

PEOPLE'S DEMOCRATIC REPUBLIC OF ALGERIA

MINISTRY OF HIGHER EDUCATION AND SCIENTIFIC RESEARCH

---

N° Series: ..... /2024



KASDI MERBAH UNIVERSITY OUARGLA

*Faculty of Hydrocarbons and Renewable Energies, Earth and Universe Science*

Hydrocarbon Production Department

## **FINAL STUDY DISSERTATION**

**In order to obtain the Master's Degree**

**Option: Professional Production**

Presented By:

**AIAD Ahmed Amine, KACEM Ahmed**

-THEME-

---

**The effectiveness of thermal control systems for  
gas hydrates formation prevention for optimal  
production activation**

---

Presented on: 08/06/2024 in front of the review committee

|             |                    |       |      |
|-------------|--------------------|-------|------|
| President:  | Mrs. BAZIOU Halima | M.A.B | UKMO |
| Examiner:   | Mr. ADJOU Zakaria  | Ph. D | UKMO |
| Supervisor: | Mrs. BAZZINE Zineb | M.A.B | UKMO |

Academic year 2023 / 2024

# Acknowledgments

Praise and gratitude to Allah Almighty for His countless blessings upon us.

We are deeply grateful to our teacher Mrs. **BAZZINE Zineb** for their support and direction, please accept our sincere thanks for giving us the honor of being our supervisor.

We sincerely express our gratitude to the review committee Mrs. **BAZIOU Halima** and Mr. **ADJOU Zakaria**, thank you for doing us the honor of agreeing to evaluate this work.

We extend our sincere thanks to Mr. **RAHAL Mohamed Lakhdar** and Mr. **Younsi Toufik** for their guidance and assistance to complete this work.

A Special thanks Our teacher Mr. **ATLILI Med Elhadi** for the effort and knowledge he has provided over these years.

All appreciation and gratitude to our teachers in Hydrocarbon Production Department, university of **KASDI MERBAH OUARGLA**

All appreciation to all the workers of **IRARA EP Sonatrach**, especially the production department **Service GL**, for their support.



## Dedication

*To my mother and father, whose unwavering support and love have been my foundation.*

*To my dear brother and sisters.*

*To my dear friend KACEM Ahmed.*

*To my dear aunt Fatima Zohra, for her care and support.*

*And to all my family and friends,*

*Thank you all. This achievement is shared with you.*

*Aiad Ahmed Amine*





*Dedications.*

*What more than being able to share the best moments of your life with the people  
you love.*

*I have the great pleasure of describing this modest work:*

*To the dearest being of my life; my mother*

*To my dear father, to my sister*

*To my dear friend Aiad ahmed amine*

*To all my family: uncles, aunts, cousins*

*I dedicate this work to all my friends with whom I have shared my life of studies  
and to all those who i know.*

*Kacem Ahmed*



## ملخص:

دراستنا تتناول فعالية المبادلات الحرارية في القضاء على تكوّن الجليد في خطوط الرفع الغازي والحفاظ على إنتاجية البئر المثلى. وتهدف إلى تعزيز أداء المبادلات الحرارية للتغلب على مشكلة الجليد بشكل كامل مما يؤدي إلى تقليل فترات التوقف الناجمة عن تكوّن الجليد وزيادة توافرية الآبار إلى أقصى حد. تم اختبار المبادلات الحرارية في حقل حاسي مسعود على 15 بئرًا، واحدة منها فشلت، في حين أن بئرين أظهرتا نسبة نجاح 100%، مما يعني أن الجليد لم يتكوّن في هذين البئرين مرة أخرى. أما باقي الآبار فقد أظهرت معدلات نجاح متفاوتة. من بين هذه الآبار، تم اختيار البئر المرشح MDZ717، حيث انخفض تكوّن الجليد ولكنه لم يُلغَ تمامًا، لدراسة أداء المبادلات الحرارية باستخدام طريقة كيرن وأدوات HYSYS، وتم استخدام Exchanger Design and Rating لإنشاء نموذج للمبادل الحراري من أجل دمجها في محاكاة HYSYS. أشارت نتائج طريقة كيرن إلى أن المبادل الحراري كافٍ للقضاء على الجليد تمامًا، ومع ذلك، لم يكن هذا هو الحال مع البئر MDZ717. وأظهرت محاكاة HYSYS، باستخدام نموذج مشابه جدًا للمبادل الحراري المستخدم في حاسي مسعود والمصمم باستخدام Exchanger Design and Rating، أن درجة حرارة الغاز بعد الخروج من المبادل بلغت 13 درجة مئوية (عند ضغط 60 بار)، وهو ما يقع في نطاق التكوين المتغير للجليد، مما يفسر السبب في عدم القضاء على الجليد تمامًا. أظهرت محاكاة HYSYS نتائج دقيقة جدًا مقارنةً بطريقة كيرن، وباستخدام نفس المحاكاة قمنا بتصميم مبادل حراري آخر واختبرناه على محاكاة البئر MDZ717، وأعطى النموذج نتيجة مرضية للغاية بزيادة درجة حرارة الغاز إلى 21 درجة مئوية، مما جعل البئر يعمل في منطقة خالية من تكوّن الجليد.

الكلمات المفتاحية: المبادل الحراري، تشكيل الهيدرات، الرفع الغازي، كيرن، HYSYS، Exchanger Design and Rating.

## Résumé:

Notre étude porte sur l'efficacité des échangeurs de chaleur dans l'élimination le problème de givrage sur les lignes de gaz lift et le maintien de la production optimale du puits. Elle vise à améliorer la performance des échangeurs pour surmonter complètement le problème de givrage, entraînant ainsi un temps d'arrêt minimal dû au problème de givrage et une disponibilité maximale des puits. Les échangeurs de chaleur à Hassi Messaoud ont été testés sur 15 puits, un puits sur les 15 a échoué, deux puits ont montré un taux de succès de 100 %, ce qui signifie que le problème de givrage ne s'est plus produit sur ces puits. Les autres puits ont montré des taux de succès variés. Parmi ces puits, le puits candidat MDZ717, où le problème de givrage a diminué mais n'a pas été complètement éliminée, a été sélectionné pour étudier la performance de l'échangeur de chaleur en utilisant la méthode Kern et les outils HYSYS. Exchanger Design and Rating a été utilisé pour créer un modèle de l'échangeur afin de l'intégrer dans la simulation HYSYS. Les résultats de la méthode Kern ont indiqué que l'échangeur est suffisant pour éliminer complètement le problème, cependant, ce n'est pas le cas avec le puits MDZ717. La simulation HYSYS, avec un modèle très similaire de l'échangeur utilisé à Hassi Messaoud

conçu avec Exchanger Design and Rating, a estimé la température du gaz à la sortie de l'échangeur à 13 °C (60 bars), ce qui tombe dans la plage de formation de glace métastable, ce qui explique pourquoi le givrage n'est pas totalement éliminée. HYSYS a montré des résultats très précis par rapport à la méthode Kern, et en utilisant la même simulation, nous avons conçu un autre échangeur et l'avons testé sur la simulation du puits MDZ717. Le modèle a donné un résultat très satisfaisant en augmentant la température du gaz à 21 °C, permettant ainsi au puits de fonctionner dans une zone sans formation de glace.

Mots clés : échangeur de chaleur, givrage, Gaz lift, Kern, HYSYS, Exchanger Design and Rating.

### **Abstract:**

Our study is about the effectiveness of heat exchanger on eliminating Hydrates on gas lift lines and maintaining the well on optimum production. And aims to enhance the exchanger performance to overcome Hydrates problem completely leading to minimal Downtime due to Hydrates and maximum well availability. The heat exchanger in Hassi Messaoud was tested on 15 wells, one well out of the 15 wells failed, two wells had 100% success rate which means Hydrates did not occur on these wells anymore. The rest of the wells had a variant success rate. Among these wells, a candidate well MDZ717, where Hydrates formation decreased but not entirely eliminated, was selected to investigate the performance of the heat exchanger by using Kern method and HYSYS tools, Exchanger Design and Rating is used to create a model of the exchanger in order to integrate it in HYSYS simulation. Kern method results indicated that the exchanger is sufficient to eliminate Hydrates completely, however, it's not the case with MDZ717. HYSYS simulation, with a very similar model of the exchanger used in Hassi Messaoud designed with Exchanger Design and Rating, estimated the temperature of gas after exiting the exchanger at 13 C° (60 bar), which falls in the range of metastable Hydrates formation, which explains the reason why Hydrates is not totally eliminated. HYSYS showed very accurate results compared to Kern method, and using the same simulation we designed another exchanger and tested it on the MDZ717 simulation, the model gave a very satisfying result by increase the temperature of the gas to 21C°, making the well operating on the free Hydrates area.

Key words: Heat exchanger, Hydrates, Gas lift, Kern, HYSYS, Exchanger Design and Rating.

# Table of contents

|  |           |
|--|-----------|
| ACKNOWLEDGMENTS.....   |           |
| DEDICATION.....  |           |
| ABSTRACT:.....   |           |
| LIST OF FIGURES:.....  |           |
| LIST OF TABLES:.....   |           |
| ABBREVIATIONS.....   |           |
| LIST OF SYMBOLS : .....                                      |           |
| <b>GENERAL INTRODUCTION .....</b>                            | <b>1</b>  |
| <b>CHAPTER I: PRESENTATION OF HASSI MESSAOUD FIELD .....</b> | <b></b>   |
| <b>I.1. PRESENTATION OF THE HASSI MESSAOUD FIELD.....</b>    | <b>3</b>  |
| I.1.1 INTRODUCTION.....                                      | 3         |
| I.1.2 HASSI MESSAOUD IN THE MAP.....                         | 4         |
| I.1.2.1 Location:.....                                       | 4         |
| I.1.2.2 Geological situation:.....                           | 4         |
| I.1.3 DESCRIPTION OF THE HMD RESERVOIR:.....                 | 5         |
| I.1.4 ZONATION AND WELL NUMBERING:.....                      | 6         |
| <b>CHAPTER II: OVERVIEW ON GAS LIFT ACTIVATION.....</b>      | <b></b>   |
| <b>II.1 INTRODUCTION.....</b>                                | <b>7</b>  |
| <b>II.2 WELLS ACTIVATION.....</b>                            | <b>7</b>  |
| II.2.1 PUMPING.....  | 8         |
| II.2.2 GAS-LIFT.....   | 8         |
| <b>II.3 GAS-LIFT APPLICATIONS:.....</b>                      | <b>9</b>  |
| <b>II.4 TYPES OF GAS-LIFT:.....</b>                          | <b>9</b>  |
| II.4.1 DEPENDING ON THE INJECTION MODE:.....                 | 9         |
| II.4.1.1 Continuous Flow Gas-Lift:.....                      | 9         |
| II.4.1.2 Intermittent Gas-Lift: .....                        | 10        |
| II.4.2 DEPENDING ON THE INJECTION SYSTEM: .....              | 11        |
| II.4.2.1 Open Gas-lift system: .....                         | 11        |
| II.4.2.2 Closed Gas-lift system: .....                       | 11        |
| <b>II.5 DIFFERENT GAS LIFT COMPLETIONS:.....</b>             | <b>11</b> |
| II.5.1 COMPLETION FOR DIRECT GAS LIFT: .....                 | 11        |
| II.5.1.1 Side pocket mandrel Completion: .....               | 11        |
| II.5.1.2 Completion with liner 2”7/8:.....                   | 12        |

|   |              |
|---|--------------|
| II.5.1.3 Completion with liner 2”7/8 and desalting: .....               | 13           |
| II.5.2 REVERSED GAS-LIFT COMPLETION: .....                              | 13           |
| II.5.2.1 Concentric tubing string (Macaroni installation): .....        | 13           |
| II.5.2.2 Casing Flow Installation: .....                                | 14           |
| II.5.2.3 Dual Gas Lift: .....   | 14           |
| II.5.2.4 Parallel gas lift: .....                                       | 15           |
| II.5.2.5 Telescopic completion: .....                                   | 15           |
| <b>II.6 PRINCIPAL GAS LIFT PARAMETERS:.....</b>                         | <b>16</b>    |
| II.6.1 WELLHEAD PRESSURE: .....   | 16           |
| II.6.2 GAS INJECTION PRESSURE: .....                                    | 16           |
| II.6.3 GAS INJECTION DEPTH: .....                                       | 16           |
| II.6.4 PRODUCTIVITY INDEX (PI): .....                                   | 16           |
| <b>II.7 INFLOW PERFORMANCE OF OIL WELLS:.....</b>                       | <b>17</b>    |
| II.7.1 INFLOW PERFORMANCE RELATIONSHIP (IPR): .....                     | 17           |
| II.7.2 DIFFERENT EQUATIONS OF IPR CURVES FOR OIL: .....                 | 17           |
| <b>II.8 HYDRATES PROBLEM IN GL PIPES IN HASSI MESSAOUD REGION:.....</b> | <b>18</b>    |
| II.8.1 REASONS OF HYDRATES FORMATION IN GL PIPELINES: .....             | 19           |
| II.8.1.1 Joule-Thomson effect: .....                                    | 19           |
| II.8.1.2 Gas-Lift Quality: .....  | 19           |
| II.8.1.3 GL and Continuous Water injection: .....                       | 19           |
| II.8.2 COMMON TECHNIQUES FOR HYDRATES PREVENTION: .....                 | 20           |
| <b>CHAPTER III: OVERVIEW ON HEAT EXCHANGERS AND HEAT TRANSFER</b>       |              |
| <b>PRINCIPLES.....</b>  | <b>.....</b> |
| <b>III.1 OVERVIEW ON HEAT TRANSFER: .....</b>                           | <b>21</b>    |
| III.1.1 DEFINITION: .....   | 21           |
| III.1.2 MODES OF HEAT TRANSFER: .....                                   | 21           |
| <b>III.2 HEAT EXCHANGERS:.....</b>                                      | <b>23</b>    |
| III.2.1 HEAT EXCHANGER CLASSIFICATION: .....                            | 23           |
| III.2.1.1 Recuperators/regenerators:.....                               | 23           |
| III.2.1.2 Transfer processes: .....                                     | 24           |
| III.2.1.3 Geometry of Construction: .....                               | 24           |
| III.2.1.4 Heat transfer mechanism:.....                                 | 24           |
| III.2.1.5 Flow arrangement: .....                                       | 24           |
| III.2.1.6 Classification According to Phase of Fluids: .....            | 25           |
| III.2.2 HEAT EXCHANGER TYPES: .....                                     | 25           |
| III.2.2.1 Double pipe Heat Exchanger: .....                             | 25           |
| III.2.2.2 Shell and tube heat exchanger:.....                           | 26           |
| III.2.2.3 Plate Heat Exchanger: .....                                   | 29           |
| <b>III.3 KERN METHOD: .....</b>   | <b>29</b>    |



|  |           |
|--|-----------|
| II.3.1 INTRODUCTION: .....   | 29        |
| III.3.2 KERN METHOD BASIC CALCULATION FOR SHELL AND TUBE EXCHANGER: .....                    | 30        |
| III.3.2.1 Calculation of the exchanged Heat Quantity: .....                                  | 30        |
| III.3.2.2 Calculation of Log Mean Temperature Difference (DTLM): .....                       | 31        |
| III.3.2.3 Calculation of the overall heat transfer coefficient $U_s$ : .....                 | 32        |
| III.3.2.4 Calculation of the heat exchange area: .....                                       | 34        |
| III.3.2.5 Calculation of the available heat exchange area: .....                             | 34        |
| <b>CHAPTER IV: PRACTICAL PART .....</b>  |           |
| <b>IV.1 PROBLEMATIC: .....</b>   | <b>35</b> |
| <b>PART ONE: GAS LIFT INJECTION RATE OPTIMIZATION WITH PIPESIM (CASE STUDY MDZ717) .....</b> | <b>37</b> |
| IV.2 OVERVIEW ABOUT PIPESIM SOFTWARE: .....  | 37        |
| IV.3 WELL MODELLING: .....   | 38        |
| IV.3.1 Well model construction: .....  | 39        |
| IV.3.2 Tubulars: .....   | 39        |
| IV.3.3 Trajectory and Depth: .....   | 40        |
| IV.3.4 Downhole equipment: .....   | 40        |
| IV.3.5 Artificial Lift: .....  | 40        |
| IV.3.6 Heat transfer: .....  | 41        |
| IV.3.7 Reservoir data: .....   | 41        |
| IV.3.8 PVT data: .....   | 42        |
| IV.3.9 Surface equipment: .....  | 43        |
| IV.4 ESTIMATION OF PRODUCTIVITY INDEX PI AND DISCHARGE COEFFICIENT $C_D$ : .....             | 44        |
| IV.4.1 Calculation of GL injection flowrates: .....  | 44        |
| IV.4.2 Calculation of water cut: .....   | 45        |
| IV.4.3 PI Evaluation: .....  | 46        |
| IV.4.4 Discharge coefficient Evaluation: .....   | 47        |
| IV.4.5 Representative Gauging selection: .....   | 48        |
| IV.5 OPTIMIZATION OF GAS LIFT INJECTION FLOWRATE: .....                                      | 49        |
| IV.6 RESULT AND DISCUSSION: .....  | 51        |
| <b>PART TWO: HEAT EXCHANGER DESIGN AND ANALYSIS (CASE STUDY MDZ717) .....</b>                | <b>52</b> |
| IV.7 HEAT EXCHANGER IN DP-HMD: .....   | 52        |
| IV.8 HYDRATES FORMATION CONDITIONS: .....  | 53        |
| IV.9 APPLICATION OF KERN METHOD: .....   | 55        |
| IV.9.1 Implementing Kern method in Python .....  | 55        |
| IV.9.2 Heat exchanger Performance verification with Kern method (Well MDZ717): .....         | 55        |
| IV.9.3 Kern Method calculation results: .....  | 58        |
| IV.10. SIMULATION AND DESIGN OF HEAT EXCHANGERS WITH HYSYS AND EDR: .....                    | 58        |
| IV.10.1 Overview about Aspen HYSYS and Aspen EDR: .....                                      | 58        |
| IV.10.1.1 Aspen HYSYS .....  | 58        |

|  |              |
|--|--------------|
| IV.10.1.2 Aspen Exchanger Design and Rating (EDR).....                 | 59           |
| IV.10.2 Model creation of the well MDZ717 and heat exchanger:.....     | 59           |
| IV.10.2.1 Adding component lists: .....                                | 60           |
| IV.10.2.2 Selecting fluid packages: .....                              | 60           |
| IV.10.2.3 Setting up the flowsheet: .....                              | 61           |
| IV.10.2.4 Designing the heat exchanger with EDR:.....                  | 62           |
| IV.10.2.5 Simulation of MDZ717 well and exchanger with HYSYS: .....    | 63           |
| IV.10.3 Design and simulation of a Proposed Heat Exchanger Model:..... | 64           |
| IV.11 RESULT AND DISCUSSION:.....                                      | 64           |
| <b>GENERAL CONCLUSION .....</b>  | <b>66</b>    |
| <b>BIBLIOGRAPHY .....</b>  | <b>.....</b> |
| <b>APPENDIX .....</b>  | <b>.....</b> |

## List of Figures:

|   |    |
|---|----|
| Figure I. 1: History of Oil Production and Well Counts in Hassi Messaoud Field. ....                | 3  |
| Figure I. 2: Geographical location of Hassi Messaoud field. ....                                    | 4  |
| Figure I. 3: Geological situation of the Hassi Messaoud field. ....                                 | 5  |
| Figure I. 4: Geological section of the Hassi Messaoud field.....                                    | 6  |
|   |    |
| Figure II. 1: Artificial Lift methods.....  | 7  |
| Figure II. 2: Basic components of GL system. ....   | 9  |
| Figure II. 3: Continuous Flow Gas-Lift. ....  | 10 |
| Figure II. 4: Intermittent Gas-Lift. ....   | 10 |
| Figure II. 5: Open gas-lift system. ....  | 11 |
| Figure II. 6: Closed gas-lift system. ....  | 11 |
| Figure II. 7: SPM Completion.....   | 12 |
| Figure II. 8: Completion with liner 2”7/8. ....   | 12 |
| Figure II. 9: Completion with liner 2”7/8 and desalting (Case of well MD322). ....                  | 13 |
| Figure II. 10: Concentric tubing string Completion. ....  | 13 |
| Figure II. 11: Casing Flow Installation. ....   | 14 |
| Figure II. 12: Dual Gas Lift. ....  | 14 |
| Figure II. 13: Parallel gas lift. ....  | 15 |
| Figure II. 14: Telescopic completion.....   | 15 |
| Figure II. 15: Inflow Performance Relationship. ....  | 17 |
| Figure II. 16: Production Losses Due to Shut-in for Variety of Reasons in HMD. ....                 | 18 |
| Figure II. 17: Example of Hydrates on Lift Gas Injection Line Downstream of Gas Lift<br>Choke. .... | 20 |
|   |    |
| Figure III. 1: Conduction. ....   | 22 |
| Figure III. 2: Convection.....  | 22 |
| Figure III. 3: Radiation. ....  | 23 |
| Figure III. 4: Flow types in heat exchangers. ....  | 25 |
| Figure III. 5: Double pipe Heat Exchanger. ....   | 26 |
| Figure III. 6: Shell and tube heat exchanger.....   | 26 |
| Figure III. 7: Tube arrangements in a shell and tube heat exchanger.....                            | 27 |

|  |    |
|--|----|
| Figure III. 8: Baffle in shell and tube heat exchanger. ....                           | 27 |
| Figure III. 9: Front Heads in shell and tube heat exchanger. ....                      | 28 |
| Figure III. 10: Rear Head in shell and tube heat exchanger. ....                       | 28 |
| Figure III. 11: TEMA Standard. ....  | 29 |
| Figure III. 12: Plate Heat Exchanger. ....   | 29 |
| Figure III. 13: Hot and cold fluid's flow. ....  | 32 |
|  |    |
| Figure IV. 1: Effect of gas rate on well production. ....                              | 35 |
| Figure IV. 2: Analysis of the first phase of 15 wells with heat exchanger DP-HMD. .... | 36 |
| Figure IV. 3: PIPESIM 2020.1 window ....   | 38 |
| Figure IV. 4: Well name and type. ....   | 39 |
| Figure IV. 5: Tubulars and Completion. ....  | 39 |
| Figure IV. 6: Trajectory and Depth. ....   | 40 |
| Figure IV. 7: Downhole equipment. ....   | 40 |
| Figure IV. 8: Artificial Lift MDZ717. ....   | 41 |
| Figure IV. 9: Heat transfer MDZ717. ....   | 41 |
| Figure IV. 10: Reservoir data. ....  | 42 |
| Figure IV. 11: PVT data. ....  | 42 |
| Figure IV. 12: Surface equipment. ....   | 43 |
| Figure IV. 13: MDZ717 PIPESIM model. ....  | 43 |
| Figure IV. 14: Liquid PI estimation inputs. ....                                       | 46 |
| Figure IV. 15: PI Evaluation MDZ717. ....  | 47 |
| Figure IV. 16: Discharge coefficient estimation inputs. ....                           | 48 |
| Figure IV. 17: Optimum GLI inputs. ....  | 49 |
| Figure IV. 18: Liquid flowrate change based on GLI rate. ....                          | 50 |
| Figure IV. 19: GLI optimization results. ....  | 50 |
| Figure IV. 20: Heat exchanger surface installation. ....                               | 52 |
| Figure IV. 21: Heat exchanger (MD322). ....  | 53 |
| Figure IV. 22: Fabrication of heat exchanger HMD. ....                                 | 53 |
| Figure IV. 23: Hydrates formation curves for Hassi Messaoud gas lift. ....             | 54 |
| Figure IV. 24: Python window. ....   | 55 |
| Figure IV. 25: Kern Method Calculation MDZ717 inputs. ....                             | 57 |
| Figure IV. 26: Kern Method Results for MDZ717 well. ....                               | 58 |
| Figure IV. 27: HYSYS V12 window. ....  | 59 |

|  |    |
|--|----|
| Figure IV. 28: Adding component lists.....   | 60 |
| Figure IV. 29: Selecting fluid packages.....   | 60 |
| Figure IV. 30: GL and Crude composition. ....  | 61 |
| Figure IV. 31: Setting up the heat exchanger streams. ....                           | 62 |
| Figure IV. 32: Geometry and sketch of the heat exchanger in DP-HMD with EDR. ....    | 62 |
| Figure IV. 33: Simulation of MDZ717 well and exchanger with HYSYS.....               | 63 |
| Figure IV. 34: Simulation of MDZ717 case and proposed exchanger model with HYSYS.... | 64 |

**List of Tables:**

|   |    |
|---|----|
| Table II. 1: Equations of IPR curves for oil. ....                | 18 |
| Table IV. 1: General Information about MDZ717.....                | 38 |
| Table IV. 2: Gauging of well MDZ717. ....                         | 44 |
| Table IV. 3: PVT data of the well MDZ717. ....                    | 45 |
| Table IV. 4: Calculated water cut percentages.....                | 45 |
| Table IV. 5: Liquid PI results.....                               | 46 |
| Table IV. 6: Discharge coefficient results.....                   | 48 |
| Table IV. 7: Representative gauging.....                          | 49 |
| Table IV. 8: Parameters of well MDZ717 at optimum condition. .... | 50 |
| Table IV. 9: Shell side and tube side data. ....                  | 56 |
| Table IV. 10: Calculation of the specific heat of gas lift. ....  | 56 |

## **Abbreviations**

GL : Gas lift

HMD : Hassi Messaoud

GLI: Gas Lift Injection

DP-HMD: Division Production of Hassi Messauod

API : American Petroleum Institute.

HYSYS : Hyprotech Systems

EDR : Exchanger Design and rating

PIPESIM : Pipeline Simulator

ESP : Electrical Submersible Pump

PCP : Progressive Cavity Pumps

GOR : Gas Oil Ratio

GLR : Gas Liquid Ratio

WC : Water Cut

SPM : Side Pocket Mandrel

CCE : Concentric

PI : Productivity Index

IPR : Inflow Performance Relationship

PVT : Pressure Volume Temperature

MD : Measured Depth

KOP : Kick Off Point

TVD : True Vertical Depth

SG : Specific Gravity

TEMA : Tubular Exchangers Manufactures Association.

DTLM : Log Mean Temperature Difference

## LIST OF SYMBOLS :

|                   |  |
|-------------------|--|
| $d_o$ :           | out diameter(m).   |
| $d_i$ :           | inner diameter(m).   |
| L:                | Length of tube (m).  |
| tw:               | tube thickness(m).   |
| Q1:               | Amount of heat lost by the hot fluid (kJ/h).   |
| Q2:               | Amount of heat received by the cold fluid (kJ/h).  |
| $\dot{M}$ :       | Heat loss flow rate of the hot fluid (kg/h).   |
| $\dot{m}$ :       | Mass flow rate of the cold fluid (kg/h).   |
| $C_{p_{gl}}$ :    | Specific heat of GL “Cold fluid” (kJ / kg k°).   |
| $C_{p_{crude}}$ : | Specific heat of Crude oil “Hot fluid” (kJ / kg k°).   |
| $t_1$ :           | Temperature of cold fluid in (C°).   |
| $t_2$ :           | Temperature of cold fluid out (C°).  |
| $T_1$ :           | Temperature of hot fluid in (C°).  |
| $T_2$ :           | Temperature of hot fluid out (C°).   |
| $Y_i$ :           | Mass fraction of the gas components.   |
| $C_{p_i}$ :       | Specific heat of each constituent (J/kg k°).   |
| $Q_{gl}$ :        | Volumetric flowrate of GL (m <sup>3</sup> /d).   |
| $\rho_{gl}$ :     | Density of GL (kg/m <sup>3</sup> ).  |
| F:                | correction factor.   |
| $U_s$ :           | the overall heat transfer coefficient (kJ/h m <sup>2</sup> k°).                                |
| $h_i$ :           | the convective heat transfer coefficient on the inside (tube side) (kJ/h m <sup>2</sup> k°).   |
| $h_o$ :           | the convective heat transfer coefficient on the outside (shell side) (kJ/h m <sup>2</sup> k°). |
| $\lambda_s$ :     | thermal conductivity of the tube wall material (steel) =45 (W/m k°).                           |
| $\lambda_{gl}$ :  | Thermal conductivity of gas lift (kJ/h.m.k°).  |

|                       |  |
|-----------------------|--|
| Nu:                   | Nusselt number.  |
| Re:                   | Number of Reynolds.  |
| Pr:                   | Prandtl number.  |
| W:                    | Fluid mass velocity (kg/h m <sup>2</sup> ).                                |
| $\mu_g$ :             | Gas dynamic viscosity.   |
| Sc:                   | Passage section of fluid (m <sup>2</sup> )                                 |
| $D_{eq}$ :            | Equivalent diameter (m <sup>2</sup> ).                                     |
| n:                    | Total number of tubes.   |
| $\dot{M}_{(o+w+g)}$ : | Mass flow rate in shell side (kg/h).                                       |
| $\mu_m$ :             | Shell side overall dynamic viscosity (kg/h m).                             |
| $\mu_i$ :             | Dynamic viscosity of each fluid (Water, Oil, Gas) (kg/h m).                |
| $X_i$ :               | Volumic fraction of each fluid (Water, Oil, Gas).                          |
| $C_{p_m}$ :           | Overall specific heat in shell side (J/kg k <sup>o</sup> ).                |
| $\lambda_m$ :         | Overall thermal conductivity in shell side (kj/h.m.k <sup>o</sup> ).       |
| $\lambda_i$ :         | Thermal conductivity of each fluid in shell side (kj/h.m.k <sup>o</sup> ). |
| $A_{cal}$ :           | The heat exchange area (m <sup>2</sup> ).                                  |
| $A_{ava}$ :           | The available heat exchange area (m <sup>2</sup> ).                        |
| $C_d$ :               | Discharge coefficient  |



# **General introduction**

The Hassi Messaoud region is crucial to Algeria's oil production, with over 500 gas lift activated wells which account for 40% of the region's total production.

Gas lift technology is extensively used to enhance oil and gas production by injecting gas into the wellbore to reduce hydrostatic pressure and facilitate the flow of hydrocarbons.

Despite its effectiveness, this method encounters significant challenges during winter due to Hydrates in the gas lift lines. Hydrates prevents the wells from producing optimally, leading to substantial production losses estimated at around 300 to 400 tons per day in Hassi Messaoud. This leads to high downtime and necessary interventions when Hydrates is severe. [15]

Several methods have been attempted to overcome the Hydrates problem in gas lift lines and the most effective solution identified is the use of heat exchangers. Engineers in the Engineering & Production department in Hassi Messaoud designed a shell and tube heat exchanger model. This model utilizes the thermal energy from the produced crude oil passing through the shell to heat the cold gas flowing through the tube.

This simple yet intelligent approach to solving the Hydrates problem requires a high crude oil temperature to heat the gas lift. The heat exchanger was tested on 15 wells and showed very good results by increasing production gain. Although successful, there is a need to further investigate and enhance the effectiveness of the heat exchanger in eliminating Hydrates and maintaining optimal production. [15]

This study aims to assess the effectiveness of the heat exchanger in Hassi Messaoud, by doing a case study on a pilot well which is MDZ717. The objective is to optimize well production using PIPESIM, evaluate the exchanger's effectiveness using the Kern method and HYSYS, and explore ways to improve its performance.

The study is divided into four chapters:

Chapter I: A presentation of the Hassi Messaoud region.

Chapter II: A review of gas lift activation and the Hydrates problem in Hassi Messaoud,

Chapter III: An overview of heat exchangers and heat transfer principles.

Chapter IV: The practical part. it includes a case study of well MDZ717 that utilizes PIPESIM to optimize the well production. Kern Method, HYSYS and EDR tools evaluate the heat exchanger effectiveness and enhance its performance.

# Chapter I: Presentation of Hassi Messaoud field

## I.1. Presentation of the Hassi Messaoud field

### I.1.1 Introduction

The Hassi-Messaoud Field is a thick sandstone reservoir covering an area of 2000 km<sup>2</sup>. It is a flattened anticline located on the North of the El-Biod-Hassi-Messaoud elevation. This elevation was formed by a sequence of horsts and grabens contained by faults in a sub-meridian direction. The faults are in general South-South-West to North-North-East trends and they run across all the producing reservoirs.

The producing reservoir is located at 3300m and consists of four distinct formations in addition to a transitional zone. These zones are subdivided into producing intervals or drains characterized by distinct properties. Overall, the field is divided into 25 separate zones that differ in their geological and geophysical properties. Reservoir pressure is maintained by water and gas injection.

Field production started in 1957. In the first twenty years, all production wells were on natural flowing. Began in 1980, the gas lift was introduced into the field development. The gas lift has been the only artificial lift method in the past. Electric Submersible Pumping (ESP) systems have been introduced into the field very recently. Other artificial lift methods such as Jet Pumps, Rod Pumps, Plungers, and Progressive Cavity Pumps (PCP) are evaluated for possible future applications in the field.

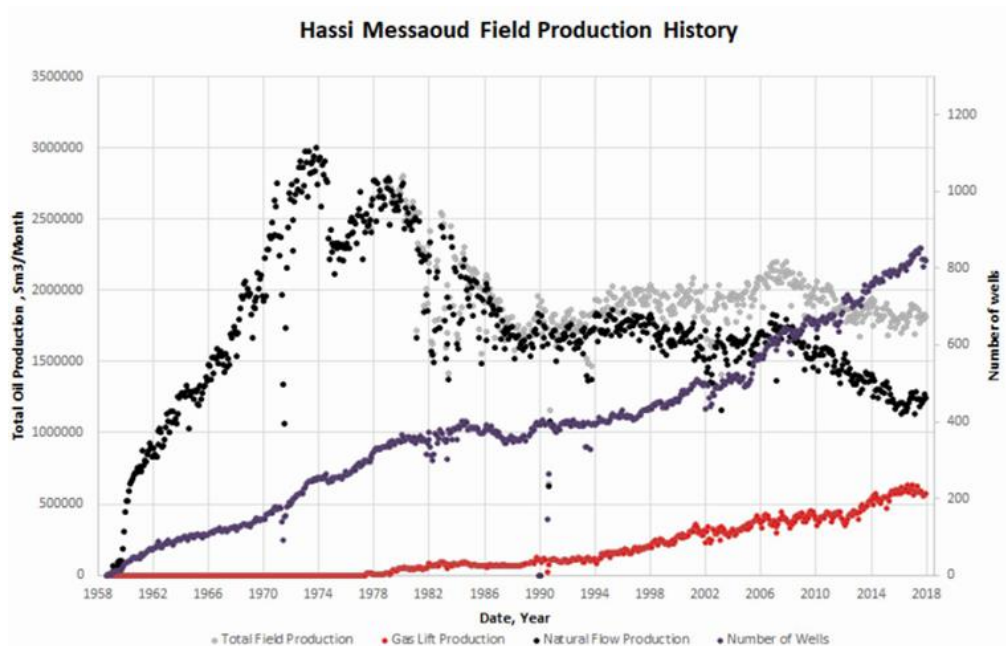
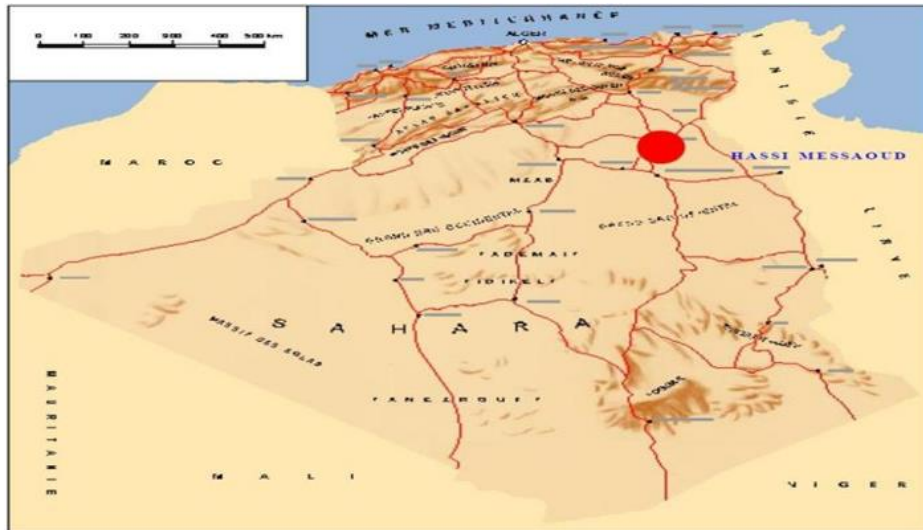


Figure I. 1: History of Oil Production and Well Counts in Hassi Messaoud Field. [17]

## I.1.2 Hassi Messaoud in the map

**I.1.2.1 Location:** The Hassi Messaoud field is located 650 km South-South-East of Algiers and 350 km from the Tunisian border. Its location in coordinates Lambert is as follows 790.000 @ 840.000 Est \* 110.000 @ 150.000 North.



**Figure I. 2:** Geographical location of Hassi Messaoud field. [1]

**I.1.2.2 Geological situation:** The Hassi Messaoud field occupies the central part of the Triassic province east of the Oued M'a depression in district IV which by its area and reserves is the largest petrogaseïfere province. It is the largest deposit in Algeria which extends over 53x44 km of area. It is limited:

- To the northwest by the deposits of Ouargla (Guellala, Ben Kahla and Haoud Berkaoui).
- To the southwest by the deposits of El Gassi, Zotti and El Agreb.
- To the south-east by the deposits; Rhourde El Baguel and Mesdar.

On a larger scale, it is limited:

- To the west by the depression of Oued M'ya.
- To the south by the pier of Amguid El Biod.
- To the north by the Djamâa - Touggourt structure.
- To the east by the shoals of Dehar, Rhourde El Baguel and the depression of Ghadames.



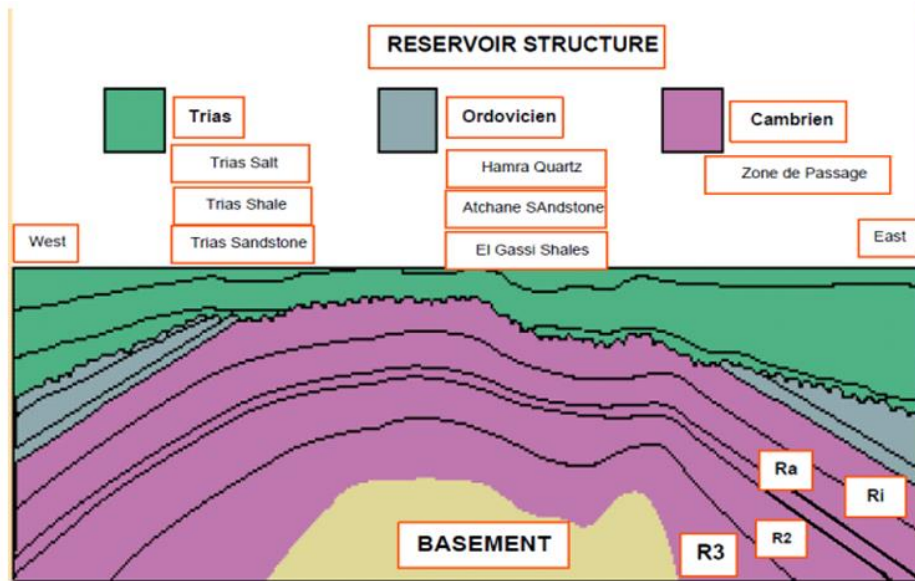


**Figure I. 4:** Geological section of the Hassi Messaoud field. [1]

### I.1.4 Zonation and well numbering:

The Hassi Messaoud field is divided into numbered areas. This division is naturally deduced from the characteristics of production and geology.

Changes in well pressures, depending on production, have made it possible to subdivide the field into 25 producing zones. A production area is defined as a set of wells that communicate with each other but little or nothing with those in neighboring areas. It should be noted that the current subdivision is not satisfactory because the same area can be subdivided into subzones.

The Hassi Messaoud field is divided from east to west into two distinct parts the south field and the north field, each has its own numbering.

**The North Field:** It is a geographical numbering supplemented by a chronological numbering, example Omo38, Onm15, Ompz16\*

O Capitalization, Ouargla permit. m area of the oil zone 1600 km<sup>2</sup>. o Minuscule, area of the oil zone of 100 km<sup>2</sup>, 3 Abscissa and 8 ordinate.

The South field Zone numbering is chronological. Ex: MD1, MD322, MDZ717.



# Chapter II: Overview on gas lift activation

## II.1 Introduction

In petroleum production, many wells initially flow naturally, driven by reservoir pressure and formation gas. This natural flow continues until the energy provided by the reservoir diminishes, causing the well to stop flowing.

When reservoir energy is insufficient or production rates exceed what the reservoir can sustain, artificial lift methods are employed to facilitate fluid extraction.

Artificial lifting methods are used for the extraction of fluids from wells that are no longer producing or to enhance the production rate from wells that are already flowing.

## II.2 Wells Activation

Wells activation modes with artificial lift can be used to activate and put wells on service, either when deposit does not contain enough energy to raise the fluid from the bottom of the well to the treatment facilities or the productivity index of the well is considered insufficient. There are two parameters that can be acted on: [2]

$$P_{re} \leq \frac{H \cdot d}{10.2} \quad (\text{II. 1})$$

- Height reduction “H” by installing a pump in the well.
- Column weight reduction “d” by injecting less dense gas (compressed air, naturel gas, nitrogen (N<sub>2</sub>) ...etc).

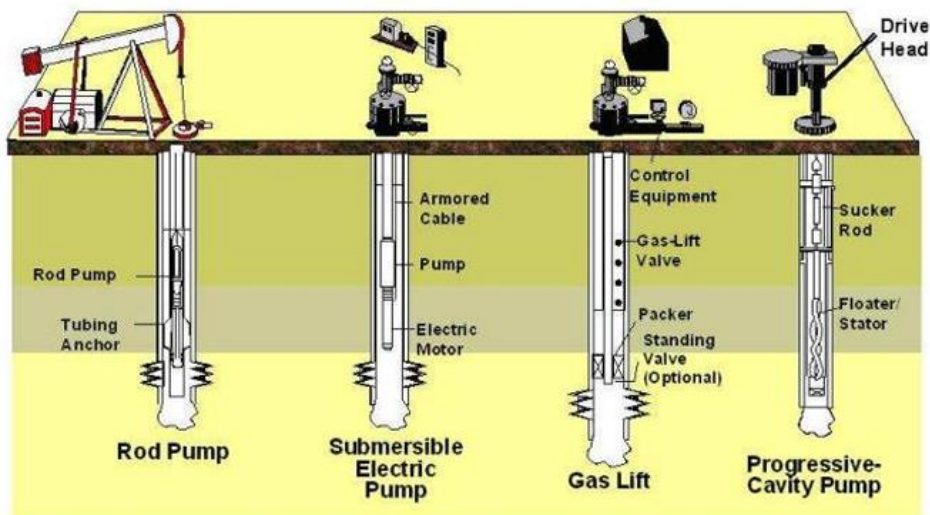


Figure II. 1: Artificial Lift methods. [3]

## II.2.1 Pumping

Pumping involves the use of some kind of a pump installed downhole to increase the pressure in the well to overcome the sum of flowing pressure losses. These methods can be classified further using several different criteria. However, the generally accepted classification is based on the way the downhole pump is driven and distinguishes between rod and rod less pumping.

- Rod pumping methods utilize a string of rods that connects the downhole pump to the surface driving mechanism which, depending on the type of pump used, makes an oscillating or rotating movement. The first kinds of pumps to be applied in water and oil wells were of the positive-displacement type requiring an alternating vertical movement to operate.
- Rod-less pumping methods, as the name implies, do not have a rod string to operate the downhole pump from the surface. Accordingly, other means are used to drive the downhole pump, such as electric or hydraulic. A variety of pump types are applied with rod less pumping, including centrifugal, positive displacement, or hydraulic pumps. Electric submersible pumping (ESP) utilizes a submerged electrical motor driving a multistage centrifugal pump.
- Jet pumping, although it is a hydraulically driven method of fluid lifting, completely differs from the rod-less pumping principles. Its downhole equipment converts the energy of a high-velocity jet stream into useful work to lift well fluids. The downhole unit of a jet pump installation is the only oil well pumping equipment known today containing no moving parts. [4]

## II.2.2 Gas-lift

The main objective of gas-lift activation is to reduce bottom hole flowing pressure and thus increase reservoir production. The gas is injected in the deepest point possible to reduce the weight of production column and with optimum parameters in order to not pass the limitations of high performance where its efficiency decreases.

Gas lift is the form of artificial lift that most closely resembles the natural flow process. It can be considered an extension of the natural flow process. In a natural flow well, as the fluid travels upward toward the surface, the fluid column pressure is reduced, gas comes out of solution, and the free gas expands. The free gas, being lighter than the oil it displaces, reduces the density of flowing fluid and further reduces the weight of the fluid column above the formation. This

reduction in the fluid column weight produces the pressure differential between the wellbore and the reservoir that causes the well to flow. [3]

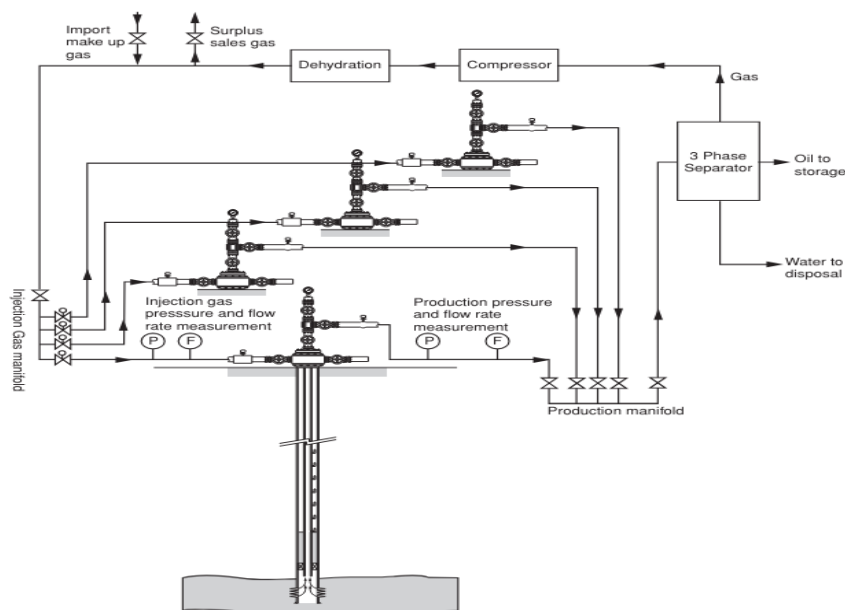


Figure II. 2: Basic components of GL system. [5]

### II.3 Gas-lift Applications:

Gas-lift is used for various purposes:

- Obtaining a stable flow rate.
- Increasing the productivity of wells.
- Starting and restarting wells after neutralisation and interventions.
- Cleaning of wellbore. [2]

### II.4 Types of Gas-lift:

#### II.4.1 Depending on the injection mode:

**II.4.1.1 Continuous Flow Gas-Lift:** Continuous flow gas lifting involves a continuous injection of lift gas into the well-stream at a predetermined depth, usually from the casing-tubing annulus to the tubing string. The injection of a proper amount of gas significantly decreases the flowing mixtures average density above the injection point. [4]

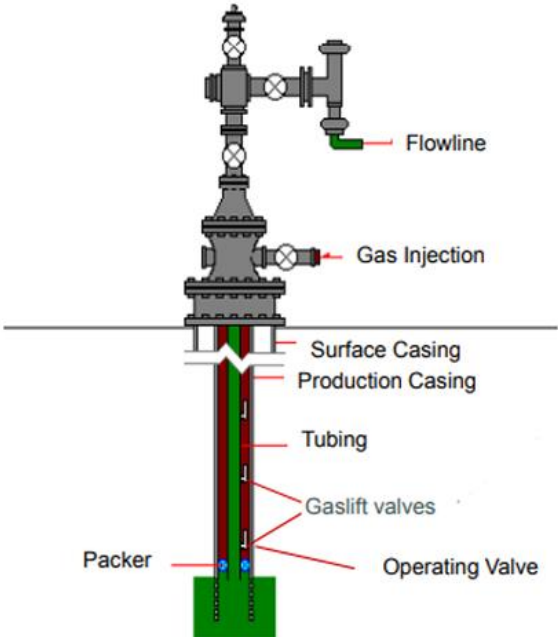


Figure II. 3: Continuous Flow Gas-Lift.

**II.4.1.2 Intermittent Gas-Lift:** Intermittent gas lift, although it uses compressed gas from the surface too, it works on a principle completely different from continuous flow gas lift. Lift gas is periodically injected into the flow string at a depth close to the perforations and physically displace a solid liquid column that was allowed to accumulate above the operating gas lift valve. [4]

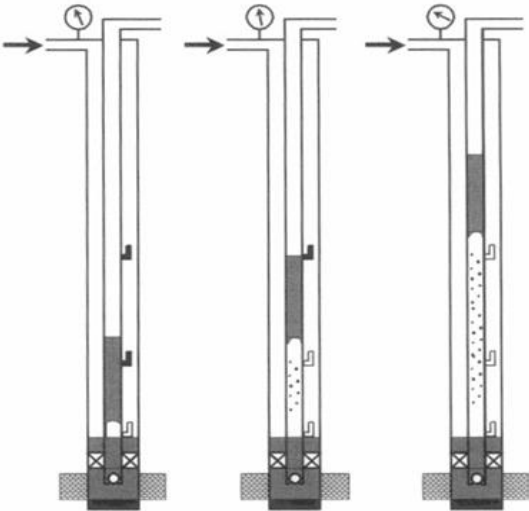


Figure II. 4: Intermittent Gas-Lift. [5]

## II.4.2 Depending on the injection system:

**II.4.2.1 Open Gas-lift system:** A low pressure gas taken from an existing gas line after compression and its use in the gas lifted wells is returned to the gas line at a low pressure. Since gas is always available at the compressor's suction, and all gas leaving the gathering system is led to the gas line, there are no capacity problems in the distribution or the gathering systems. [4]

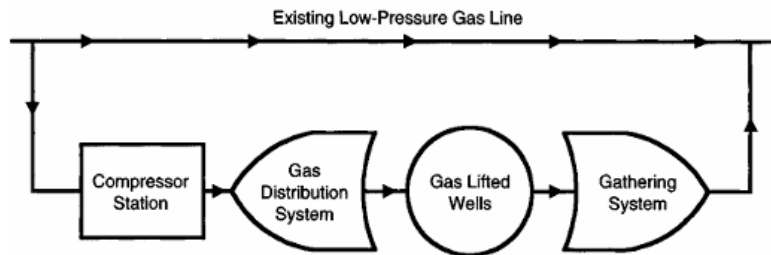


Figure II. 5: Open gas-lift system. [4]

**II.4.2.2 Closed Gas-lift system:** The closed system returns all gas from the separators back to the suction of the compressors. This system requires outside gas for initial make-up only, then, it operates without any outside supplement of gas. After the system is charged with gas at startup, its operational gas requirement equals the sum of the gas rate required for fuel and the gas rate covering leakage losses in system components. [4]

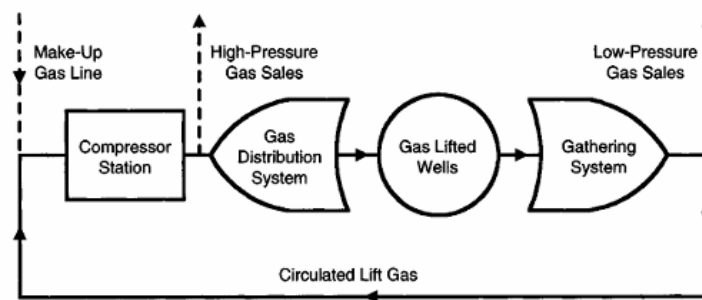


Figure II. 6: Closed gas-lift system. [4]

## II.5 Different gas lift completions:

### II.5.1 Completion for direct gas lift:

**II.5.1.1 Side pocket mandrel Completion:** Gas injection is carried out in the annular tubing-casing and through SPM (Side pocket mandrel) valves and production is carried through the tubing. It is the most widely used gas lift design in the world.

The SPM discharge valves and the orifice are operated by cable for tubing with a nominal diameter of 2" 7/8 and more, placed at different depths and allow the oil column to be gradually lightened. The packer is sometimes equipped with a by-pass to allow the gas to go as low as possible into the well. [6]

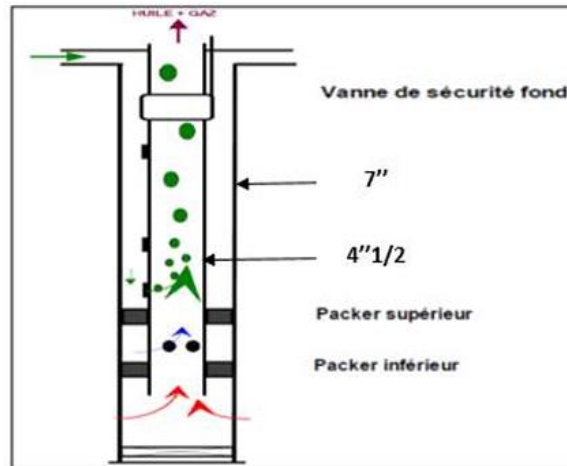


Figure II. 7: SPM Completion. [6]

**II.5.1.2 Completion with liner 2"7/8:** In this completion, a 2"7/8 liner is lowered into the 4"1/2 tubing and the gas injection is done through the annular space (4"1/2 and 2"7/8) while oil production in the 2"7/8 liner. It is the most common gas lift design in Hassi-Messoud field, due to its simplicity and ease of operation. [6]

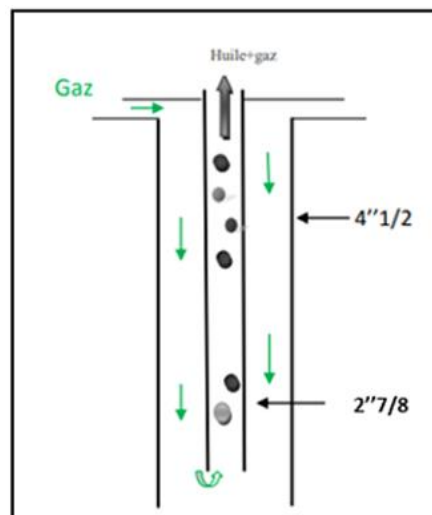
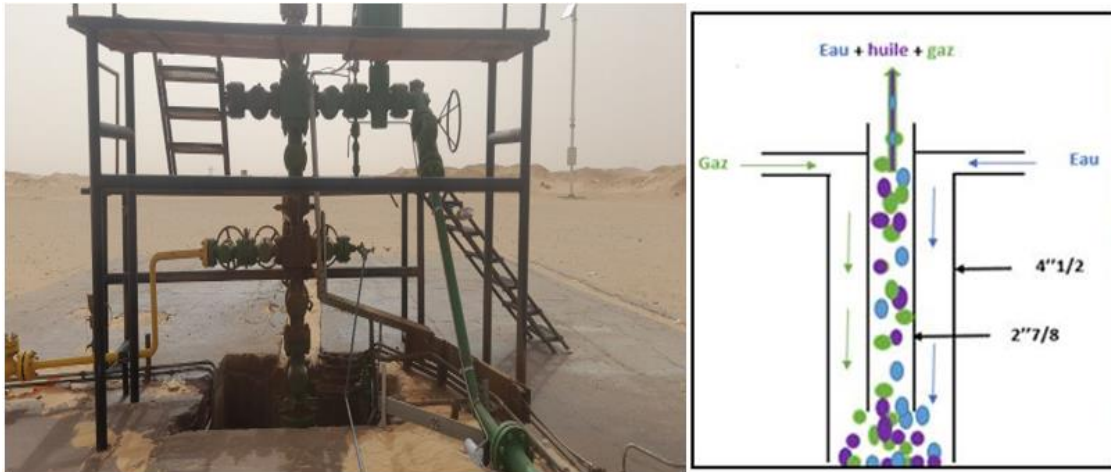


Figure II. 8: Completion with liner 2"7/8. [6]

**II.5.1.3 Completion with liner 2"7/8 and desalting:** This type of completion is used both for gas lifting and well desalination by water injection. The injection of gas and water is done in the same annular part between the 4"1/2 tubing and the 2"7/8 liner. [6]



**Figure II. 9:** Completion with liner 2"7/8 and desalting (Case of well MD322). [6]

## II.5.2 Reversed gas-lift Completion:

**II.5.2.1 Concentric tubing string (Macaroni installation):** The gas is injected into a small concentric tube, also called Macaroni, this type of profile is very common because it avoids heavy Work-Over.

This solution is generally found in wells where the gas-lift has not been planned at the end of drilling the well and the installation of a concentric tube is a simple and inexpensive way to activate the well. [6]

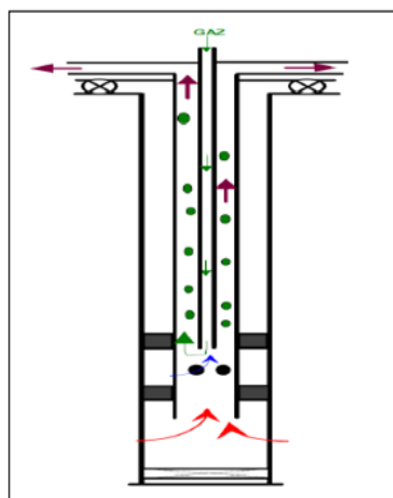


**Figure II. 10:** Concentric tubing string Completion. [6]



**II.5.2.2 Casing Flow Installation:** In a casing flow installation, gas is injected down the tubing and production rises in the casing-tubing annulus.

It is generally used in continuous flow gas lift wells producing extremely large liquid rates that exceed the capacity of the tubing string run in the well. Its main drawback is that the casing is exposed to well fluids restricting application to noncorrosive liquids. [4]

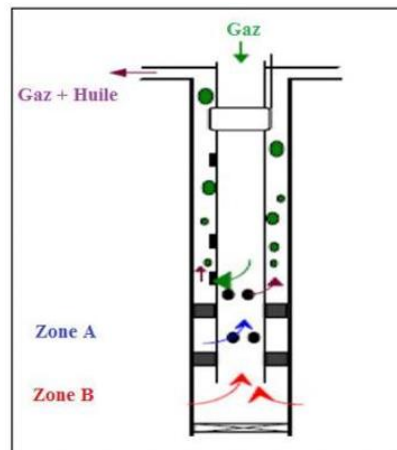


**Figure II. 11:** Casing Flow Installation. [6]

**II.5.2.3 Dual Gas Lift:** Double completions are neither easy to lower nor easy to raise but offer the possibility of producing two incompatible reservoirs in the same well for commingle production. Among the problems of this completion:

- The great complexity of annular sub-surface safety valves.
- The size of pocket mandrel. In general, it is not possible to remove a tube alone because the mandrels cannot overlap when the tubing is reassembled first. [6]

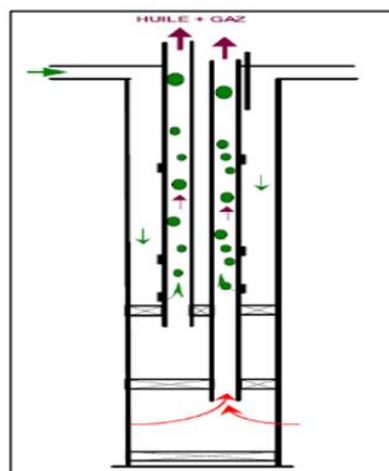


**Figure II. 12:** Dual Gas Lift. [6]

**II.5.2.4 Parallel gas lift:** This production method has the same disadvantages as the double gas lift in terms of setting up the completion. The gas is injected into one tubing while the second produces from the reservoir.

This completion is used when the available gas must not come into contact with the casing, The parallel gas lift often exists in old wells initially in multiple completion. [6]

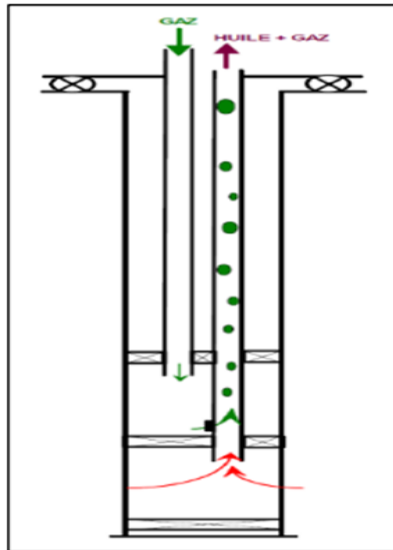


**Figure II. 13:** Parallel gas lift. [6]

**II.5.2.5 Telescopic completion:** This completion is used in salt wells. The gas lift is injected through the annular space (4"1/2 and 2"7/8). Water injection is done through the CCE and oil production through the annular space (2"7/8 and CCE). [6]

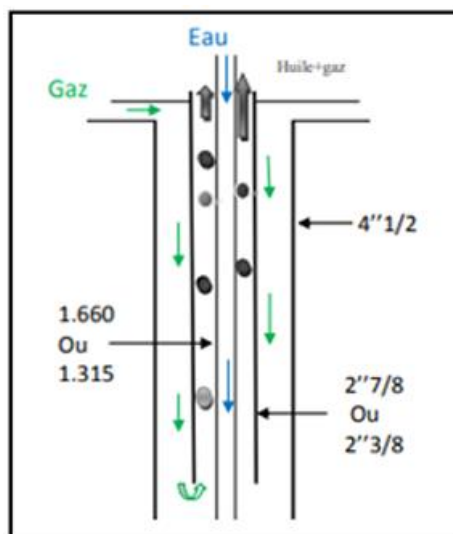


**Figure II. 14:** Telescopic completion. [6]

## II.6 Principal gas lift parameters:

### II.6.1 Wellhead pressure:

The lower the head pressure, the less gas will be required to produce the same amount of fluid. In addition, a low volume of injected gas makes it possible to have space-saving surface installations, thus reducing the collection pressure. A low head pressure therefore improves the efficiency of the well and neighboring wells. [7]

### II.6.2 Gas injection pressure:

The gas pressure to be injected affects the number of discharge valves, so injection with high pressure can allow operation without discharge valves (single point), which greatly simplifies well design, operation and maintenance. [7]

### II.6.3 Gas injection depth:

The deeper the injection point, the more effective the injected gas is. A deep injection point provides a very clear improvement in well production, especially for high IP wells.

Similarly, a significant portion of a well's possible production may be lost if gas is injected from a leaking discharge valve instead of the operating valve. Some completions are equipped with a packer with a by-pass to allow the gas to go as close as possible to the reservoir. [7]

### II.6.4 Productivity Index (PI):

Productivity Index (PI=J) is the number of barrels of liquid produced per day for each pound per square inch (psi) of reservoir pressure drawdown. Draw-down is defined as the difference in the stabilized static bottomhole pressure and the dynamic bottomhole pressure.

The gas-lift and like other well activation methods lower the dynamic bottomhole pressure, therefore the gas lift is affected by the productivity index. The effect is confirmed in wells with a significant PI where the gas lift provides spectacular flow rates. [8]

$$PI = \frac{q}{P_{re} - P_{wf}} \quad (II. 2)$$

Where:

- PI: Productivity Index (BLPD/psi)
- q: Liquid Production Rate (BLPD)

- $P_{re}$ : Reservoir Pressure (psig)
- $P_{wf}$ : Flowing bottomhole pressure (psig)

## II.7 Inflow Performance of Oil Wells:

A well's inflow performance is usually expressed in terms of productivity which simply indicates the number of barrels of oil or liquid that a well is capable of producing at a given reservoir pressure. One way of expressing well productivity is with the Productivity Index (P.I) technique. This involves measuring a well's producing rate, and flowing bottomhole pressure at that rate, then using this information to calculate a PI for the well.

### II.7.1 Inflow Performance Relationship (IPR):

The Inflow Performance Relationship is essential for understanding and optimizing the production of hydrocarbons from reservoirs. It helps engineers and operators determine how changes in production rates or reservoir conditions affect the performance of the well.

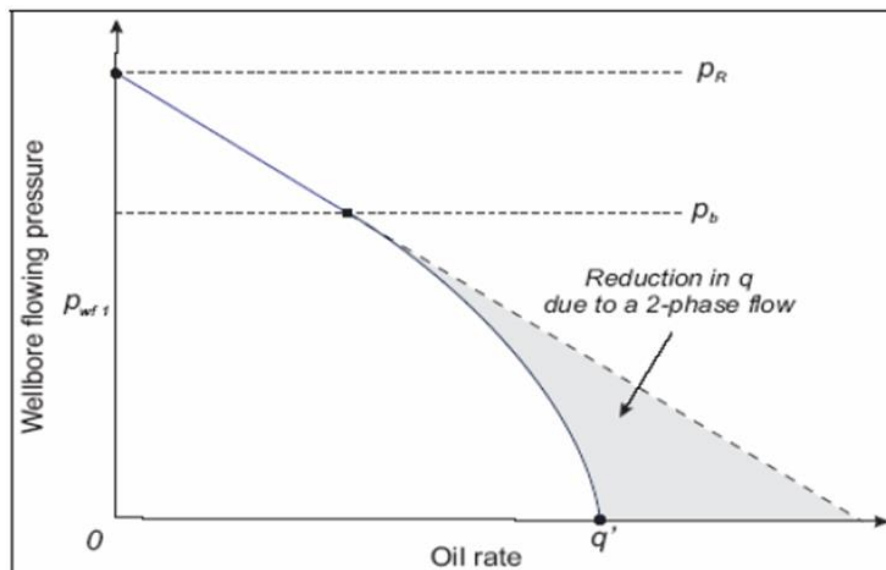


Figure II. 15: Inflow Performance Relationship. [5]

### II.7.2 Different equations of IPR curves for oil:

- Straight line IPR: Use for high permeability, single-phase flow, and early reservoir development.
- Vogel IPR: Use for reservoirs below bubble point pressure, moderate to low permeability, and primarily depletion drive reservoirs.

- Fetkovich IPR: Use for both gas and oil reservoirs, all stages of development, and reservoirs with varying flow regimes.

**Table II. 1:** Equations of IPR curves for oil. [8]

|                   |   |
|-------------------|---|
| Straight line IPR | $q = J * (P_{re} - P_{wf})$   |
| Vogel IPR         | $\frac{q_0}{q_{0,max}} = 1 - 0.2 \left( \frac{P_{wf}}{P_{re}} \right) - 0.8 \left( \frac{P_{wf}}{P_{re}} \right)^2$ |
| Fetkovich IPR     | $\frac{q}{q_{max}} = 1 - \left( \frac{P_{wf}}{P_{re}} \right)^2$  |

$q_{0,max}$ : Maximum incoming flow, corresponding to zero dynamic pressure ( $P_{wf}=0$ ) (AOF: absolute open flow).

$q_0$ : Incoming flow corresponding to  $P_{wf}$

## II.8 Hydrates problem in GL pipes in Hassi Messaoud region:

There are more than 500 wells on gas-lift activation in Hassi Messaoud region with a contribution of 40% of total production. Hydrates formation in the lift gas injection lines has caused significant production losses during winter months in Hassi-Messaoud field. These losses have taken place even with different techniques have been used to mitigate these problems.

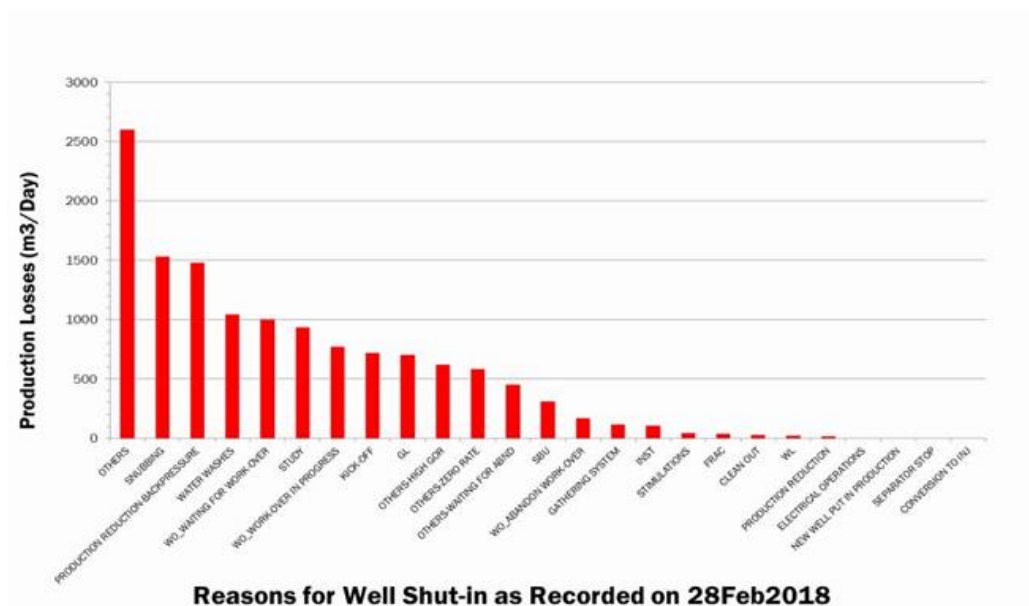


**Figure II. 16:** Production Losses Due to Shut-in for Variety of Reasons in HMD. [17]

## II.8.1 Reasons of Hydrates formation in GL pipelines:

**II.8.1.1 Joule-Thomson effect:** Joule-Thomson effect can be defined as the phenomenon of temperature change produced when a gas is allowed to expand adiabatically from a region of high pressure to a region of extremely low pressure.

This cooling of the gas is basically due to the decrease in the kinetic energy of the gaseous molecules as some part of this kinetic energy is utilized in overcoming intermolecular van der Waals force of attraction during expansion. [10]

**II.8.1.2 Gas-Lift Quality:** The gas used in the injection operation is not entirely clean due to the presence of moisture, impurities, or contaminants such as water vapor or hydrocarbons. As the gas passes through the GL choke valve, it undergoes adiabatic expansion, transitioning from a high-pressure to a low-pressure environment (Joule-Thomson effect). This expansion causes a significant temperature drop, rapidly freezing the contaminants and impurities in the gas, leading to the formation of hydrates inside the GL pipes. The low temperature slows the circulation of GL into the well, and the Hydrates formation inside the pipes blocks the gas flow through the choke valve and GL pipeline, negatively impacting the well's performance.

**II.8.1.3 GL and Continuous Water injection:** The simultaneous injection of water for desalting and gas through the CCE promotes Hydrates formation in the GL line and at the wellhead due to the low gas temperature and the presence of injected water. This results in severe issues such as the interruption of water and gas injection and the formation of salt deposits.



**Figure II. 17:** Example of Hydrates on Lift Gas Injection Line Downstream of Gas Lift Choke.

### II.8.2 Common techniques for Hydrates prevention:

There are several techniques available to prevent Hydrates phenomena in gas injection operations:

- Skid methanol injection: Methanol is injected to lower the freezing point of water, thereby preventing Hydrates formation.
- Injection of heated desalinated water: This method involves injecting heated water to maintain the temperature above the freezing point, preventing hydrates from forming.
- Glycol injection: Glycol is used as an antifreeze agent, mixing with water to lower its freezing point and inhibit Hydrates formation.
- Installing heat exchangers next to wellheads: Heat exchangers are installed near wellheads to transfer heat to the gas, ensuring it remains above the freezing point as it is injected. In the next chapter, heat exchangers will be discussed in greater details.

# Chapter III: Overview on heat exchangers and heat transfer principles



### III.1 Overview on Heat Transfer:

#### III.1.1 Definition:

Heat transfer is the study of heat flow, as the form of energy that can be transferred from one system to another as a result of temperature difference, the transfer of energy as heat is always from the hotter system to the colder system, and heat transfer stops when the two system reach the same temperature.

#### III.1.2 Modes of Heat transfer:

Heat can be transferred in three different modes:

##### Conduction:

Conduction is the transfer of thermal energy through a material or between materials that are in direct contact, in solid the mechanism of transferring the heat is through atomic vibrations or the movement of free electron while in liquids and gases it occurs through molecular collisions.

Conduction occurs more readily in solids, where the particles are closer together than in liquids and gases where particles are further apart.

The rate of heat conduction through a medium depends on the geometry of the medium, its thickness, and the material of the medium, as well as the temperature difference across the medium.

Fourier's Law is used to describe the conduction of heat in materials:

$$\frac{dQ}{dt} = -\lambda S \frac{dT}{dL} \quad (\text{III. 1})$$

- $dQ/dt$ : is the rate at which heat is transferred by conduction (W).
- $dT$ : Temperature change.
- $dL$ : Thickness of the material through which heat flux is passing.
- $S$ : Cross-sectional area through which heat flux is passing.
- $\lambda$ : Thermal conductivity coefficient of the material.

Fourier's law states that the negative gradient of temperature and the time rate of heat transfer is proportional to the area at right angles of that gradient through which the heat flows. [10]

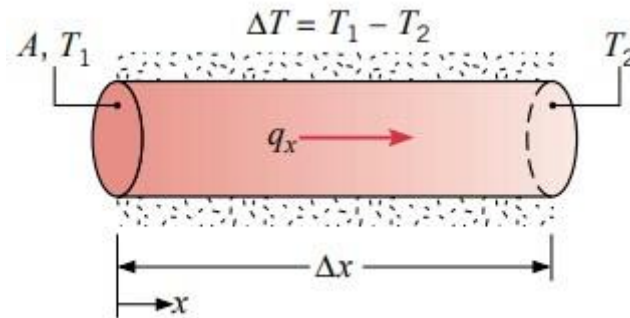


**Figure III. 1:** Conduction. [10]

### Convection:

Convection is the transfer of heat between a solid and a fluid, when the thermal energy being transmitted by the movement of the fluid. [11]

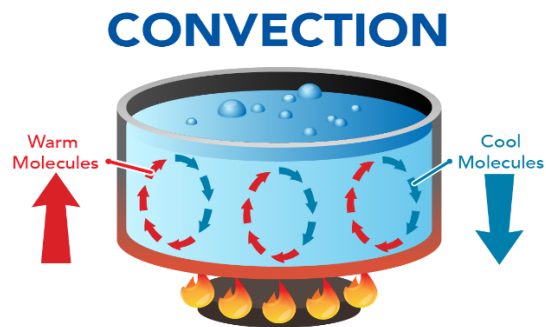


**Figure III. 2:** Convection. [11]

This transfer mechanism is described by Newton's law:

$$\frac{dQ}{dt} = hA(T - T_0) \quad (\text{III. 2})$$

Where:

- $dQ/dt$ : is the rate at which heat is transferred by convection (W)
- $h$ : is the convection heat-transfer coefficient ( $\text{W} \cdot \text{m}^{-2} \cdot ^\circ\text{C}^{-1}$ )
- $A$ : is the exposed surface area ( $\text{m}^2$ )
- $T$ : is the temperature of the immersed object ( $^\circ\text{C}$ )
- $T_0$ : is the temperature of the fluid which is under convection ( $^\circ\text{C}$ )

**Radiation:**

Heat transfer by radiation is the transfer of thermal energy between two surfaces at different temperature levels, in the absence of an intervening medium between them. This occurs due to electromagnetic waves emitted from a hot source.

The mechanism of heat flow by radiation consists three distinct phases, first by the conversion of thermal energy of the hot source into electromagnetic waves, then, the passage of wave motion through intervening space and finally transformation of waves into heat. [11]

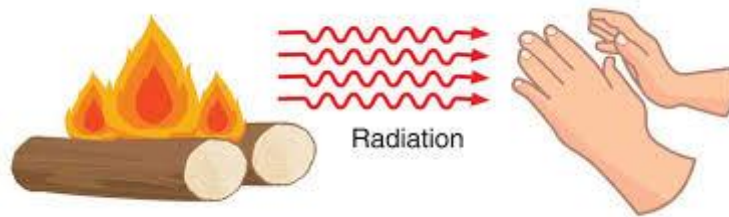


**Figure III. 3:** Radiation. [12]

The basic rate equation for radiation heat transfer is the Stefan Boltzmann law.

$$E_b = \sigma_b AT^4 \quad (\text{III. 3})$$

Where:

- $E_b$ : is the energy radiated per unit time.
- $T$ : the absolute temp of the surface.
- $\sigma_b$ : is the Stefan-Boltzmann constant ( $\sigma_b = 5.67 \times 10^{-8} \text{ W/m}^2\text{K}^4$ ).

**III.2 Heat Exchangers:**

Heat exchangers are devices that provide transfer of thermal energy between two or more fluids at different temperatures. Heat exchangers are used in a wide variety of application specifically in process industry.

**III.2.1 Heat exchanger classification:****III.2.1.1 Recuperators/regenerators:**

- Recuperative Heat Exchangers:

Heat is transferred indirectly through a separating wall or interface between the fluids.

➤ Regenerative Heat Exchangers:

Heat transfer occurs within a solid matrix, with one fluid storing heat while the other extracts it in alternating cycles. [12]

### III.2.1.2 Transfer processes:

➤ Direct contact:

Heat is transferred between the cold and hot fluids through direct contact between these fluids. There is no wall between the hot and cold streams, and the heat transfer occurs through the interface between the two streams.

➤ Indirect contact:

The heat is exchanged between hot and cold fluids through a heat transfer surface, a wall separating the two fluids. The cold and hot fluids flow simultaneously. [12]

### III.2.1.3 Geometry of Construction:

- Tubular Heat Exchanger (Double-Pipe, Shell and tube)
- Plate Heat Exchanger,
- Other types: Spiral heat exchanger, Compact heat exchanger. [12]

### III.2.1.4 Heat transfer mechanism:

- Single-phase convection on both sides.
- Single-phase convection on one side, two-phase convection on the other side.
- Two-phase convection on both sides. [12]

### III.2.1.5 Flow arrangement:

- Parallel Flow: Both fluids flow in the same direction, parallel to each other, within the heat exchanger.
- Counter flow: Fluids flow in opposite directions, enhancing heat transfer efficiency compared to parallel flow.
- Cross flow: Fluids flow perpendicular to each other, creating a crosswise flow pattern. This arrangement is common in plate heat exchangers.

- **Mixed flow:** When one of the fluids changes direction or flow direction several times relative to the other. This type of circulation actually represents a combination of the other three types. [12]

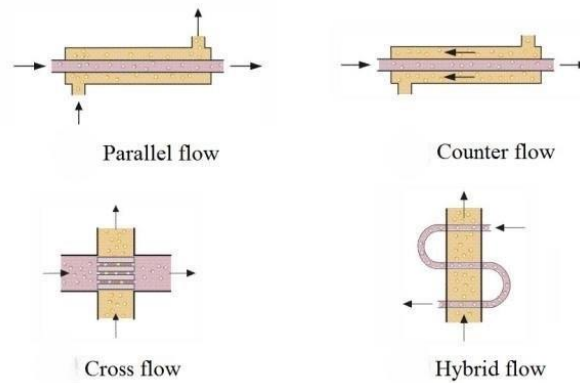


**Figure III. 4:** Flow types in heat exchangers. [12]

### III.2.1.6 Classification According to Phase of Fluids:

- Gas-liquid:** One fluid is in the gaseous phase and the other in the liquid phase. Common examples are radiators in vehicles, air coolers, and condensers in refrigeration systems.
- Liquide-liquid:** Both fluids are in the liquid phase. Examples include shell-and-tube heat exchangers, plate heat exchangers, and double-pipe heat exchangers used in process industries.
- Gas-gas:** In these heat exchangers, both fluids involved are in the gaseous phase. Examples include air-to-air heat exchangers used in ventilation systems and gas-to-gas heat recovery systems. [12]

## III.2.2 Heat exchanger types:

### III.2.2.1 Double pipe Heat Exchanger:

The simplest type of heat exchanger possible, consisting of just two concentric tubes, and appropriate end fittings to move the fluids from one section of the exchanger to the next. Additional double-pipe sections can be added in series or parallel to provide the required amount of heat transfer surface.

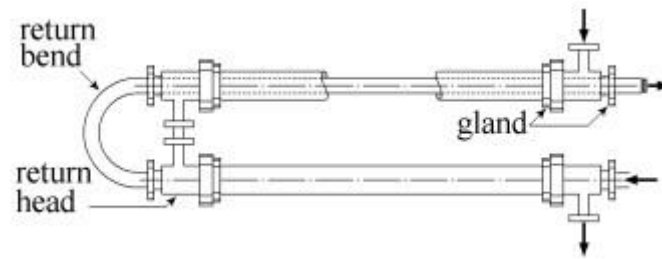


Figure III. 5: Double pipe Heat Exchanger. [12]

### III.2.2.2 Shell and tube heat exchanger:

Shell-and-tube heat exchangers are the most versatile type of heat exchangers. They are used in the process industries. They provide relatively large ratios of heat transfer area to volume and weight, and they can be easily cleaned. They offer great flexibility to meet almost any service requirement. Reliable design methods and shop facilities are available for their successful design and construction. [12]

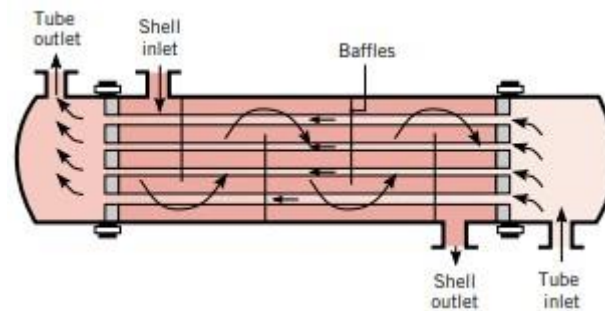
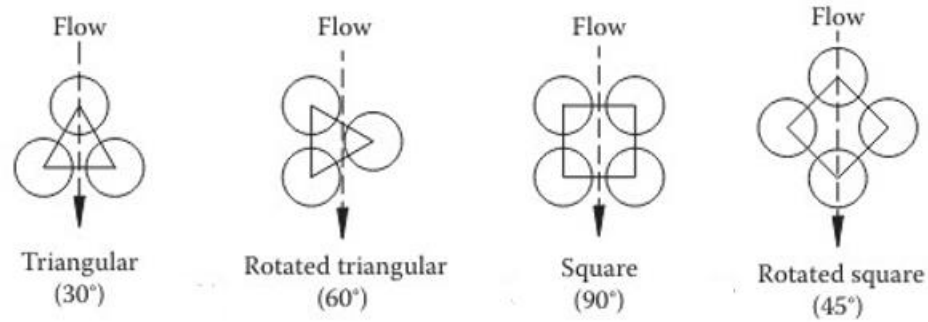


Figure III. 6: Shell and tube heat exchanger. [13]

#### ❖ Component of a shell and tube heat exchanger:

**Tubes:** Tubes are the primary components where heat exchange occurs. They carry one of the fluids through the exchanger. Commonly made of metals like steel, copper, or special alloys. Can be arranged in single or multiple passes to enhance heat transfer efficiency.

Tube arrangement in a shell and tube heat exchanger is crucial for determining the heat transfer efficiency and pressure drop of the system. In the next figure shown the common types of tube arrangements.



**Figure III. 7:** Tube arrangements in a shell and tube heat exchanger. [13]

**Baffles:** Baffles are plates or barriers installed inside the shell to direct the flow of the shell-side fluid across the tube's multiple times, enhance fluid turbulence and increase the heat transfer coefficient on the shell side its types include segmental, disc and doughnut, or helical baffles.

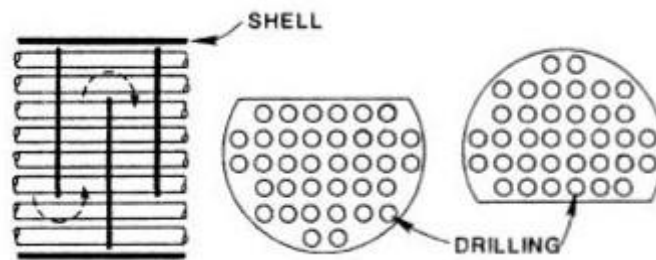


**Figure III. 8:** Baffle in shell and tube heat exchanger. [13]

**Shell:** The shell is the outer cylindrical vessel that houses the tube bundle and allows the shell-side fluid to flow around the tubes, usually made of metal.

**Front Head:** The front head is the component at the end of the heat exchanger where the tube side fluid enters the tubes. It also allows for easy access to the tubes for maintenance. Can be a channel with a removable cover, a bonnet (integral cover), or a channel integral with the tube sheet.

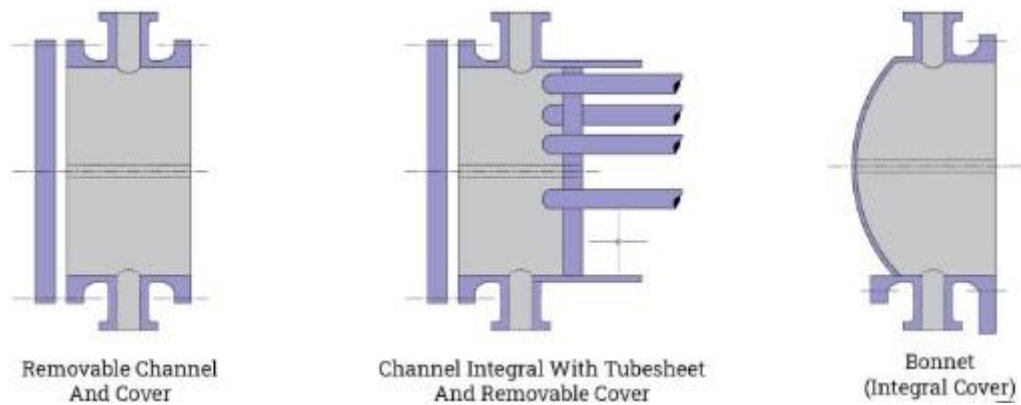


**Figure III. 9:** Front Heads in shell and tube heat exchanger. [13]

**Rear Head:** The rear head is located at the opposite end of the front head and allows the tube-side fluid to exit the tubes. It can also facilitate maintenance and cleaning. Can include fixed tube sheets, floating heads, or U-tubes.

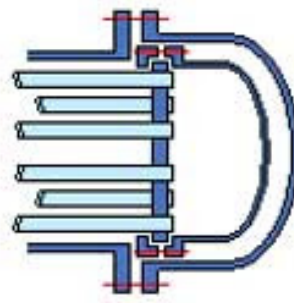


**Figure III. 10:** Rear Head in shell and tube heat exchanger. [13]

**Nozzles:** Nozzles are the inlet and outlet connections for both the shell-side and tube-side fluids. They are typically welded onto the shell and front/rear heads. They Provide access points for fluids to enter and exit the heat exchanger, ensuring a controlled flow rate and direction.

**TEMA Standard:** The Tubular Exchanger Manufacturers Association (TEMA) sets standards for the design, fabrication, and use of shell and tube heat exchangers. These standards ensure consistency, reliability, and safety in heat exchanger performance. [13]



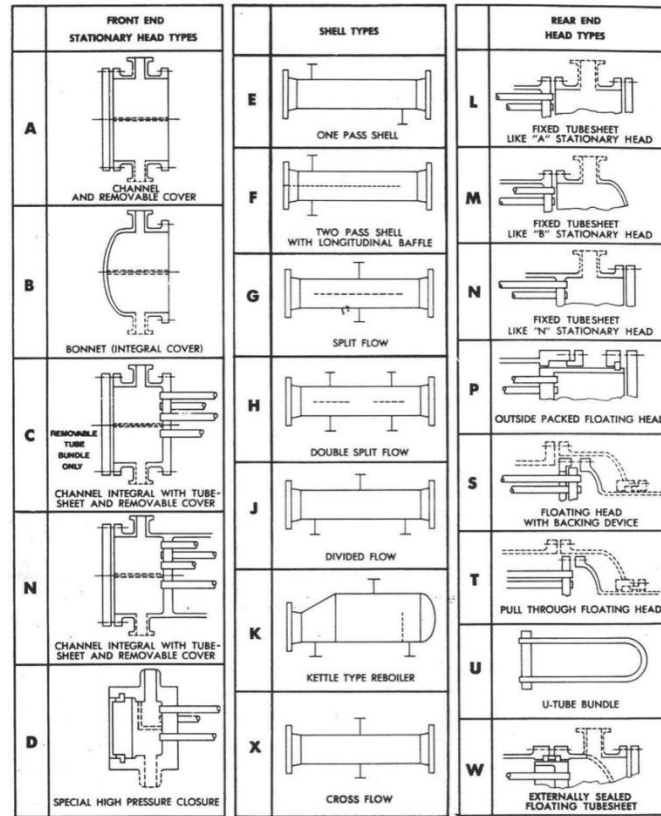


Figure III. 11: TEMA Standard. [13]

III.2.2.3 Plate Heat Exchanger:

A plate heat exchanger is usually comprised of a stack of corrugated or embossed metal plates in mutual contact, each plate having four apertures serving as inlet and outlet ports, and seals designed so as to direct the fluids in alternate flow passages.

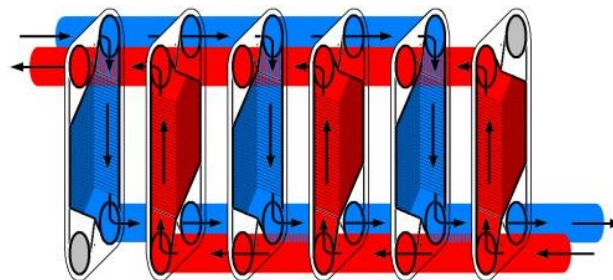


Figure III. 12: Plate Heat Exchanger. [13]

III.3 Kern method:

II.3.1 Introduction:

The thermal design of heat exchangers is directed to calculate an adequate surface area to handle the thermal duty for the given specification. The most common problem in heat exchanger design is the sizing problem, which is concerned with the determination of the dimensions of the heat exchanger.

In sizing, an appropriate heat exchanger type is selected and the size to meet the specified hot and cold fluid inlet and outlet temperatures, flow rates, and pressure drop requirements, is determined.

There are two methods for calculating and sizing heat exchangers:

- The analytical methods include DTLM method and the NUT method.
- The numerical methods include finite volume method and the enthalpy-temperature diagram method.

For the calculation of tubular or shell-and-tube heat exchangers, the mathematical analysis of the transfer becomes very complex. In fact, two main methods are used: Kern method (which we used in the study) and Donohue method. Those methods are included as representatives of the simple "integral" approach and, until recently, commonly used in the industry.

### III.3.2 Kern method basic calculation for Shell and tube exchanger:

The Kern method, which was an attempt to correlate data for standard exchangers by a simple equation analogous to equations for flow in heat exchanger. Although the Kern equation is not particularly accurate, it is widely used because of its simplicity and practicality, making it a valuable tool for preliminary design and performance estimation of shell-and-tube heat exchangers. [14]

This calculation method is based on the following data:

- ❖ The composition of the fluids.
- ❖ The flow rate of the fluids.
- ❖ The inlet and outlet conditions of the fluids.
- ❖ The physical properties of the fluids.

#### III.3.2.1 Calculation of the exchanged Heat Quantity:

$$Q_1 = \dot{M} C_{p_{crude}} (T_1 - T_2) \quad (\text{III. 4})$$

$$Q_2 = \dot{m} C p_{gas} (t_2 - t_1) \quad (\text{III. 5})$$

$$Q = Q_1 = Q_2$$

$$Q = \dot{m} C p_{gl} (t_2 - t_1) \quad (\text{III. 6})$$

$Q_1$ : Amount of heat lost by the hot fluid (kJ/h).

$Q_2$ : Amount of heat received by the cold fluid (kJ/h).

$\dot{M}$ : Heat loss flow rate of the hot fluid (kg/h).

$\dot{m}$ : Mass flow rate of the cold fluid (kg/h).

$C p_{gl}$ : Specific heat of GL “Cold fluid” (kJ / kg k°).

$C p_{crude}$ : Specific heat of Crude oil “Hot fluid” (kJ / kg k°).

$t_1$  : Temperature of cold fluid in (C°).

$t_2$  : Temperature of cold fluid out (C°).

$T_1$  : Temperature of hot fluid in (C°).

$T_2$  : Temperature of hot fluid out (C°).

$$C p_{gl} = \sum C p_i Y_i \quad (\text{III. 7})$$

$$\dot{m} = \frac{Q_{gl} * \rho_{gl}}{24} \quad (\text{III. 8})$$

$Y_i$ : Mass fraction of the gas components.

$C p_i$ : Specific heat of each constituent (J/kg k°).

$Q_{gl}$ : Volumetric flowrate of GL (m<sup>3</sup>/d).

$\rho_{gl}$ : Density of GL (kg/m<sup>3</sup>).

### III.3.2.2 Calculation of Log Mean Temperature Difference (DTLM):

The Logarithmic Mean Temperature Difference represents the logarithmic average of the temperature difference ( $\Delta T$ ) between the inlet and the outlet of the exchanger [°C].

$$\Delta T_{LM} = \frac{(T_1 - t_2) - (T_2 - t_1)}{\ln \frac{T_1 - t_2}{T_2 - t_1}} \quad (\text{III. 9})$$

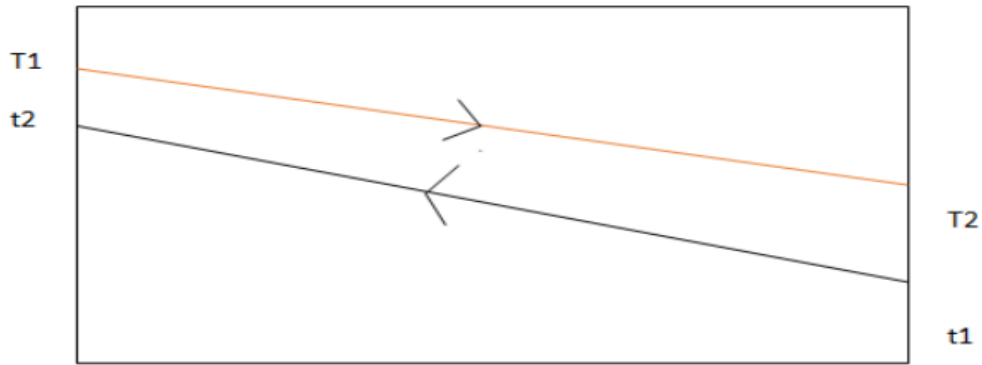


**Figure III. 13:** Hot and cold fluid's flow.

❖ **Correction of Log Mean Temperature Difference (DTLMC):**

$$\Delta T_{LMC} = \Delta T_{LM} * F \quad (\text{III. 10})$$

Where: F is determined from the graph  $F = f(R, E)$ : (Appendix)

$$R = \frac{T_1 - T_2}{t_2 - t_1} \quad (\text{III. 11})$$

$$E = \frac{t_2 - t_1}{T_1 - t_1} \quad (\text{III. 12})$$

**III.3.2.3 Calculation of the overall heat transfer coefficient  $U_s$ :**

$$U_s = \frac{1}{\frac{1}{h_i} + \frac{1}{h_o} + \frac{t_w}{\lambda_s}} \quad (\text{III. 13})$$

With:

$U_s$ : the overall heat transfer coefficient ( $\text{kJ/h m}^2 \text{K}^\circ$ ).

$h_i$ : the convective heat transfer coefficient on the inside (tube side) ( $\text{kJ/h m}^2 \text{K}^\circ$ ).

$h_o$ : the convective heat transfer coefficient on the outside (shell side) ( $\text{kJ/h m}^2 \text{K}^\circ$ ).

$t_w$ : the thickness of the tube wall (m).

$\lambda_s$ : thermal conductivity of the tube wall material (steel) =45 ( $\text{W/m K}^\circ$ ) (1 W = 0.239 Cal / S, 1S =  $2.7 \cdot 10^{-4}$ , 1 Cal = 4.18J)

❖ **Calculation of  $h_i$  (tube side):**

$$h_i = \frac{N_u * \lambda_{gl}}{d_i} \quad (\text{III. 14})$$

$d_i$ : Inside diameter of tube (m).

$\lambda_{gl}$ : Thermal conductivity of gas lift,  $\lambda_{gl} = 0.108$  (kj/h.m.k°).

$N_u$ : Nusselt number.

$$N_u = 0.021R_e^{0.8}P_r^{0.43} \quad (\text{III. 15})$$

$R_e$ : Number of Reynolds.

$P_r$ : Prandtl number.

$$R_e = \frac{W*d_i}{\mu_g} \quad (\text{III. 16})$$

$W$ : Fluid mass velocity (kg/h m<sup>2</sup>).

$\mu_g$ : Gas dynamic viscosity ( $\mu_g = 0.125$  kg/h m).

$$W = \frac{\dot{m}}{S_c} \quad (\text{III. 17})$$

$S_c$ : Passage section of fluid (m<sup>2</sup>)

$$P_r = \frac{Cp_{gl}*\mu_g}{\lambda_{gl}} \quad (\text{III. 18})$$

#### ❖ Calculation of $h_o$ (shell side):

$$h_o = \frac{N_u*\lambda_m}{D_{eq}} \quad (\text{III. 19})$$

$D_{eq}$ : Equivalent diameter (m<sup>2</sup>).

$$\Delta S_c = \frac{\pi D_{eq}^2}{4} = \left( \frac{\pi D_i^2}{4} \right) - \left( \frac{n*\pi d_o^2}{4} \right) \quad (\text{III. 20})$$

$D_i$ : Inner diameter shell side (m<sup>2</sup>).

$d_o$ : outer diameter tube side (m<sup>2</sup>).

$n$ : Total number of tubes.

$$N_u = 0.021R_e^{0.8}P_r^{0.43} \quad (\text{III. 21})$$

$$R_e = \frac{W*D_{eq}}{\mu_m} \quad (\text{III. 22})$$

$$W = \frac{\dot{M}_{(o+w+g)}}{\Delta S_c} \quad (\text{III. 23})$$

$\dot{M}_{(o+w+g)}$ : Mass flow rate in shell side (kg/h).

$$\mu_m = \sum \mu_i X_i = \mu_o X_o + \mu_w X_w + \mu_g X_g \quad (\text{III. 24})$$

$\mu_m$ : Shell side overall dynamic viscosity (kg/h m).

$\mu_i$ : Dynamic viscosity of each fluid (Water, Oil, Gas) (kg/h m).

$X_i$ : Volumic fraction of each fluid (Water, Oil, Gas).

$$Cp_m = \sum Cp_i X_i = Cp_o X_o + Cp_w X_w + Cp_g X_g \quad (\text{III. 25})$$

$Cp_m$ : Overall specific heat in shell side (J/kg k°)

$Cp_i$ : Specific heat of each fluid (Water, Oil, Gas) (J/kg k°)

$$\lambda_m = \sum \lambda_i X_i = \lambda_o X_o + \lambda_w X_w + \lambda_g X_g \quad (\text{III. 26})$$

$\lambda_m$ : Overall thermal conductivity in shell side (kj/h.m.k°).

$\lambda_i$ : Thermal conductivity of each fluid in shell side (kj/h.m.k°).

$$P_r = \frac{Cp_m \mu_m}{\lambda_m} \quad (\text{III. 27})$$

#### III.3.2.4 Calculation of the heat exchange area:

$$A_{cal} = \frac{Q}{U_s \Delta T_{LM}} \quad (\text{III. 28})$$

#### III.3.2.5 Calculation of the available heat exchange area:

$$A_{ava} = \pi d_o l \quad (\text{III. 29})$$

# Chapter IV: Practical part

### IV.1 Problematic:

In Hassi Messoud, over 520 wells are activated by gas lift, contributing 40% to the region's overall production. For these wells to operate at optimal flow rates, gas lift parameters need to be optimized for each well. The relationship between production rate and Gas-Lift Injection (GLI) rate is critical (Figure IV.1), as maintaining the GLI at an optimal value is essential for efficient production.

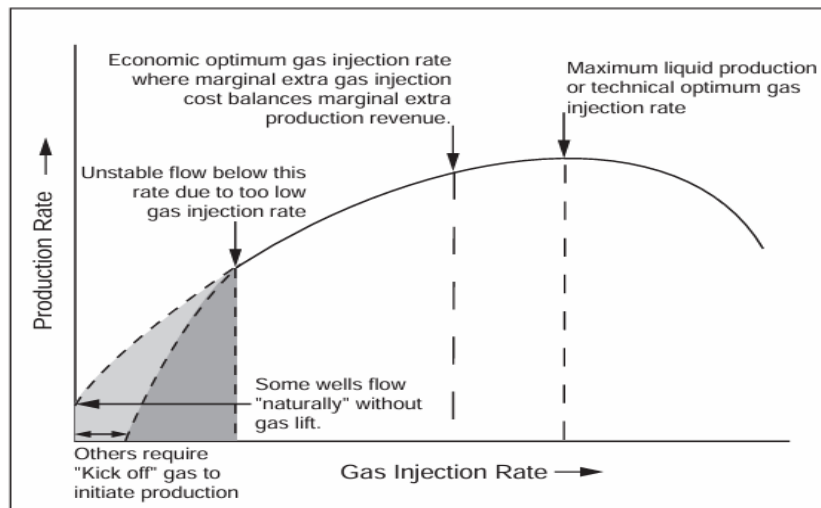


**Figure IV. 1:** Effect of gas rate on well production. [5]

A significant issue faced by gas lift-activated wells is Hydrates in the GL lines, especially during winter. Wells with double injection (gas and water) are particularly affected due to the contact between cold gas and water at the wellhead, as well as the presence of impurities and water in the gas composition. With the presence of the hydrates and Hydrates formation temperature and pressure conditions, water in GL or from the desalting operation to freeze instantly. Hydrates can stall the GL flow or completely block the GL line and wellhead, negatively impacting the well production rate, with an estimated decrease of approximately 400 tons per day.

A common method to minimize Hydrates in Hassi Messoud is increasing the GLI flow rate. While this approach is somewhat effective, it does not solve the issue entirely and is impractical because increasing the GL flow rate deviates from the optimal GLI, leading to a loss in production, waste of gas, and surface problems (Figure IV.1).



Several solutions were tested by DP-HMD to overcome this problem, such as using methanol skids, but without success. This led to the study of sizing a heat exchanger that utilizes the heat from the crude oil to warm the gas lift line before injecting the gas into the wellbore.

The exchanger was tested on 15 wells during the winter period, with 14 wells showing a high success rate.

| DP-Hassi Messaoud   |         | Saison Hivernale 2021-22<br>Avant Echangeur |                     | Saison Hivernale 2022-23<br>Après Echangeur |                     |                             |                           |                                       |                               |
|---------------------|---------|---|---------------------|---|---------------------|-----------------------------|---------------------------|---------------------------------------|-------------------------------|
| Champ               | Puits   | Fréquence                                   | Temps d'arrêt (hrs) | Fréquence                                   | Temps d'arrêt (hrs) | Gain en disponibilité (hrs) | Gain en disponibilité (%) | Gain en nombre d'intervention (ΔFreq) | Gain estimé en Production (T) |
| NORD                | OMIZ633 | 41  | 352,16              | 15  | 123,59              | 228,57                      | 65%                       | 26                                    | 481                           |
| NORD                | OMGZ81  | 17  | 127,32              | 2   | 18,67               | 108,65                      | 85%                       | 15                                    | 335                           |
| NORD                | OMGZ801 | 28  | 205,83              | 33  | 252,01              | -46,18                      | -22%                      | -5                                    | -66                           |
| NORD                | OMKZ15  | 25  | 177,42              | 10  | 98,99               | 78,43                       | 44%                       | 15                                    | 215                           |
| NORD                | ONI551  | 29  | 288,99              | 9   | 87,32               | 201,67                      | 70%                       | 20                                    | 328                           |
| SUD                 | ONMZ201 | 15  | 128,6               | 0   | 0                   | 128,6                       | 100%                      | 15                                    | 390                           |
| SUD                 | MD660   | 10  | 80,41               | 1   | 10,5                | 69,91                       | 87%                       | 9                                     | 287                           |
| SUD                 | MD420   | 34  | 257,65              | 2   | 17,33               | 240,32                      | 93%                       | 32                                    | 367                           |
| SUD                 | MD179   | 26  | 249,92              | 3   | 12,67               | 237,25                      | 95%                       | 23                                    | 171                           |
| SUD                 | MD322   | 12  | 102,84              | 0   | 0                   | 102,84                      | 100%                      | 12                                    | 263                           |
| NORD                | ONMZ513 | 19  | 149,99              | 5   | 43,34               | 106,65                      | 71%                       | 14                                    | 149                           |
| NORD                | OMKZ103 | 13  | 80,57               | 3   | 28,75               | 51,82                       | 64%                       | 10                                    | 143                           |
| SUD                 | MDZ717  | 5   | 44,42               | 4   | 38,51               | 5,91                        | 13%                       | 1                                     | 31                            |
| SUD                 | ONM61   | 18  | 135,24              | 5   | 39,16               | 96,08                       | 71%                       | 13                                    | 61                            |
| NORD                | OMNZ102 | 4   | 35,92               | 3   | 21,17               | 14,75                       | 41%                       | 1                                     | 39                            |
| Total               |         |   |                     |   |                     |                             |                           | 201                                   | 3194                          |
|                     |         | Fréquence                                   | Temps d'arrêt (hrs) | Fréquence                                   | Temps d'arrêt (hrs) | Gain en disponibilité (hrs) | Gain en disponibilité (%) |                                       |                               |
| Moyenne (par puits) |         | 19,73                                       | 161,15              | 6,33  | 52,80               | 108,35                      | 67%                       |                                       |                               |

**Figure IV. 2:** Analysis of the first phase of 15 wells with heat exchanger DP-HMD. [15]

The experience with the OMGZ801 well, however, was not successful for the following reasons:

- The well does not produce in a stable flow regime.
- The performance of the well negatively influences the performance of the exchanger (the well is exposed to wellbore problems).
- The well is probably within the temperature limit necessary to avoid Hydrates.

Figure IV.2 shows that only two wells (MD322 and ONMZ201) achieved 100% availability with zero downtime due to Hydrates. The other 11 wells showed improvements in availability, but downtime due to Hydrates was not completely eliminated. According to DP-HMD, the minimum crude oil temperature required for the exchanger to be effective is 28°C.

In this chapter, we investigate the performance of the exchanger constructed by EP-HMD in preventing Hydrates by conducting a case study on the least successful well MDZ717 (with 13% gain in availability) and explore ways to increase its availability for optimal production conditions, by using Kern method and Aspen HYSYS tools.

To conduct this study, we designed an exchanger model using Exchanger Design & Rating (EDR) very similar to the exchanger in DP-HMD, and we compared its performance to our proposed heat exchanger model.

This chapter has two parts:

- ✓ Part 1: We use PIPESIM software to model and optimize the gas lift injection rate of well MDZ717.
- ✓ Part 2: We investigate the effectiveness of the exchanger in preventing Hydrates under optimal well conditions using two tools: the Kern method and Aspen HYSYS software. Additionally, we use HYSYS simulation and EDR to enhance Hydrates elimination by designing our proposed model and comparing the results of the two exchangers.

## **Part One: Gas lift injection rate optimization with PIPESIM (case study MDZ717)**

### **IV.2 Overview about PIPESIM Software:**

PIPESIM was originally developed by a company called Baker Jardine. Baker Jardine was formed in 1985 to provide software and consulting services to the oil and gas industry. In April 2001, Baker Jardine was acquired by Schlumberger.

Schlumberger has invested in the redevelopment of the industry's leading Production Engineering software to ensure that it can solve challenging multiphase flow problems. PIPESIM couples a leading-edge Graphical User Interface with a field-proven computation engine.

PIPESIM offers a wide-ranging capability for modelling entire production systems from the reservoir to the processing facility, such as: [18]

- Well Performance analysis
- Pipeline and Facilities
- Network analysis module.

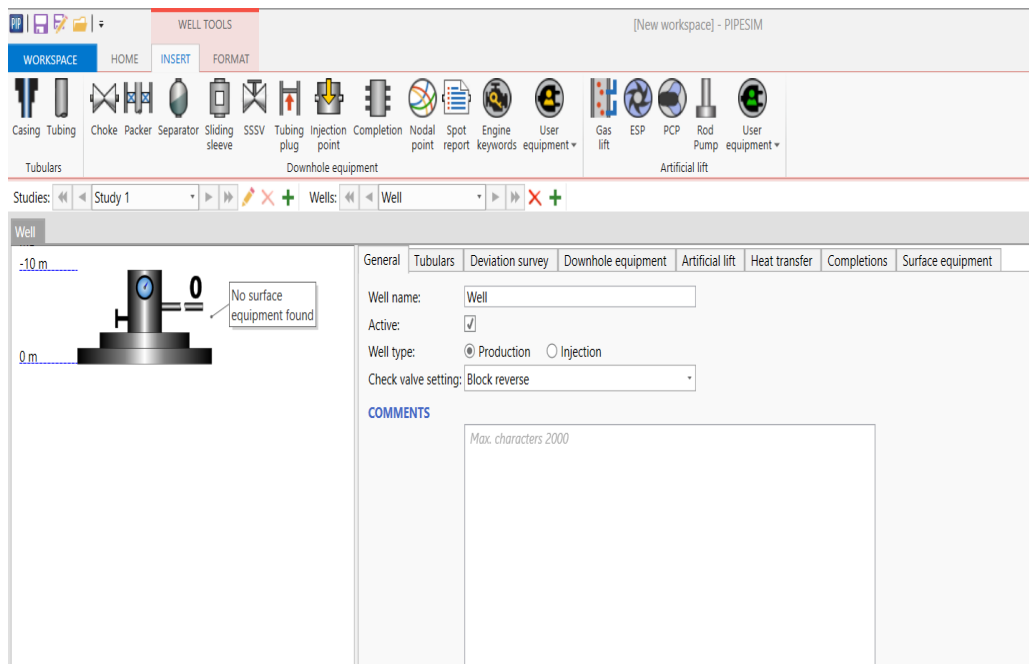


**Figure IV. 3:** PIPESIM 2020.1 window

### IV.3 Well Modelling:

This part contains the steps of modelling MDZ717 well using PIPESIM, this modelling will allow us to optimize the performance of the well by optimizing GL parameters such as injection flowrate. Several data points are required to build the model and achieve optimization.

**Table IV. 1:** General Information about MDZ717.

|                      |                             |
|----------------------|-----------------------------|
| <i>Well</i>          | MDZ717                      |
| <i>Zone</i>          | HZS                         |
| <i>Drilling date</i> | 09/12/2018                  |
| <i>Coordinates</i>   | X: 808741.906 Y: 111858.329 |
| <i>Situation</i>     | GAS LIFT (31/08/2021)       |
| <i>Status</i>        | Open                        |

### IV.3.1 Well model construction:

In the general tap of PIPESIM, the well name and type (production or injection) can be entered.

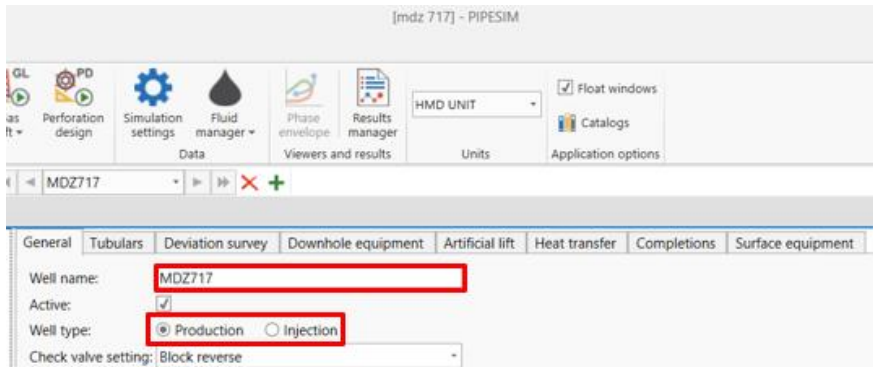


Figure IV. 4: Well name and type.

### IV.3.2 Tubulars:

In the Tubulars tab, completion of the well can be inputted, such as: Casing, Tubing, inside and outside diameters, Measured Depth...etc (Appendix). the well MDZ717 has a 7” casing, 7” liner, 4”1/2 tubing and 1”660 CCE, therefor, to determine the fluid passage, the equivalent diameter was calculated and found to be 2.78 inch.

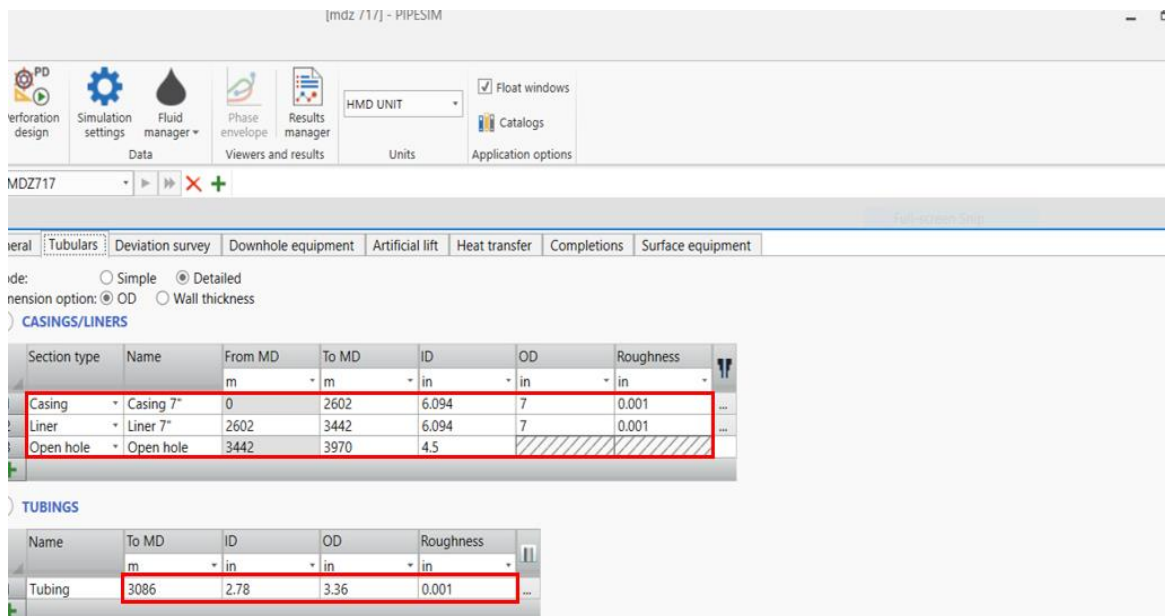


Figure IV. 5: Tubulars and Completion.

### IV.3.3 Trajectory and Depth:

In the Deviation survey tab, measured depth (MD) and Total Vertical Depth (TVD) were inserted (Appendix).

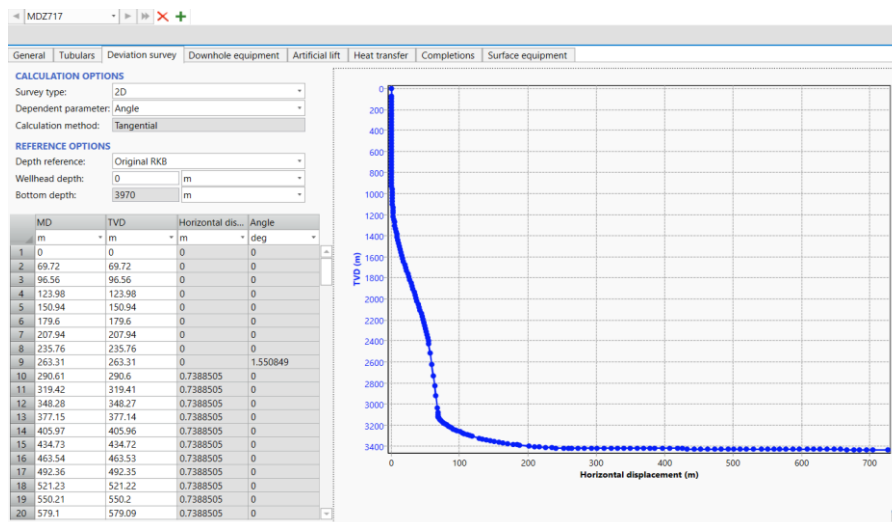


Figure IV. 6: Trajectory and Depth.

### IV.3.4 Downhole equipment:

The downhole equipment can be inserted in the downhole equipment tab along with the node point.

| Equipment | Name   | Active                              | MD   |
|-----------|--------|-------------------------------------|------|
| 1         | Packer | <input checked="" type="checkbox"/> | 3086 |
| 2         | NA     | <input checked="" type="checkbox"/> | 3442 |

Figure IV. 7: Downhole equipment.

### IV.3.5 Artificial Lift:

in the Artificial lift tab, either gas lift or pump lift can be inserted. MDZ717 is a GL activated so “GAS LIFT” option is selected. Gas lift valve is put in the deepest injection point.

General | Tubulars | Deviation survey | Downhole equipment | Artificial lift | Heat transfer | Completions | Surface equipment

**GAS LIFT**

Injection option:  Fixed injection ports  Injection valve system  
 Alhanati stability check:

| Gas lift | Active                              | MD   | Injection basis | Inj. quantity | Injection unit     | Port size |
|----------|-------------------------------------|------|-----------------|---------------|--------------------|-----------|
| 1        | <input checked="" type="checkbox"/> | 3085 | Injection g...  | 0             | sm <sup>3</sup> /d | 1         |

**GAS PROPERTIES**

Gas specific gravity:  Specify  Use fluid model

**PUMP LIFT**

| Equipment | Name | Active | MD |
|-----------|------|--------|----|
|           |      |        | m  |

Figure IV. 8: Artificial Lift.

### IV.3.6 Heat transfer:

Well head and wellbore temperature are set in the Heat transfer tab along with the Heat transfer coefficient  $U = 8 \text{ Btu}/(\text{h} \cdot \text{degF} \cdot \text{ft}^2)$ .

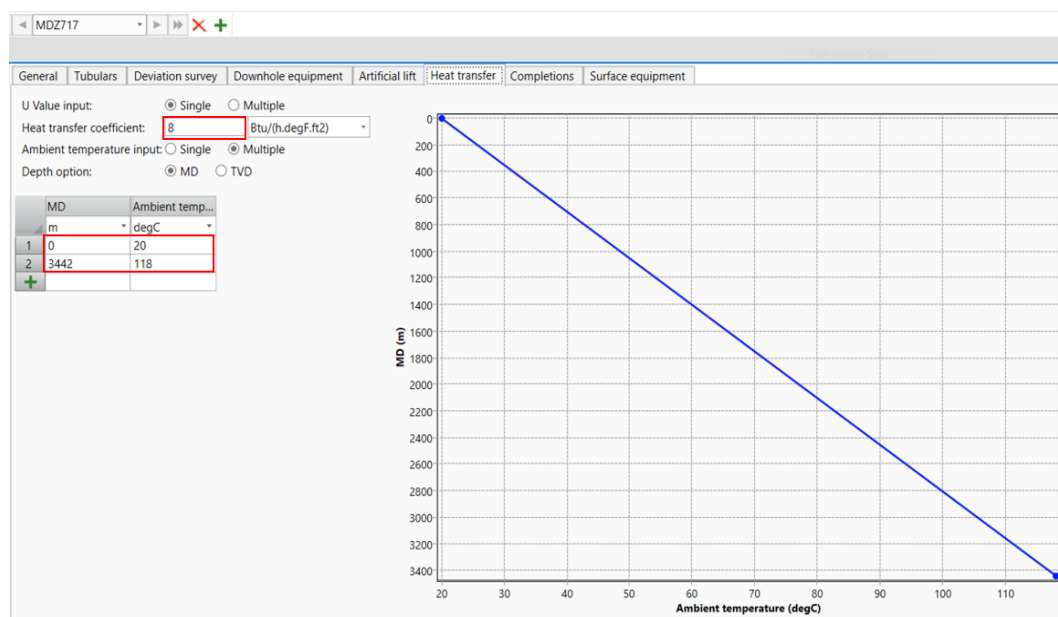


Figure IV. 9: PIPESIM heat transfer tab.

### IV.3.7 Reservoir data:

In this part, perforation, reservoir pressure and PI should be inserted, we set temporarily  $PI = 1$  ( $\text{Sm}^3/\text{d} \cdot \text{bar}$ ) and it will be determined later after selecting a representative gauging date because the Flowing Wellbore Pressure in MDZ717 well tests were not measured.

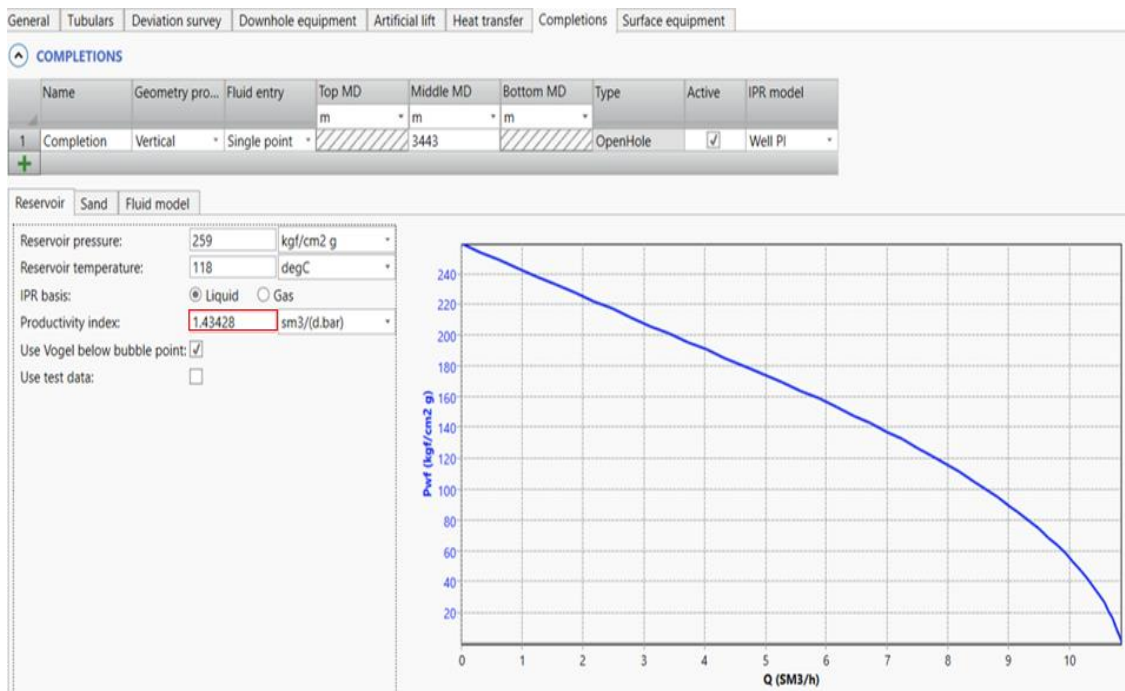


Figure IV. 10: Reservoir data.

### IV.3.8 PVT data:

In the “Fluid model” window, a fluid model can be created using the PVT data of the well, the fluid model represents the properties of fluids.

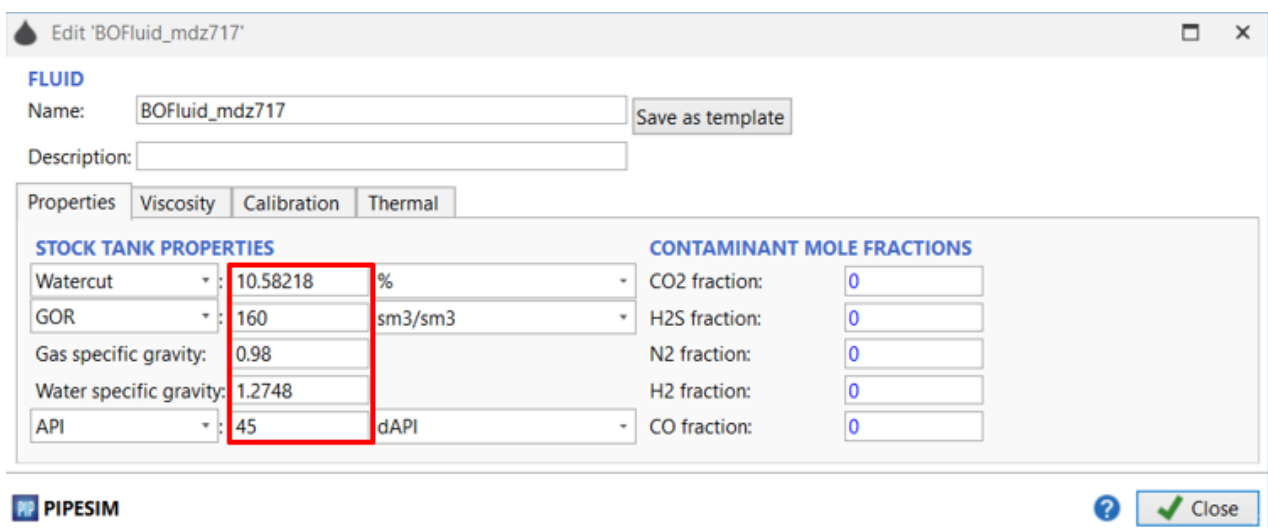


Figure IV. 11: PVT data.

### IV.3.9 Surface equipment:

In this window, surface equipment can be selected, well choke is set on 16mm diameter and the discharge coefficient. The pipeline is represented with the flowline up to the separator (point J).

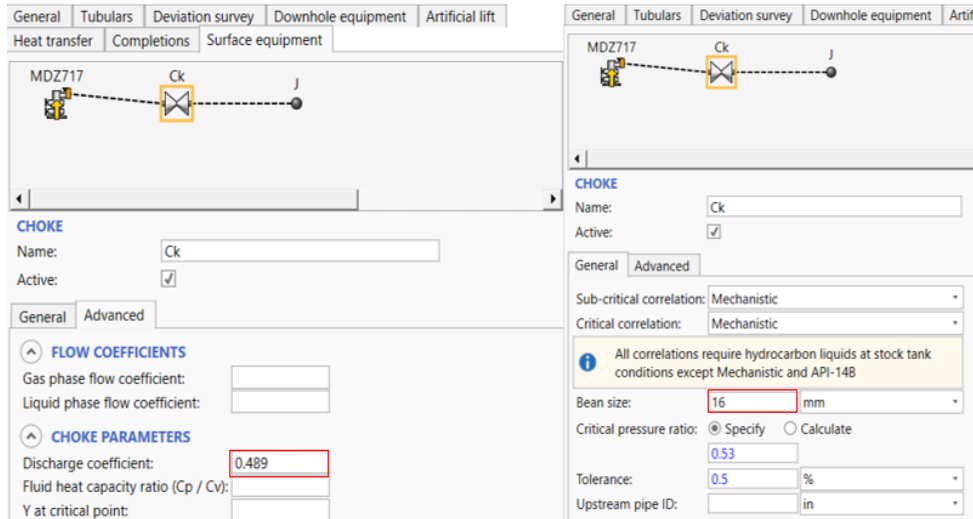


Figure IV. 12: Surface Equipment.

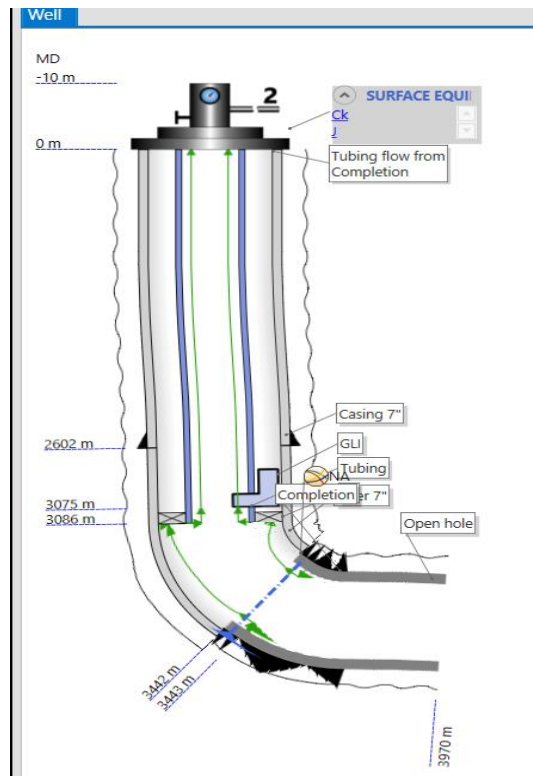


Figure IV. 13: MDZ717 PIPESIM model.



#### IV.4 Estimation of Productivity Index PI and Discharge Coefficient $C_d$ :

The productivity index is crucial for understanding the well's capability to produce fluids under varying pressure conditions, while the discharge coefficient helps in evaluating the efficiency of fluid flow through the wellbore and surface equipment.

The absence of Flowing wellbore pressure in the well tests makes us use an indirect method to find the PI value. We have to estimate the productivity index (PI) then discharge coefficient ( $C_d$ ) from the last 6 gauging measurements.

**Hagedorn & Brown** correlation is the used correlation in HMD region in PIPESIM, with it we can find reasonable PI and  $C_d$  values. To achieve accurate and reliable estimates, we need to select the most representative gauging data. By doing so, we can ensure that our estimations reflect the true performance of the well, leading to better optimization of the GLI rate.

##### IV.4.1 Calculation of GL injection flowrates:

Not all the GL injecting flowrate were measured in the gauging data, therefor, the missing injecting flow rate were calculated.

**Table IV. 2:** Gauging of well MDZ717.

| Measurement date | Bean size (mm) | Flowrate (m <sup>3</sup> /h) |         | Pressure (kg/cm <sup>2</sup> ) |             |              | GL Parameters       |                 |                    | Water flowrate (l/h) |          | Liquid Flow rate (m <sup>3</sup> /h) |
|------------------|----------------|------------------------------|---------|--------------------------------|-------------|--------------|---------------------|-----------------|--------------------|----------------------|----------|--------------------------------------|
|                  |                | Oil                          | Gas     | Wellhead Press                 | Pipe. Press | Separ. Press | Press. Reseau (Bar) | Inj press (Bar) | GL Flowrate (M3/J) | Recovered            | Injected |                                      |
| 5/25/2023        | 16             | 5.29                         | 2907.85 | 39.8                           | 16.2        | 16.39        | 208                 | 110             | 31392              | 730                  | -        | 6.02                                 |
| 8/26/2023        | 16             | 1.25                         | 2561.88 | 25.5                           | 15.3        | 5.52         | -                   | -               | 35841              | 250                  | -        | 1.5                                  |
| 9/22/2023        | 16             | 4.4                          | 2721.84 | 33.2                           | 15          | 15.08        | 200                 | 74              | 26940              | 630                  | -        | 5.03                                 |
| 9/23/2023        | 16             | 4.56                         | 3131.98 | 36.3                           | 15.1        | 15.21        | 203                 | 77              | 34279              | 460                  | -        | 5.02                                 |
| 1/9/2024         | 16             | 6.55                         | 2444.76 | 34.6                           | 18.8        | 18.71        | 205                 | 60              | 12504.6            | 488                  | -        | 7.038                                |
| 2/18/2024        | 16             | 5.56                         | 2559.35 | 35.3                           | 14.7        | 14.68        | -                   | -               | 19186.44           | 658                  | -        | 6.218                                |

**Table IV. 3:** PVT data of the well MDZ717.

| <b>PVT Data</b>           |                |                                  |
|---------------------------|----------------|----------------------------------|
| Oil API Gravity           | 45             | API                              |
| Oil Specific Gravity      | 0.8017         |                                  |
| Gas Specific Gravity      | 0.98           | 0.793                            |
| Water Salinity            | 350,000        | ppm                              |
| Water Gravity             | 1.2748         |                                  |
|                           |                |                                  |
| RS at Saturation Pressure | <b>160</b>     | Sm <sup>3</sup> /Sm <sup>3</sup> |
|                           |                |                                  |
| Fluid Model               | Black Oil      |                                  |
|                           |                |                                  |
| <b>Laboratory Data</b>    |                |                                  |
| Saturation Pressure       | <b>153.966</b> | kg/cm <sup>2</sup> _g            |
| Temperature               | 118            | °C                               |

**IV.4.2 Calculation of water cut:**

Water cut influences the liquid flow rate values, so taking into consideration the quantity of water produced is important for accurate results.

**Table IV. 4:** Calculated water cut percentages.

| <b>Measurement date</b> | <b>Water Cut %</b> |
|-------------------------|--------------------|
| 5/25/2023               | 12.12624585        |
| 8/26/2023               | 16.66666667        |
| 9/22/2023               | 12.52485089        |
| 9/23/2023               | 9.163346614        |
| 1/9/2024                | 6.933788008        |
| 2/18/2024               | 10.58218077        |

The water cut value to be included in the Fluid model will be determined after finding a reliable gauging data.

### IV.4.3 PI Evaluation:

In the system analysis tab, liquid PI is estimated based on the wellhead pressure of each gauging date with the variables: Water cut, Liquid flowrate and GL flowrate of the last 6 gauging.

With the last 6 gauging, the PIPESIM shows us the evolution of the PI (Table IV.5). This allows us to understand the behaviour of the well through the different interventions carried out there.

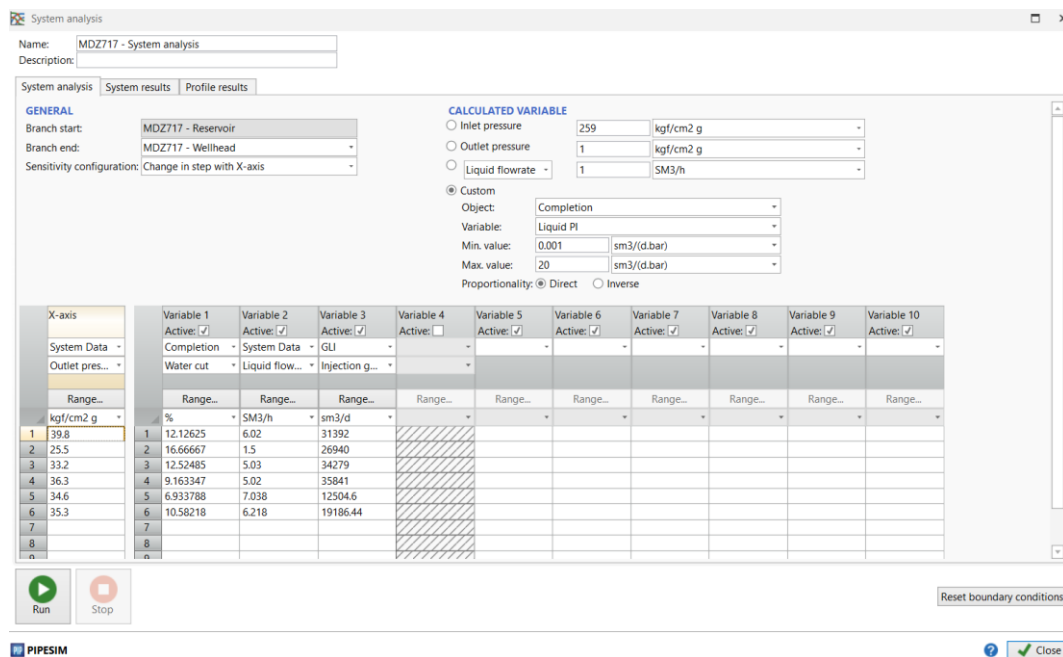
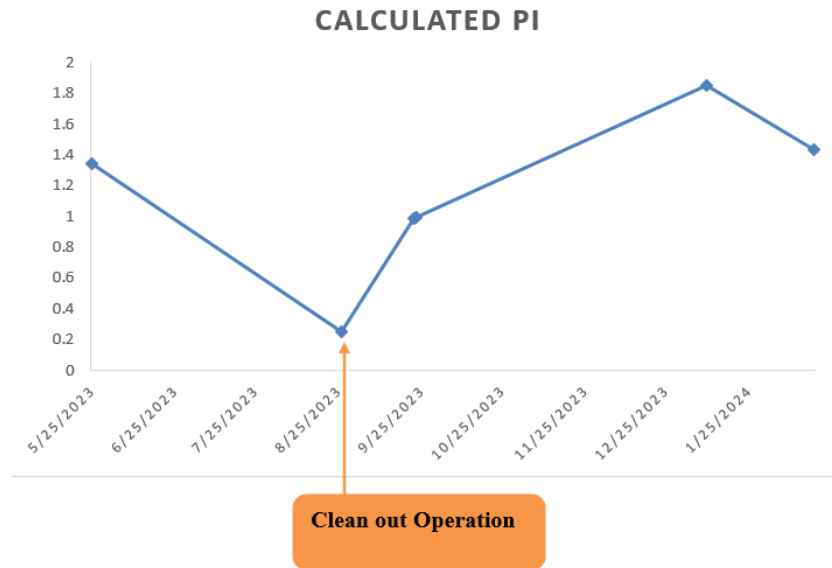


Figure IV. 14: Liquid PI estimation inputs.

Table IV. 5: Liquid PI results.

| Measurement date | $P_{wh}$ (kg/cm <sup>2</sup> ) | Liquid Flow (m <sup>3</sup> /h) | Liquid PI (Sm <sup>3</sup> /d.bar) |
|------------------|--------------------------------|---------------------------------|------------------------------------|
| 5/25/2023        | 39.80035                       | 6.02                            | 1.339737                           |
| 8/26/2023        | 25.49992                       | 1.5                             | 0.2513448                          |
| 9/22/2023        | 33.19993                       | 5.03                            | 0.986932                           |
| 9/23/2023        | 36.29977                       | 5.02                            | 0.9961556                          |
| 1/9/2024         | 34.59974                       | 7.038                           | 1.853956                           |
| 2/18/2024        | 35.3                           | 6.218                           | 1.43428                            |



**Figure IV. 15:** PI Evaluation MDZ717.

Figure IV.15 shows that there is a diminution in PI from the first to the second gauging. After the second gauging, well history indicates a Clean out operation around the 2<sup>nd</sup> and 3<sup>rd</sup> gauging dates, which explains why PI value starts to increase reaching a max value on the 5<sup>th</sup> gauging, meaning that the well is stimulated at that value. The decrease of PI is then related to an asphaltene deposition. [16]

The PI for gauging 2 (0.2513448) stands out as an outlier being significantly lower as well as gauging number 5 (1.853956) which is significantly high, thus, suggesting an inconsistency or error in that measurement.

#### IV.4.4 Discharge coefficient Evaluation:

The discharge coefficient ( $C_d$ ) is a dimensionless number that characterizes the efficiency of fluid flow through the choke valve. It quantifies how well the actual flow rate matches the theoretical flow rate, accounting for factors such as friction, turbulence, and flow separation that cause deviations from ideal conditions.

In the system analysis tab,  $C_d$  is estimated based on the pipeline pressure of each gauging date with the variables: Water cut, Liquid flowrate, GL flowrate and Productivity index of the last 6 gauging.

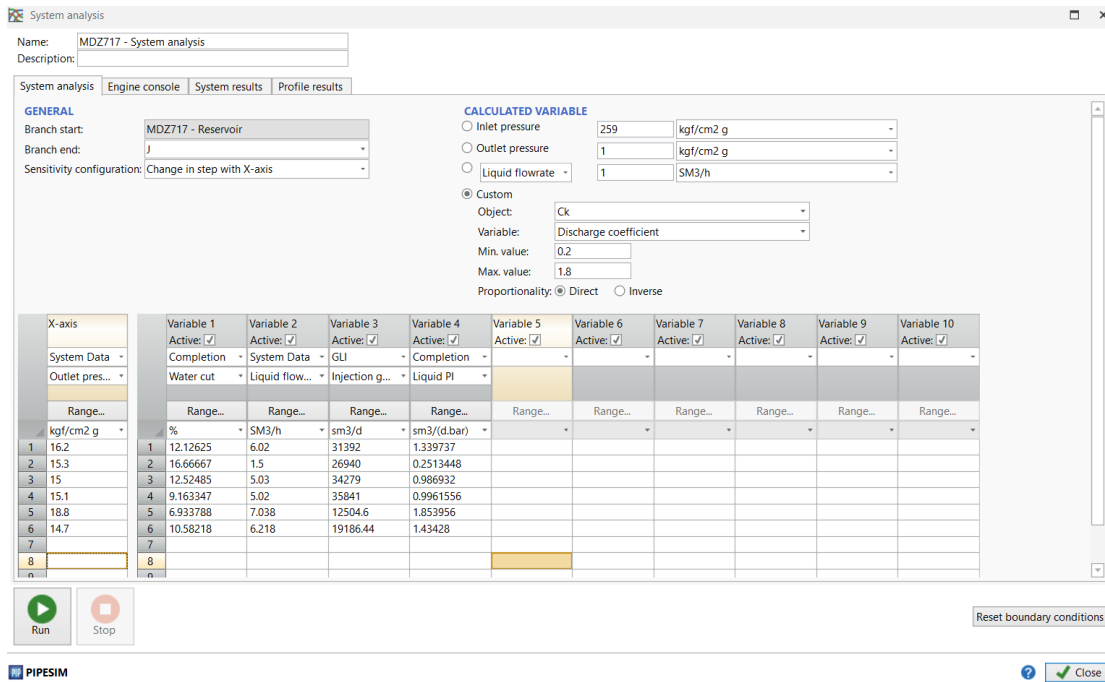


Figure IV. 16: Discharge coefficient estimation inputs.

Table IV. 6: Discharge coefficient results.

|   | Measurement date | Pipe press (kg/cm <sup>2</sup> ) | C <sub>d</sub> |
|---|------------------|----------------------------------|----------------|
| 1 | 5/25/2023        | 16.19971                         | 0.502          |
| 2 | 8/26/2023        | 15.29978                         | 0.399          |
| 3 | 9/22/2023        | 15.00027                         | 0.562          |
| 4 | 9/23/2023        | 15.10011                         | 0.525          |
| 5 | 1/9/2024         | 18.79966                         | 0.501          |
| 6 | 2/18/2024        | 14.70006                         | 0.489          |

From table IV.6, the most consistent C<sub>d</sub> values, those close to each other, are found in gauging 1 (0.502), 5 (0.501), and 6 (0.489). The C<sub>d</sub> values for gauging 2 (0.399) and 3 (0.562) are outliers, indicating potential measurement or flow inconsistencies.

**IV.4.5 Representative Gauging selection:**

The discharge coefficient (0.489) is close to the most consistent values (0.502 and 0.501) and indicates stable flow conditions.

The PI value (1.43428) is reasonable, not an outlier like in gauging 2 and 5, and reflects the well's productivity accurately under consistent conditions.

The combination of a consistent  $C_d$  and a reasonable PI suggests that (02/18/2024) gauging measurement is reliable and representative of the well's actual performance.

**Table IV. 7:** Representative gauging.

| Date       | Liquid PI Sm <sup>3</sup> /(d.bar) | DC    | Water cut % |
|------------|------------------------------------|-------|-------------|
| 02/18/2024 | 1.43428                            | 0.489 | 10.58218077 |

### IV.5 Optimization of gas lift injection flowrate:

After completing the modelling of the well and inserting the values of productivity index, discharge coefficient and water cut into the model, system analysis is used to estimate the optimum GLI rate (Gas Lift Injection).

System analysis | Engine console | System results | Profile results

**GENERAL**

Branch start: MDZ717 - Reservoir

Branch end: Ck

Sensitivity configuration: Permuted

**CALCULATED VARIABLE**

Inlet pressure 259 kgf/cm<sup>2</sup> g

Outlet pressure 14.7 kgf/cm<sup>2</sup> g

Liquid flowrate

Custom

| X-axis             | Variable 1                                  | Variable 2                                  | Variable 3                                  | Variable 4                                  |
|--------------------|---|---|---|---|
| GLI                | Active: <input checked="" type="checkbox"/> | Active: <input checked="" type="checkbox"/> | Active: <input checked="" type="checkbox"/> | Active: <input checked="" type="checkbox"/> |
| Injection g...     | Ck  |   |   |   |
| Range...           | Bean size                                   |   |   |   |
| sm <sup>3</sup> /d | Range...                                    | Range...                                    | Range...                                    | Range...                                    |
| 1 0                | mm  |   |   |   |
| 2 10000            | 1 16  |   |   |   |
| 3 20000            | 2   |   |   |   |
| 4 30000            | 3   |   |   |   |
| 5 40000            | 4   |   |   |   |
| 6 50000            | 5   |   |   |   |
|                    | 6   |   |   |   |

**Figure IV. 17:** Optimum GLI inputs.

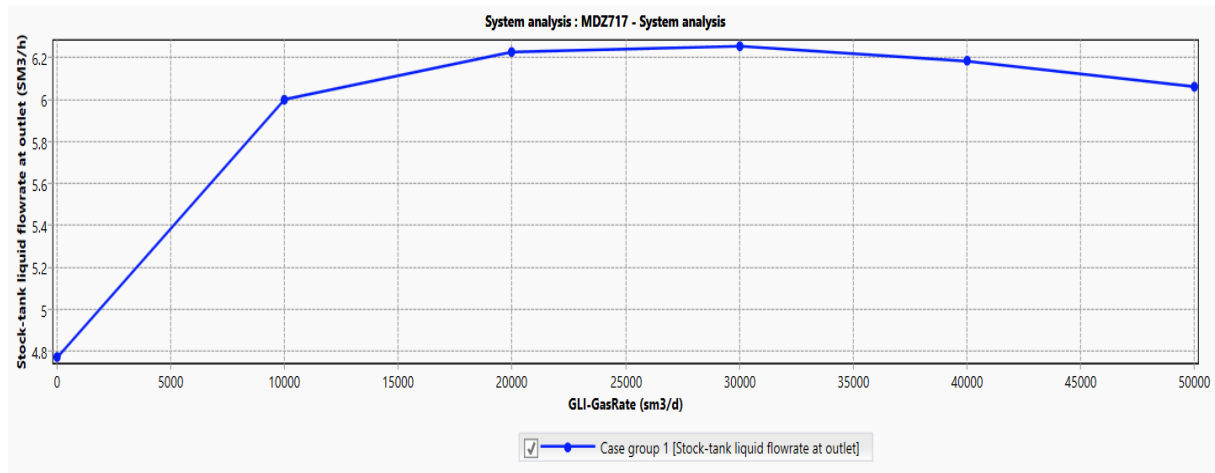


Figure IV. 18: Liquid flowrate change based on GLI rate.

|   | GLI-GasRate<br>sm3/d | Stock-tank liq...<br>SM3/h | GLI-GasRate<br>sm3/d | Stock-tank wa...<br>% |
|---|----------------------|----------------------------|----------------------|-----------------------|
|   | Case group 1 [...]   | Case group 1 [...]         | Case group 1 [...]   | Case group 1 [...]    |
| 1 | 0                    | 4.772617                   | 0                    | 10.582                |
| 2 | 10000.09             | 5.998177                   | 10000.09             | 10.582                |
| 3 | 19999.91             | 6.228458                   | 19999.91             | 10.582                |
| 4 | 29998.87             | 6.255175                   | 29998.87             | 10.582                |
| 5 | 40000.38             | 6.184271                   | 40000.38             | 10.582                |
| 6 | 49999.06             | 6.059373                   | 49999.06             | 10.582                |

Figure IV. 19: GLI optimization results.

The optimum gas lift injection rate is 10000 ( $\text{sm}^3/\text{d}$ ) which correspond with the liquid flow rate value of 5.998 ( $\text{sm}^3/\text{h}$ ), this value is considered the economic optimum gas injection rate where marginal extra gas injection cost balances marginal extra production revenue (Figure IV.1).

Table IV. 8: Parameters of well MDZ717 at optimum condition.

| Parameters   | Value   |
|--|---------|
| Gas lift injection rate ( $\text{sm}^3/\text{d}$ ) | 10000   |
| Oil flow rate ( $\text{sm}^3/\text{h}$ )           | 5.3652  |
| Gas flow rate ( $\text{sm}^3/\text{h}$ )           | 1192.29 |
| Water flow rate ( $\text{sm}^3/\text{h}$ )         | 0.6348  |
| Pipe line pressure ( $\text{kg}/\text{cm}^2$ )     | 14.7    |
| Pipe line temperature ( $^{\circ}\text{C}$ )       | 26      |

## IV.6 Result and discussion:

Part one focuses on optimizing the gas lift injection (GLI) rate for well MDZ717 to achieve optimal production using PIPESIM. The economically optimal GLI is 10,000  $\text{sm}^3/\text{d}$ , resulting in a liquid production rate of 5.99  $\text{sm}^3/\text{h}$ . At the maximum GLI rate of 30,000  $\text{sm}^3/\text{d}$ , the liquid flow only increases to 6.25  $\text{sm}^3/\text{h}$ . This marginal gain of 0.25  $\text{sm}^3/\text{h}$  indicates a high cost for minimal benefit.

Maintaining these conditions is challenging due to Hydrates effects that negatively impact well performance, leading to significant production losses. To address this, engineers at DP-HMD constructed a heat exchanger to mitigate the impact of Hydrates on production. Although the heat exchanger showed positive results, It did not completely eliminate Hydrates formation for most wells.

In the next part, we will evaluate the efficiency of the heat exchanger in eliminating Hydrates and maintaining optimal production for well MDZ717 using the Kern method and HYSYS tools. We will explore ways to improve the elimination of Hydrates, aiming to minimize downtime and maximize production gains.



## Part Two: Heat exchanger design and analysis (case study MDZ717)

In this part, we will test the effectiveness of the heat exchanger used by DEP in eliminating Hydrates in the optimum conditions of MDZ717 well. This evaluation will utilize the Kern method and HYSYS simulation. To facilitate an accurate HYSYS simulation, a highly similar model of the heat exchanger was designed using Aspen EDR. This approach will enhance our ability to predict the heat exchanger's performance in this case study and identify ways to improve its efficiency.

### IV.7 Heat exchanger in DP-HMD:

The heat exchanger used by Engineering and production department in HMD is installed on the wellhead level at the surface. The exchanger has 18" diameter shell and 2" diameter tube, the hot crude oil passes through the shell side and the cold gas passes through the tube side. The exchanger is connected to the production pipeline with valves that can be closed in case of not using the exchanger and the same for the GL pipeline.

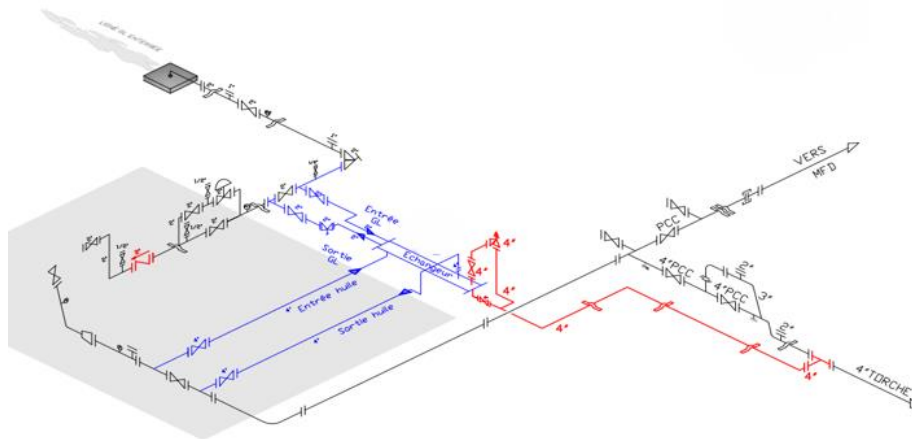


**Figure IV. 20:** Heat exchanger surface installation. [15]

The exchanger has an automatic safety valve that opens and switches the fluids in the exchanger into torch in case of gas leak inside the exchanger. Each of the gas inlet, outlet and oil inlet have a thermometer for temperature measurement, and the safety valve has a manometer

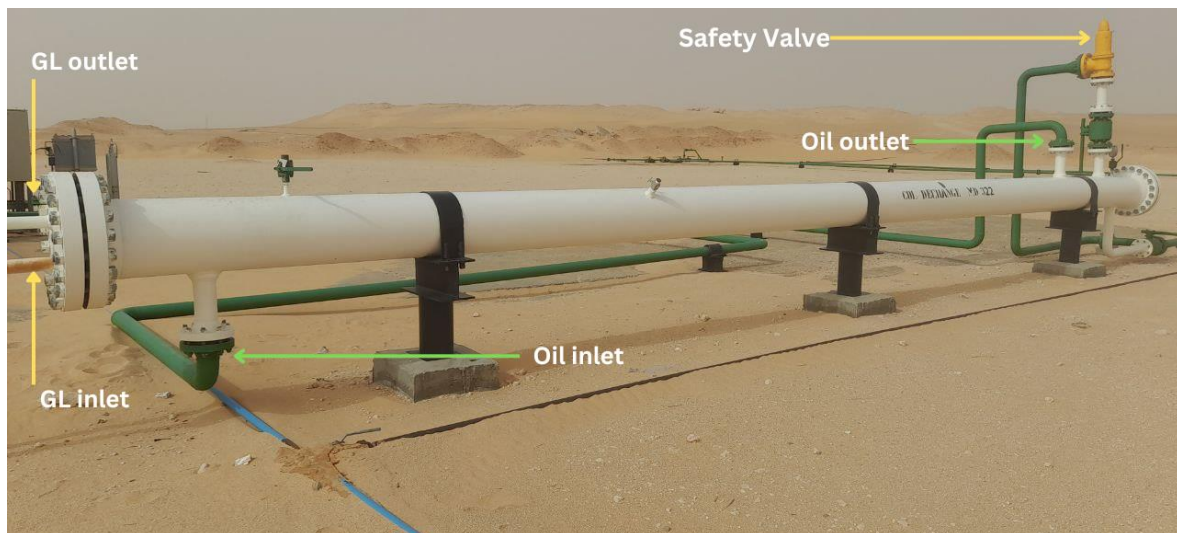


Figure IV. 21: Heat exchanger (MD322).

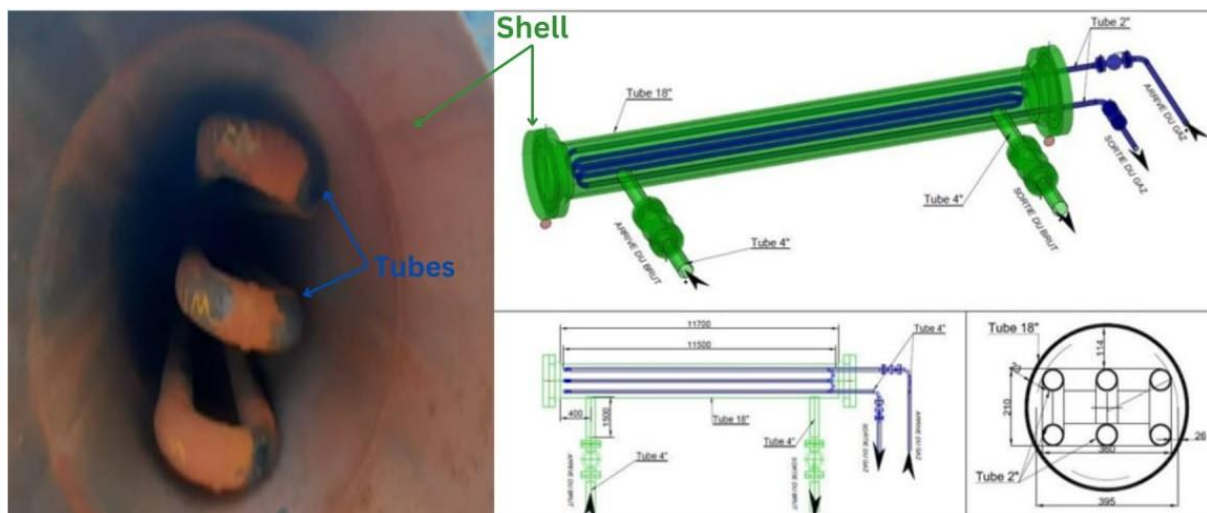
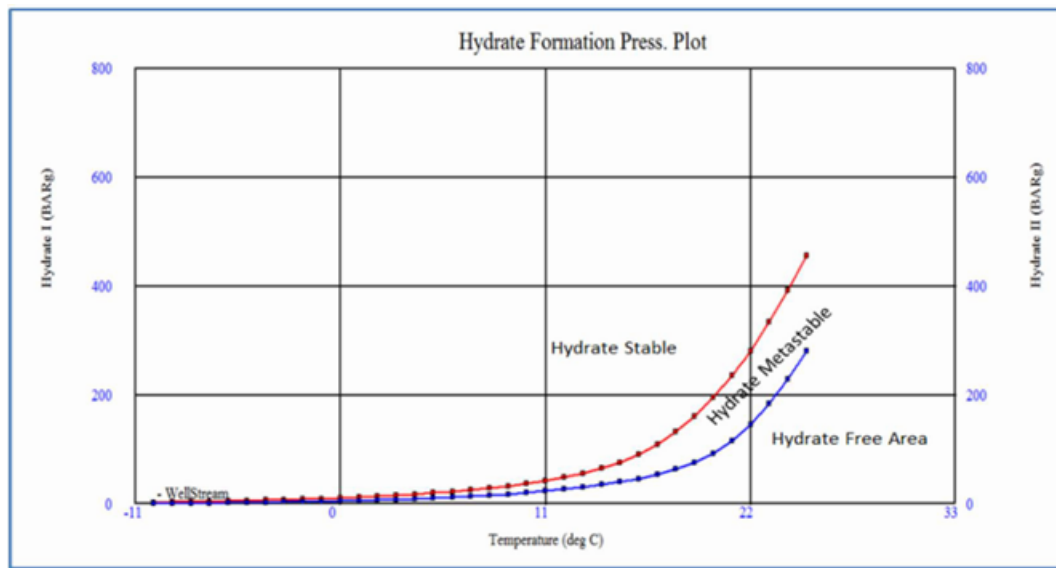


Figure IV. 22: Fabrication of heat exchanger HMD. [15]

## IV.8 Hydrates formation conditions:

The root cause of hydrates formation is that the lift gas used is directly taken from the gas to be injected into the reservoir without adequate dehydration. This insufficiently dehydrated wet gas can freeze when it experiences a significant temperature drop, which is caused by the large pressure drop across the lift gas injection choke in the gas lift line.



**Figure IV. 23:** Hydrates formation curves for Hassi Messaoud gas lift. [17]

Figure IV.22 illustrates hydrates formation under varying temperature and pressure conditions, it demonstrates three ranges:

1. **Hydrates Stable:** This zone represents the conditions under which hydrates formation occurs and stabilizes. Hydrates in gas lift wells form at these specific temperatures and pressures. It is crucial to avoid operating within this zone to prevent hydrates and ensure optimal well performance.
2. **Hydrates Metastable zone:** The Metastable Zone refers to a range of temperature and pressure conditions where hydrates formation is possible but not guaranteed to be stable. In this zone, hydrates can form but may also dissolve or transition depending on slight changes in environmental conditions. Operations in this zone are risky because hydrates can intermittently form, potentially disrupting gas lift operations. Operating within this zone explains why some wells showed improvements but did not achieve complete success.
3. **Hydrates Free Area:** The Hydrates Free Area is a range of temperature and pressure conditions where the formation of hydrates is highly unlikely. Operating within this zone ensures that hydrates does not occur, thereby maintaining optimal gas lift operations and preventing disruptions caused by hydrates formation. This area represents the safest and most efficient operating conditions for gas lift wells.

In this case study with MDZ717 well, with GL line pressure of 60 bars at the optimum conditions, the minimum required to be safe from Hydrates stable conditions is 12 C°. This

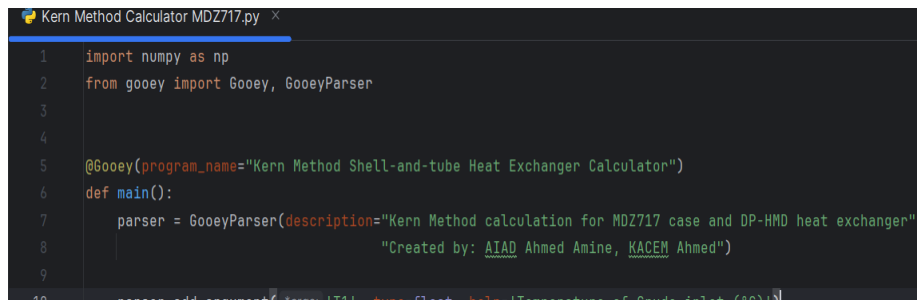
temperature is operating under the metastable zone which means Hydrates might still occur. The gas lift injection pressure in HMD is in the range of 60 to 95bars which means to operate safely from Hydrates zone, the GL needs to be maintained above 20 C° at least, operating above this temperature means 100% efficiency of the exchanger and guarantee zero downtime due to Hydrates, by extension maximum production gain.

## IV.9 Application of Kern method:

### IV.9.1 Implementing Kern method in Python

Python is a computer programming language often used to build websites and software, automate tasks and analyses data. Python is a general-purpose language, not specialized for any specific problems, and used to create various programs.

To make the calculation easier and faster, we wrote Kern method equations in a python code, which make the calculating of results quicker. This python code is particularly for the MDZ717 case with a fixed heat exchanger dimension.



```

1  import numpy as np
2  from goocy import Goocy, GoocyParser
3
4
5  @Goocy(program_name="Kern Method Shell-and-tube Heat Exchanger Calculator")
6  def main():
7      parser = GoocyParser(description="Kern Method calculation for MDZ717 case and DP-HMD heat exchanger"
8                          "Created by: AIAD Ahmed Amine, KACEM Ahmed")
9
10

```

Figure IV. 24: Python window.

### IV.9.2 Heat exchanger Performance verification with Kern method (Well MDZ717):

The Kern method involves calculating the necessary heat exchange area for a heat exchanger, taking into account numerous factors and data points. The objective is to verify the heat exchanger's effectiveness in preventing Hydrates in the GL line of MDZ717 well

Using the data from PIPESIM MDZ717 (Table IV.8) well and the dimensions of the heat exchanger, the necessary heat exchange area ( $A_{cal}$ ) can be calculated and compared with the available heat exchange area of the heat exchanger ( $A_{ava}$ ). If " $A_{cal} < A_{ava}$ " then the heat exchanger is able to make the heat exchange in order for the gas to reach a specified temperature in specified conditions, else if " $A_{cal} > A_{ava}$ " then the heat exchange surface of the heat exchanger is not sufficient in the specified conditions.

**Table IV. 9:** Shell side and tube side data.

| Parameters                          | Shell Side                    |                                |                               | Tube Side                 |
|-------------------------------------|-------------------------------|--------------------------------|-------------------------------|---------------------------|
|                                     | Oil                           | Gas                            | Water                         |                           |
| Inlet temperature (C°)              | 26                            |                                |                               | 0                         |
| Outlet temperature (C°)             | 24                            |                                |                               | 12                        |
| Outside diameter (inch)             | 18                            |                                |                               | 2                         |
| Inside diameter (inch)              | 17.24                         |                                |                               | 1.88                      |
| Thickness (m)                       | 0.0096                        |                                |                               | 0.003                     |
| Construction material               | Steel                         |                                |                               | Steel                     |
| Fluids flowrate                     | 5.3652<br>(m <sup>3</sup> /h) | 1192.29<br>(m <sup>3</sup> /h) | 0.6348<br>(m <sup>3</sup> /h) | 10000 (m <sup>3</sup> /d) |
| Dynamic viscosity<br>(kg/h m)       | 31.20                         | 0.125                          | 3.69                          | 0.125                     |
| Thermal conductivity<br>(kj/m h k°) | 0.215                         | 0.125                          | 0.489                         | 0.108                     |
| Specific heat (kJ/kg k°)            | 2.16                          | 1.9                            | 4.186                         | 1.94                      |
| Specific gravity                    | 0.8                           | 0.793                          | 1.2                           | 0.742                     |

**Table IV. 10:** Calculation of the specific heat of gas lift.

| GL Components | $Y_i$       | $C_{pi}(J/Kg*K)$ | $C_{p_i}Y_i$ |
|---------------|-------------|------------------|--------------|
| <b>H2O</b>    | 0.025219925 | 4180             | 105.4192875  |
| <b>C1</b>     | 0.599390153 | 2208.5           | 1323.753153  |
| <b>C2</b>     | 0.311584274 | 1708.5           | 532.3417321  |

|             |             |                |                        |
|-------------|-------------|----------------|------------------------|
| <b>C3</b>   | 0.003771051 | 1630           | 6.146812941            |
| <b>iC4</b>  | 0           | 1675           | 0                      |
| <b>nC4</b>  | 0           | 1675           | 0                      |
| <b>iC5</b>  | 0           | 1619           | 0                      |
| <b>nC5+</b> | 0.00036292  | 1619           | 0.587567906            |
| <b>C6+</b>  | 0.000422527 | 2260           | 0.954910364            |
| <b>N2</b>   | 0.0377592   | 1040           | 39.26956802            |
| <b>CO2</b>  | 0.046709875 | 832.5          | 38.88597098            |
|             |             | $C_{p_{gl}} =$ | 1.941939715 (kJ/kg k°) |

In order to put the value of F, the option field needs to be empty when the pressing start then the E and R values are calculated and shown, from (Appendix) the value of F is determined and can be put after pressing edit, when pressing start again the calculation will be done.

Kern Method Shell-and-tube Heat Exchanger Calculator

Settings  
Kern Method calculation for MDZ717 case and DP-HMD heat exchanger. Created by: AIAD Ahmed Amine, KACEM Ahmed

**Required Arguments**

|   |   |
|---|---|
| <b>T1</b><br>Temperature of Crude inlet (°C)<br>26                        | <b>T2</b><br>Temperature of Crude outlet (°C)<br>24           |
| <b>t1</b><br>Temperature of Gas-Lift inlet (°C)<br>0                      | <b>t2</b><br>Temperature of Gas-Lift outlet (°C)<br>12        |
| <b>Qgl</b><br>Flow rate of injected Gas Lift (m <sup>3</sup> /d)<br>10000 | <b>Qo</b><br>Flow rate of oil (m <sup>3</sup> /h)<br>5.3652   |
| <b>Qg</b><br>Flow rate of gas (m <sup>3</sup> /h)<br>1192.29              | <b>Qw</b><br>Flow rate of water (m <sup>3</sup> /h)<br>0.6348 |

**options**

**F**  
Correction Factor F  
0.98

Cancel Start

Figure IV. 25: Kern Method Calculation MDZ717 inputs.

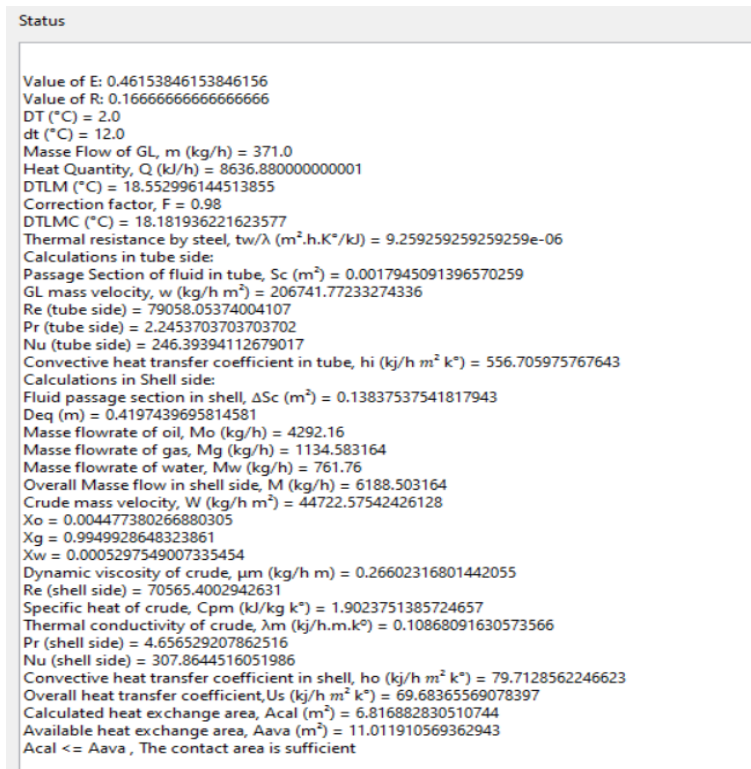


**Figure IV. 26:** Kern Method Results for MDZ717 well.

### IV.9.3 Kern Method calculation results:

The results from Kern Method calculations (Figure IV.25) for well MDZ717 reveal that the calculated heat transfer area exceeds the available heat transfer area of the DP-HMD heat exchanger. This indicates that the heat exchanger is more than sufficient to maintain the gas lift (GL) temperature above the hydrates stable zone, ensuring optimal production. To further confirm these findings, we will next design the heat exchanger using Aspen EDR and utilize it in HYSYS to simulate the GL pipeline heating process for well MDZ717.

## IV.10. Simulation and design of Heat exchangers with HYSYS and EDR:

### IV.10.1 Overview about Aspen HYSYS and Aspen EDR:

#### IV.10.1.1 Aspen HYSYS

Aspen HYSYS is a chemical process simulator currently developed by AspenTech used to mathematically model chemical processes, from unit operations to full chemical plants and refineries. HYSYS is able to perform many of the core calculations of chemical engineering, including those concerned with mass balance, energy balance, vapor-liquid equilibrium, heat transfer, mass transfer, chemical kinetics, fractionation, and pressure drop. HYSYS is used

extensively in industry and academia for steady-state and dynamic simulation, process design, performance modelling, and optimization. [19]

### IV.10.1.2 Aspen Exchanger Design and Rating (EDR)

ASPEN Exchanger Design & Rating software can be used for thermal analysis of various types of exchangers including shell and tube, air cooled, fired heater, plate, plate-fin, and coil wound.

This software can be used for:

- Calculating the size of an exchanger based on the specified process requirements (such as inlet and outlet temperatures, flow rates, and other factors).
- Calculating the outlet conditions given the exchanger geometry.
- Calculating pressure drop.

EDR can be integrated with HYSYS in order to use the heat exchanger design in the HYSYS simulation process. [19]

### IV.10.2 Model creation of the well MDZ717 and heat exchanger:

First step after executing HYSYS is creating a new case.

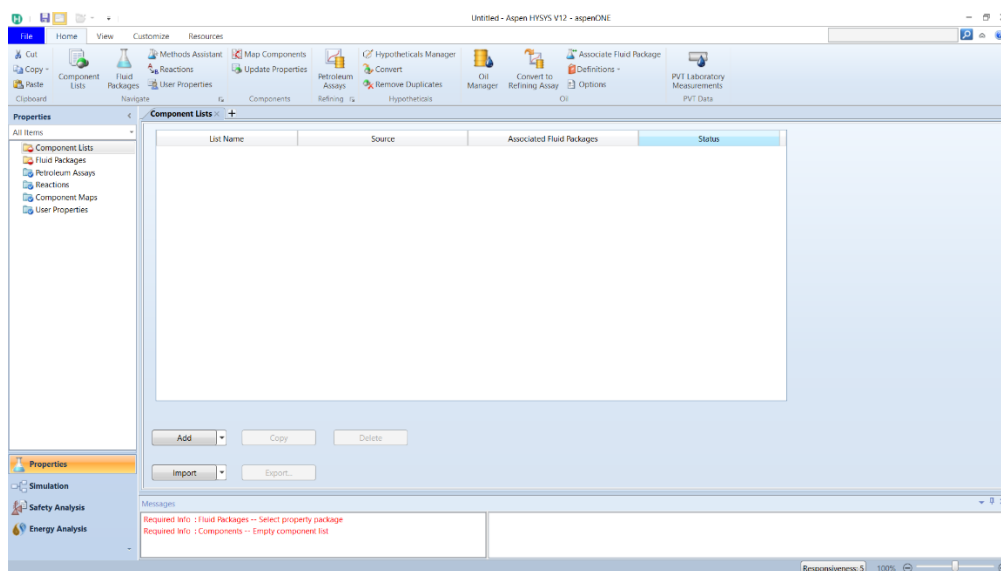


Figure IV. 27: HYSYS V12 window.



### IV.10.2.1 Adding component lists:

In the properties window component lists can be created and used in HYSYS simulation. In our case we selected two component lists (GL and Crude oil), however, it is possible to create one list because GL components can be included along with the crude components.

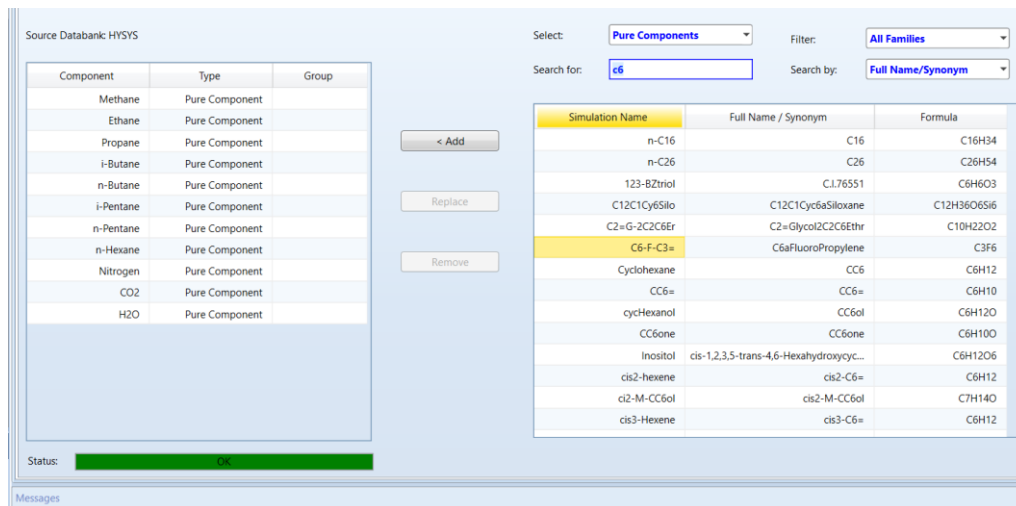


Figure IV. 28: Adding component lists.

### IV.10.2.2 Selecting fluid packages:

In the properties tab, an Equation of State (EOS) can be selected from the HYSYS database. In our simulation, we selected Peng-Robinson (PR) Fluid package because it's the common EOS for modelling the behavior of gases and liquids in the petroleum industry.

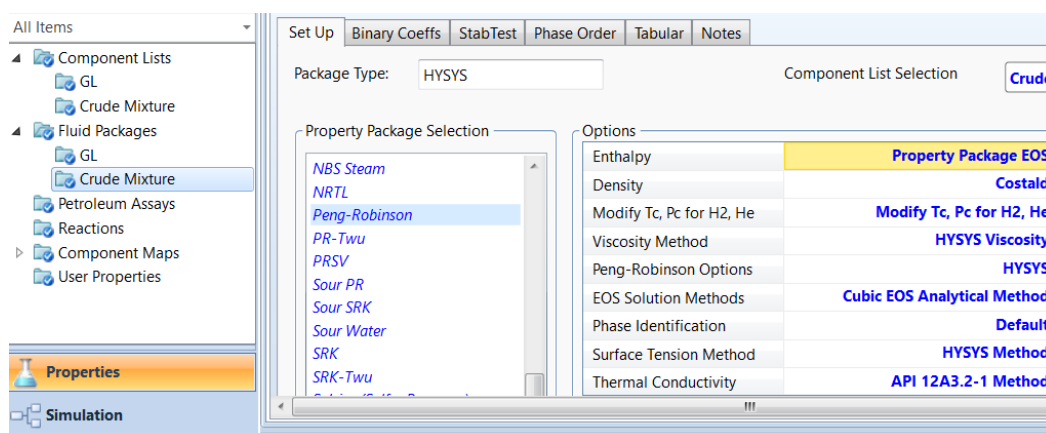


Figure IV. 29: Selecting fluid packages.

### IV.10.2.3 Setting up the flowsheet:

In the simulation tab, we can set up the flowsheet by adding streams and materials. In our example, we selected a mixture to mix crude fluids (oil, water, gas) because their mass fractions were from samples in surface separator (Appendix), therefore, we used HYSYS to recombine the crude. The inlet data of GL and crude are: Temperature, pressure and mass flow. HYSYS calculates the other data and the results in the outlets.

| Worksheet |  | GL inlet | GL outlet | Crude inlet |        | Crude outlet |
|-----------|--|----------|-----------|-------------|--------|--------------|
| Methane   |  | 0.7074   | 0.7074    | Nitrogen    | 0.0089 | 0.0089       |
| Ethane    |  | 0.2140   | 0.2140    | CO2         | 0.0096 | 0.0096       |
| Propane   |  | 0.0017   | 0.0017    | Methane     | 0.3026 | 0.3026       |
| i-Butane  |  | 0.0000   | 0.0000    | Ethane      | 0.0916 | 0.0916       |
| n-Butane  |  | 0.0000   | 0.0000    | Propane     | 0.0411 | 0.0411       |
| i-Pentane |  | 0.0000   | 0.0000    | i-Butane    | 0.0054 | 0.0054       |
| n-Pentane |  | 0.0001   | 0.0001    | n-Butane    | 0.0209 | 0.0209       |
| n-Hexane  |  | 0.0001   | 0.0001    | i-Pentane   | 0.0067 | 0.0067       |
| Nitrogen  |  | 0.0271   | 0.0271    | n-Pentane   | 0.0128 | 0.0128       |
| CO2       |  | 0.0214   | 0.0214    | n-Hexane    | 0.0170 | 0.0170       |
| H2O       |  | 0.0282   | 0.0282    | n-Heptane   | 0.0165 | 0.0165       |
|           |  |          |           | n-Octane    | 0.0174 | 0.0174       |
|           |  |          |           | n-Nonane    | 0.0140 | 0.0140       |
|           |  |          |           | n-Decane    | 0.0160 | 0.0160       |
|           |  |          |           | n-C11       | 0.0121 | 0.0121       |
|           |  |          |           | n-C12       | 0.0100 | 0.0100       |
|           |  |          |           | n-C13       | 0.0089 | 0.0089       |
|           |  |          |           | n-C14       | 0.0070 | 0.0070       |
|           |  |          |           | n-C15       | 0.0062 | 0.0062       |
|           |  |          |           | n-C16       | 0.0049 | 0.0049       |
|           |  |          |           | n-C17       | 0.0041 | 0.0041       |
|           |  |          |           | n-C18       | 0.0036 | 0.0036       |
|           |  |          |           | n-C19       | 0.0032 | 0.0032       |
|           |  |          |           | n-C20       | 0.0026 | 0.0026       |
|           |  |          |           | n-C21       | 0.0022 | 0.0022       |
|           |  |          |           | n-C22       | 0.0019 | 0.0019       |
|           |  |          |           | n-C23       | 0.0016 | 0.0016       |
|           |  |          |           | n-C24       | 0.0014 | 0.0014       |
|           |  |          |           | n-C25       | 0.0012 | 0.0012       |

Figure IV. 30: GL and Crude composition.

We selected simple end point heat exchanger in the beginning to set the inlets and outlets names. We can input the inlets only in the worksheet window (Temperature, pressure, mass flow and mass fraction of compositions) and let HYSYS calculate the outlets after importing EDR model.

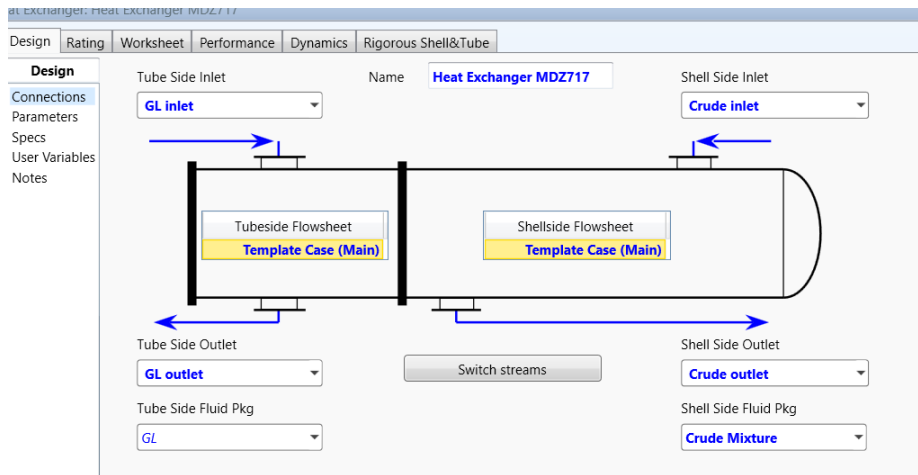


**Figure IV. 31:** Setting up the heat exchanger streams.

**IV.10.2.4 Designing the heat exchanger with EDR:**

In the Rigorous Shell&Tube tab, an import option is available to import an EDR file, the heat exchanger can be designed and modified in HYSYS after pressing View EDR browser.

In the EDR browser tab, the geometry of the heat exchanger can be specified along with Process settings, in the process tab we defined the allowable pressure drop to 0.2 bar and resistance fouling to 0.0001 m<sup>2</sup>-K/W for both streams.

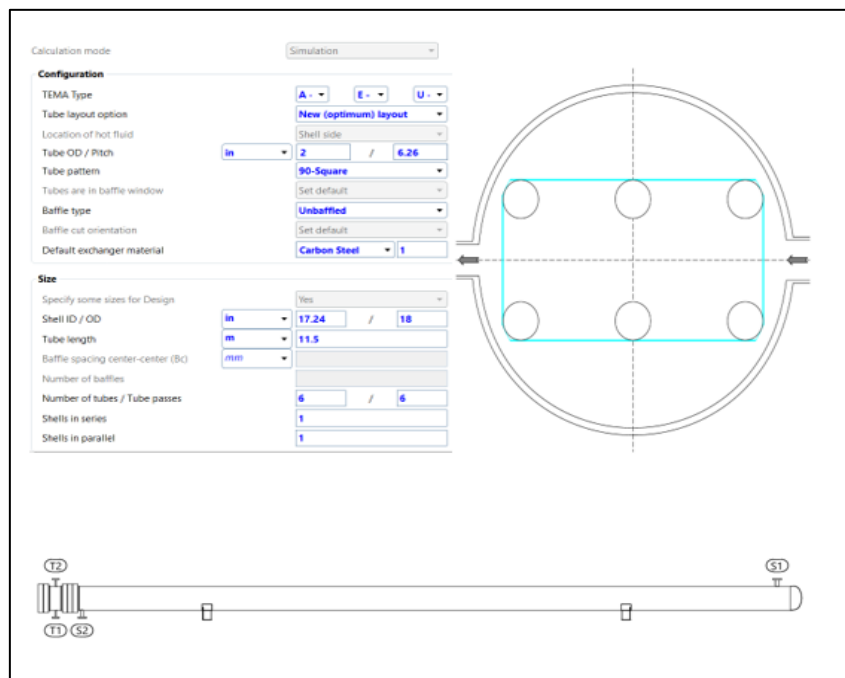


**Figure IV. 32:** Geometry and sketch of the heat exchanger in DP-HMD with EDR.

### IV.10.2.5 Simulation of MDZ717 well and exchanger with HYSYS:

After designing the heat exchanger and completing all necessary steps, the flowsheet is configured in HYSYS. HYSYS then computes all parameters that were not manually inserted and ensures convergence. The inputs inserted are the parameters of both GL and crude inlets, those parameters are: temperature, pressure, mass flow, and compositions. Meanwhile, the outlet side parameters are calculated by HYSYS as part of its simulation process.

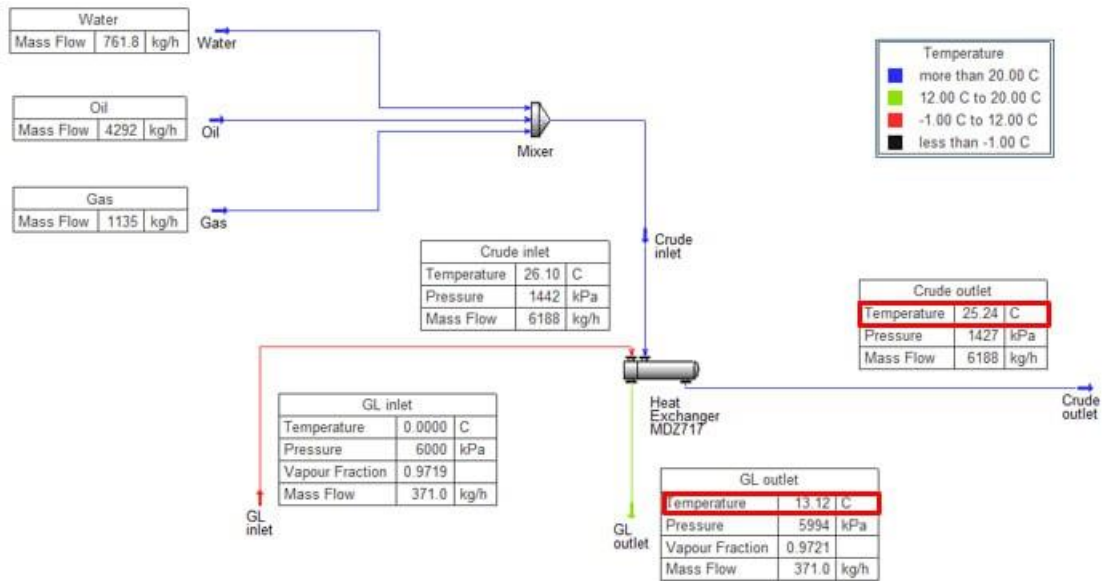


**Figure IV. 33:** Simulation of MDZ717 well and exchanger with HYSYS.

The outlet parameters of the crude and gas lift (GL) were computed using HYSYS, revealing that the GL temperature is 13.12°C. This temperature falls within the metastable range of Hydrates formation (Figure IV.23), indicating a potential risk associated with operating under these conditions. This result helps explain why the Hydrates problem for this well has not been completely resolved, as operating within the metastable range can still lead to intermittent Hydrates issues.

This result, compared to the Kern Method calculation, is deemed more reliable as it reflects the actual operating conditions of the well. While the Kern Method provides valuable insights, the HYSYS simulation incorporates various dynamic factors and accurately models the behavior of the gas lift system under real-world conditions. Therefore, the temperature obtained from the HYSYS simulation offers a more comprehensive understanding of the well's performance and potential Hydrates risks.

### IV.10.3 Design and simulation of a Proposed Heat Exchanger Model:

By utilizing EDR and implementing modifications to the DP HMD heat exchanger, we explored various adjustments to enhance its efficiency and achieve a safe operating zone, thereby aiming for 100% well availability and zero downtime due to Hydrates for maximum production gain. After iterative improvements, we developed a finalized model and tested it using the MDZ717 HYSYS simulation. This allowed us to compare its performance directly with the DP-HMD exchanger, ensuring that our modifications effectively addressed the Hydrates issue and optimized production.

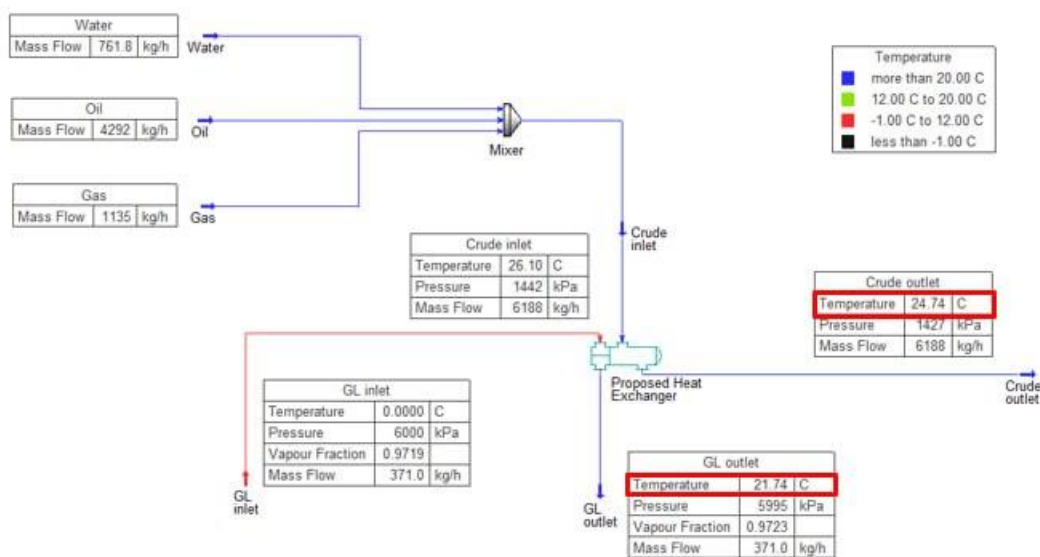


**Figure IV. 34:** Simulation of MDZ717 case and proposed exchanger model with HYSYS.

The simulation shows that with the proposed heat exchanger model, the GL outlet temperature is calculated to be 21.74°C (at 60 bar). Reaching a temperature above 20°C means operating in the Hydrates-free area, ensuring complete safety under these conditions. This guarantees zero downtime due to Hydrates, 100% availability, and maximum production gain.

### IV.11 Result and discussion:

This part investigated why the DP-HMD system couldn't entirely eliminate Hydrates in the well MDZ717. We approached this investigation using the Kern method to compare the calculated heat transfer area with the available transfer area of the exchanger. The results showed that the calculated area was 6.8 m<sup>2</sup>, while the available area was 11 m<sup>2</sup>. This indicated that the exchanger should be sufficient to eliminate Hydrates completely, which was not the case for the MDZ717 well.

To gain a more detailed understanding, we used HYSYS to simulate the gas lift heating process for the MDZ717 well. We designed a model of the exchanger using EDR, closely resembling the one used in DP-HMD. The simulation showed that the GL pipeline temperature rose to 13.12°C under optimal production conditions. This temperature is within the metastable Hydrates zone (Figure IV.23), posing a risk and failing to prevent Hydrates formation entirely. This explains why the MDZ717 well did not achieve 100% success in preventing Hydrates in real data and demonstrates that the HYSYS simulation provides a more accurate analysis than the Kern method.

To improve the well's availability and minimize downtime due to Hydrates, we made changes to the model and tested it under the same conditions for the MDZ717 well. The results showed that the proposed exchanger could raise the GL temperature to 21.74°C, which is within the Hydrates-free area. This indicates that it is possible to enhance the availability of the MDZ717 well for optimal production, ensuring maximum gain and zero downtime due to Hydrates.

# **General conclusion**

The problem of Hydrates in gas lift (GL) wells causes big production issues. Hydrates leads to major production losses and operational difficulties. Our investigation aimed to understand and solve this issue by looking at how well the DP-HMD heat exchanger works in keeping optimum GL conditions.

First, we optimized the gas lift injection (GLI) rate to achieve the best production using PIPESIM. We found that the best GLI was 10,000 sm<sup>3</sup>/d. However, because of Hydrates is it hard to keep these conditions, so we looked closely at how the heat exchanger was performing.

We used the Kern method to compare the calculated heat transfer area (6.8 m<sup>2</sup>) with the available area of the existing heat exchanger (11 m<sup>2</sup>). Although this suggested the exchanger should prevent Hydrates completely, real-world data showed that Hydrates still accrued.

To get a more accurate picture, we used HYSYS to simulate the gas lift heating process for well MDZ717. We designed a model of the heat exchanger using EDR to match the DP-HMD exchanger. The simulation showed that the GL pipeline temperature increased to 13.12°C, which is within the risky metastable Hydrates zone. This explained why the well didn't completely avoid Hydrates. This also showed that HYSYS is more accurate than the Kern method.

Next, we improved the heat exchanger model and tested it under the same conditions. The new model raised the GL temperature to 21.74°C, which is in the Hydrates-free zone. This means the well could operate without Hydrates problems, ensuring 100% availability and maximum production.

Our analysis and simulations show the importance of precise modeling for optimizing well performance. By fixing the issues with the existing heat exchanger and proposing a better model, we showed that it is possible to greatly improve the efficiency and reliability of well MDZ717 regardless of its low crude temperature. The combined approach of GLI optimization and a better heat exchanger design effectively solves the Hydrates problem, ensuring consistent optimal production conditions.

In the end we recommend:

- Employing advanced simulation software like HYSYS for constructing and analyzing heat exchanger models. HYSYS provides more accurate and realistic simulations of the gas lift heating process, helping to identify and resolve Hydrates.



- Modifying the dimensions of the heat exchanger to enhance its performance. Increasing the heat transfer area can ensure that the gas lift temperature stays in the Hydrates-free zone, thereby maintaining optimal production conditions.
- Integrating baffles into the heat exchanger design. Baffles create turbulence in the fluid flow, which improves heat transfer efficiency. This can help in achieving a higher outlet temperature, reducing the risk of Hydrates.
- Enhanced Dehydration: Ensure that the gas lift supply is sufficiently dehydrated before injection. Proper dehydration can significantly reduce the risk of hydrates formation, thus improving the overall efficiency of the gas lift process.
- Designing the heat exchanger and GLI optimization to the specific conditions of each well. Factors such as reservoir characteristics, ambient temperature, and gas composition should be considered to develop the most effective solution.
- Installation of heat exchanger in series should be considered, due to its high performance.

All these recommendations and studies should take into account the economic and technical challenges.

# **Bibliography**

## References

- [1] ROUINA Kheireddine, RABEHI Nacer, ZEMANI Youssef Ouissini, EVALUATION AND INTERPRETATION OF WELL TESTING DATA FROM CASES OF WELLS IMPLANTED IN UNCONVENTIONAL RESERVOIRS (WELL OMKZ421 HMD), MEMORY, KASDI MERBAH UNIVERSITY OUARGLA, 2022 / 2023.
- [2] TOTAL, Le PROCESS, le puits activé par gaz lift SUPPORT DE FORMATION : Cours EXP-PR-PR030-FR, 17/04/2007
- [3] Schlumberger, Gas Lift Design and Technology, Chevron Main Pass 313 Optimization Project, 09/12/2000.
- [4] Gas Lift Manual, Takacs, Gabon, Oklahoma, 2005.
- [5] Production technology, institute of petroleum engineering. Heriot- Watt.
- [6] M. NDIAYE Cheikh Ahmeth Tidiane, Optimisation des paramètres Gas Lift par le PIPESIM, Formation d'induction, INPG, 2023/2024.
- [7] Récupération assistée par gas-lift, Serpro et Groupe socotec industrie, septembre 2001.
- [8] GAS LIFT, BOOK 6 OF THE VOCATIONAL TRAINING SERIES, THIRD EDITION, AMERICAN PETROLEUM INSTITUTE, 1994.
- [9] Paper: Physical Chemistry, Dr Lokesh Kumar Agarwal, Mohanlal Sukhadia University.
- [10] Heat Transfer: A Practical Approach" by Yunus A. Cengel and Afshin J. Ghajar.
- [11] [https://www.rajagiritech.ac.in/home/mech/Course\\_Content/Semester%20VI/ME%20302%20Heat%20and%20Mass%20Transfer/Module%201.pdf](https://www.rajagiritech.ac.in/home/mech/Course_Content/Semester%20VI/ME%20302%20Heat%20and%20Mass%20Transfer/Module%201.pdf) (19/05/2024).
- [12] Heat Exchangers: Selection, Rating, and Thermal Design by Sadik Kakac, Hongtan Liu, and Anchasa Pramuanjaroenkij.
- [13] Heat Exchanger Design Handbook, Kuppan Thulukkanam, 2000.
- [14] Review of Methods of Donohue, Kern, Bell-Delaware and C.F. Braun, J. Taborek
- [15] SH / DP/ DR – HMD /Direction Eng. & Production Dept./ Contrôle Sud Service Artificial Lift: Echangeur de chaleur.
- [16] SH / DP/ DR – HMD /Direction Eng. & Production Dept./ Contrôle Sud Service Artificial Lift: L'historique des puits.
- [17] Article: Hydrates Mitigation and Flare Reduction Using Intermittent Gas Lift in Hassi Messaoud, Algeria, Ala Eddine Aoun, Faouzi Maougal, and Lahcene Kabour, Sonatrach; Tony Liao, Brahim AbdallahElhadj, and Sabrina Behaz, Halliburton. SPE.
- [18] PIPESIM User Guide, Version 2012.1, Schumberger.

[19] An Applied Guide to Process and Plant Design, Sean Moran, 03/30/2015.

# Appendix

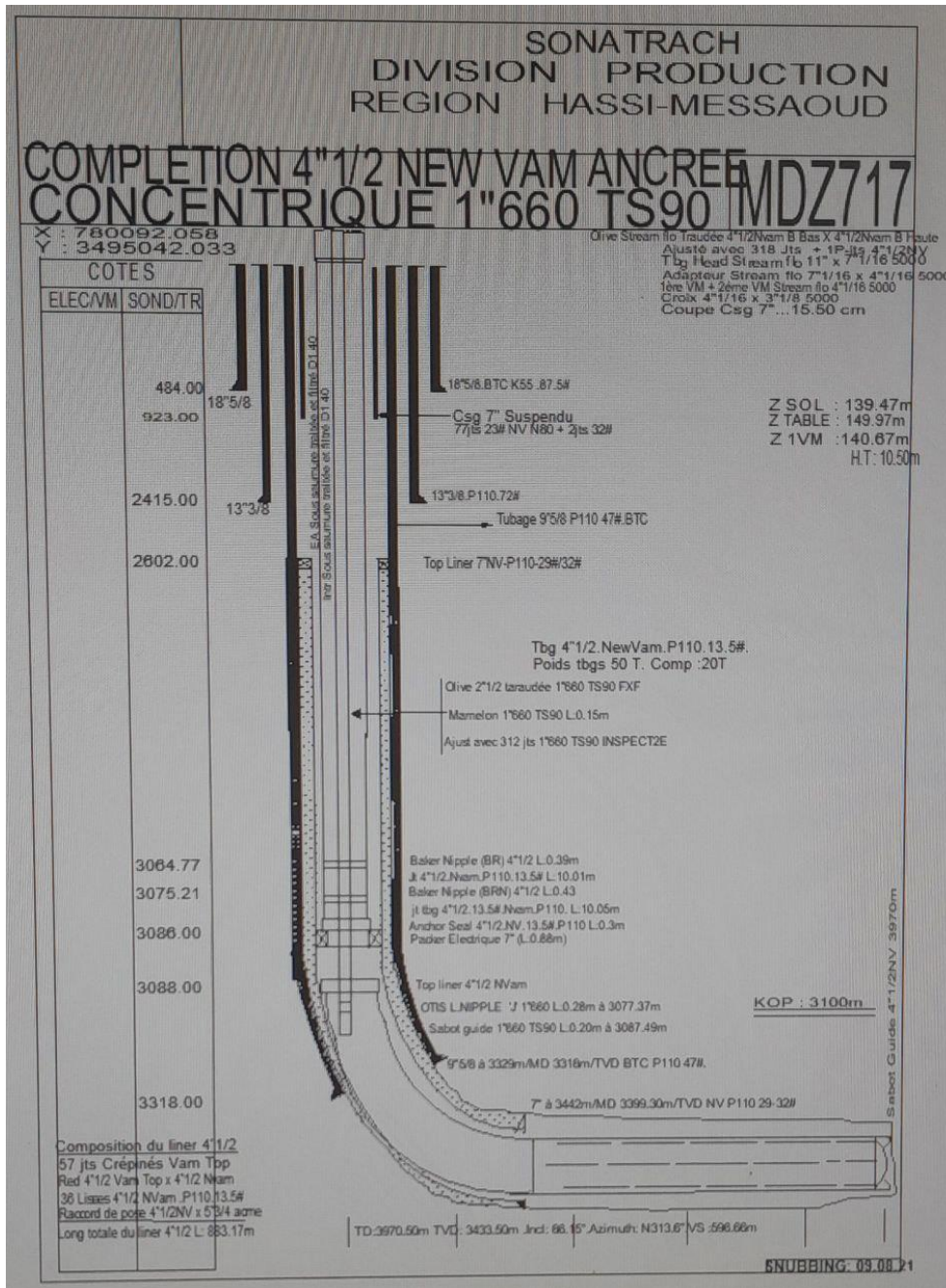
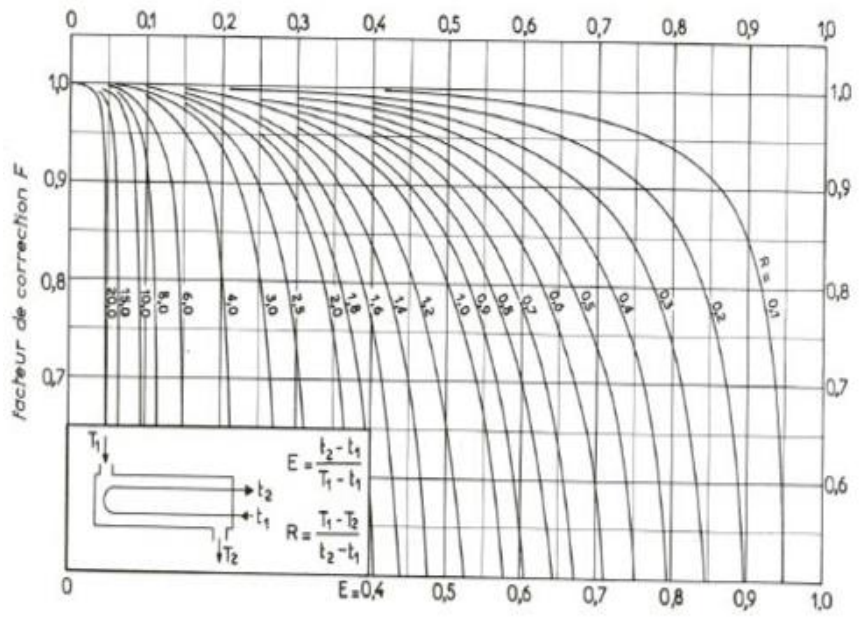


**Figure 01:** Completion schematic of well MDZ717



a. une passe côté calandre, deux passes (ou plus) côté tubes.

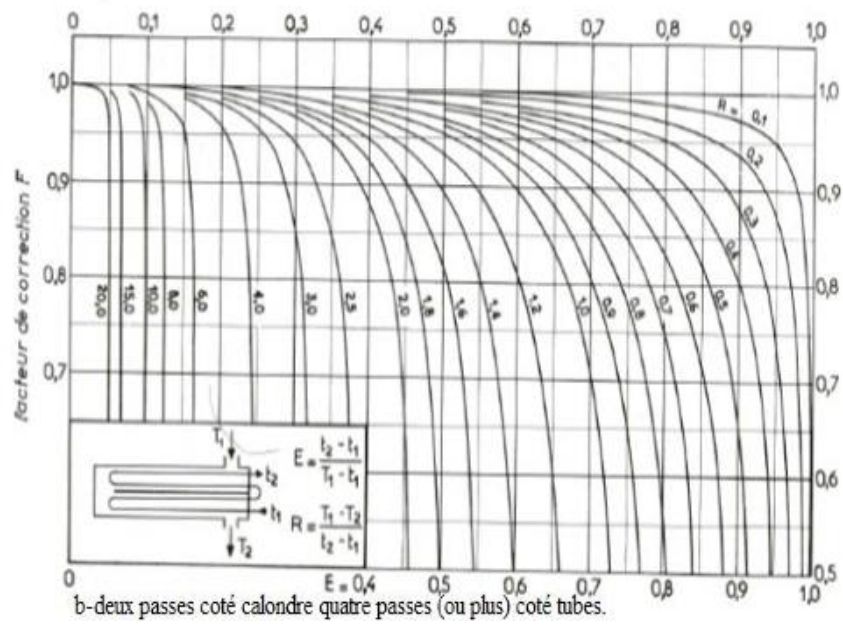


Figure 02: Correction factor F

| Component     | MW     | Separator Oil |        | Component     | MW     | Separator Gas |        |
|---------------|--------|---------------|--------|---------------|--------|---------------|--------|
|               | g/mol  | Wt %          | Mole % |               | g/mol  | Wt %          | Mole % |
| N2            | 28.01  | 0.02          | 0.07   | N2            | 28.01  | 2.72          | 2.14   |
| CO2           | 44.01  | 0.15          | 0.41   | CO2           | 44.01  | 4.19          | 2.10   |
| H2S           | 34.08  | 0.00          | 0.00   | H2S           | 34.08  | 0.00          | 0.00   |
| C1            | 16.04  | 0.92          | 6.99   | C1            | 16.04  | 51.11         | 70.35  |
| C2            | 30.07  | 1.87          | 7.58   | C2            | 30.07  | 23.77         | 17.46  |
| C3            | 44.10  | 2.51          | 6.94   | C3            | 44.10  | 10.68         | 5.35   |
| i-C4          | 58.12  | 0.61          | 1.28   | i-C4          | 58.12  | 1.17          | 0.44   |
| n-C4          | 58.12  | 2.62          | 5.49   | n-C4          | 58.12  | 3.52          | 1.34   |
| i-C5          | 72.15  | 1.21          | 2.04   | i-C5          | 72.15  | 0.71          | 0.22   |
| n-C5          | 72.15  | 2.40          | 4.06   | n-C5          | 72.15  | 1.08          | 0.33   |
| C6            | 84.00  | 4.08          | 5.92   | C6            | 84.00  | 0.64          | 0.17   |
| Mcylo-C5      | 84.16  | 0.62          | 0.90   | Mcylo-C5      | 84.16  | 0.06          | 0.02   |
| Benzene       | 78.11  | 0.39          | 0.62   | Benzene       | 78.11  | 0.04          | 0.01   |
| Cyclo-C6      | 84.16  | 0.52          | 0.75   | Cyclo-C6      | 84.16  | 0.04          | 0.01   |
| C7            | 96.00  | 4.73          | 6.00   | C7            | 96.00  | 0.19          | 0.04   |
| Mcylo-C6      | 98.19  | 1.21          | 1.50   | Mcylo-C6      | 98.19  | 0.03          | 0.01   |
| Toluene       | 92.14  | 0.48          | 0.64   | Toluene       | 92.14  | 0.01          | 0.00   |
| C8            | 107.00 | 5.75          | 6.55   | C8            | 107.00 | 0.05          | 0.01   |
| C2-Benzene    | 106.17 | 0.36          | 0.41   | C2-Benzene    | 106.17 | 0.00          | 0.00   |
| mp-Xylene     | 106.17 | 0.71          | 0.82   | mp-Xylene     | 106.17 | 0.00          | 0.00   |
| o-Xylene      | 106.17 | 0.28          | 0.32   | o-Xylene      | 106.17 | 0.00          | 0.00   |
| C9            | 121.00 | 5.19          | 5.22   | C9            | 121.00 | 0.01          | 0.00   |
| C10           | 134.00 | 6.61          | 6.01   | C10           | 134.00 | 0.00          | 0.00   |
| C11           | 147.00 | 5.47          | 4.53   | C11           | 147.00 | 0.00          | 0.00   |
| C12           | 161.00 | 4.95          | 3.74   | C12           | 161.00 | 0.00          | 0.00   |
| C13           | 175.00 | 4.73          | 3.29   | C13           | 175.00 | 0.00          | 0.00   |
| C14           | 190.00 | 4.00          | 2.56   | C14           | 190.00 | 0.00          | 0.00   |
| C15           | 206.00 | 3.79          | 2.24   | C15+          | 206.00 | 0.00          | 0.00   |
| C16           | 222.00 | 3.24          | 1.78   | Calculated MW |        |               | 22.08  |
| C17           | 237.00 | 2.89          | 1.48   |               |        |               |        |
| C18           | 251.00 | 2.67          | 1.30   |               |        |               |        |
| C19           | 263.00 | 2.48          | 1.15   |               |        |               |        |
| C20           | 275.00 | 2.14          | 0.95   |               |        |               |        |
| C21           | 291.00 | 1.90          | 0.79   |               |        |               |        |
| C22           | 305.00 | 1.71          | 0.68   |               |        |               |        |
| C23           | 318.00 | 1.51          | 0.58   |               |        |               |        |
| C24           | 331.00 | 1.35          | 0.50   |               |        |               |        |
| C25           | 345.00 | 1.26          | 0.44   |               |        |               |        |
| C26           | 359.00 | 1.09          | 0.37   |               |        |               |        |
| C27           | 374.00 | 1.05          | 0.34   |               |        |               |        |
| C28           | 388.00 | 0.97          | 0.31   |               |        |               |        |
| C29           | 402.00 | 0.84          | 0.26   |               |        |               |        |
| C30           | 479.22 | 8.72          | 2.21   |               |        |               |        |
| Calculated MW | g/mol  |               | 121.77 |               |        |               |        |

Figure 03: Oil and Gas samples.

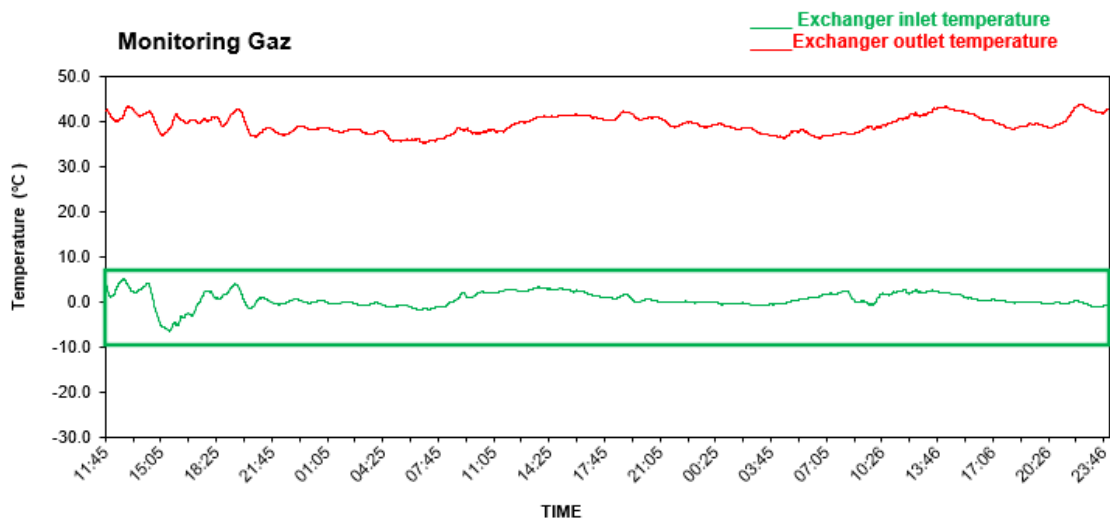


Figure 04: Evaluation of the heat exchanger (OMGZ81)



**Table 01: Data Survey MDZ717**

| N° | MD (m)  | Incl (°) | Azimuth (°) | TVD (m) | Latitude N/S (m) | Longitude E/W (m) | DLS (°/30m) | VS (m) | Remarques |
|----|---------|----------|-------------|---------|------------------|-------------------|-------------|--------|-----------|
| 1  | 0.00    | 0.00     | 0.00        | 0.00    | 0.00             | 0.00              | 0.00        | 0.00   |           |
| 2  | 69.72   | 0.06     | 176.19      | 69.72   | -0.04            | 0.00              | 0.03        | -0.03  |           |
| 3  | 96.56   | 0.08     | 97.80       | 96.56   | -0.05            | 0.02              | 0.10        | -0.05  |           |
| 4  | 123.98  | 0.25     | 106.91      | 123.98  | -0.07            | 0.10              | 0.19        | -0.12  |           |
| 5  | 150.94  | 0.25     | 89.86       | 150.94  | -0.09            | 0.21              | 0.08        | -0.21  |           |
| 6  | 179.60  | 0.26     | 92.17       | 179.60  | -0.09            | 0.34              | 0.02        | -0.31  |           |
| 7  | 207.94  | 0.38     | 91.32       | 207.94  | -0.10            | 0.50              | 0.13        | -0.42  |           |
| 8  | 235.76  | 0.55     | 94.65       | 235.76  | -0.11            | 0.72              | 0.19        | -0.59  |           |
| 9  | 263.31  | 0.64     | 90.49       | 263.31  | -0.12            | 1.01              | 0.11        | -0.80  |           |
| 10 | 290.61  | 0.62     | 93.65       | 290.60  | -0.13            | 1.31              | 0.04        | -1.02  |           |
| 11 | 319.42  | 0.54     | 91.65       | 319.41  | -0.15            | 1.60              | 0.09        | -1.24  |           |
| 12 | 348.28  | 0.53     | 85.99       | 348.27  | -0.14            | 1.87              | 0.06        | -1.42  |           |
| 13 | 377.15  | 0.39     | 80.33       | 377.14  | -0.12            | 2.10              | 0.15        | -1.57  |           |
| 14 | 405.97  | 0.33     | 59.86       | 405.96  | -0.06            | 2.27              | 0.15        | -1.64  |           |
| 15 | 434.73  | 0.23     | 58.62       | 434.72  | 0.01             | 2.39              | 0.10        | -1.68  |           |
| 16 | 463.54  | 0.14     | 50.00       | 463.53  | 0.07             | 2.47              | 0.10        | -1.70  |           |
| 17 | 492.36  | 0.12     | 37.75       | 492.35  | 0.11             | 2.51              | 0.04        | -1.70  |           |
| 18 | 521.23  | 0.15     | 30.95       | 521.22  | 0.17             | 2.55              | 0.04        | -1.68  |           |
| 19 | 550.21  | 0.18     | 29.41       | 550.20  | 0.24             | 2.59              | 0.03        | -1.66  |           |
| 20 | 579.10  | 0.15     | 19.27       | 579.09  | 0.32             | 2.63              | 0.04        | -1.63  |           |
| 21 | 607.84  | 0.16     | 29.62       | 607.83  | 0.39             | 2.66              | 0.03        | -1.61  |           |
| 22 | 636.73  | 0.19     | 37.21       | 636.72  | 0.46             | 2.71              | 0.04        | -1.59  |           |
| 23 | 665.56  | 0.19     | 35.64       | 665.55  | 0.54             | 2.76              | 0.01        | -1.57  |           |
| 24 | 694.36  | 0.24     | 45.77       | 694.35  | 0.62             | 2.83              | 0.07        | -1.57  |           |
| 25 | 723.25  | 0.24     | 49.75       | 723.24  | 0.70             | 2.92              | 0.02        | -1.57  |           |
| 26 | 752.09  | 0.29     | 73.05       | 752.08  | 0.76             | 3.04              | 0.12        | -1.61  |           |
| 27 | 780.89  | 0.35     | 71.54       | 780.88  | 0.81             | 3.19              | 0.06        | -1.69  |           |
| 28 | 809.60  | 0.35     | 75.24       | 809.59  | 0.86             | 3.36              | 0.02        | -1.77  |           |
| 29 | 838.44  | 0.41     | 74.21       | 838.43  | 0.91             | 3.55              | 0.06        | -1.86  |           |
| 30 | 867.13  | 0.38     | 70.16       | 867.12  | 0.97             | 3.73              | 0.04        | -1.95  |           |
| 31 | 895.89  | 0.36     | 63.12       | 895.88  | 1.04             | 3.90              | 0.05        | -2.02  |           |
| 32 | 924.77  | 0.38     | 71.39       | 924.76  | 1.12             | 4.08              | 0.06        | -2.09  |           |
| 33 | 953.58  | 0.40     | 82.58       | 953.56  | 1.16             | 4.27              | 0.08        | -2.20  |           |
| 34 | 982.39  | 0.49     | 84.74       | 982.37  | 1.18             | 4.49              | 0.10        | -2.34  |           |
| 35 | 1011.20 | 0.54     | 83.33       | 1011.18 | 1.21             | 4.75              | 0.05        | -2.50  |           |

|    |         |      |       |         |      |       |      |       |
|----|---------|------|-------|---------|------|-------|------|-------|
| 36 | 1040.06 | 0.62 | 86.87 | 1040.04 | 1.23 | 5.04  | 0.09 | -2.69 |
| 37 | 1068.87 | 0.70 | 91.71 | 1068.85 | 1.24 | 5.37  | 0.10 | -2.92 |
| 38 | 1097.70 | 0.78 | 92.62 | 1097.68 | 1.22 | 5.74  | 0.08 | -3.19 |
| 39 | 1126.61 | 0.88 | 95.16 | 1126.58 | 1.19 | 6.16  | 0.11 | -3.51 |
| 40 | 1155.49 | 0.97 | 95.94 | 1155.46 | 1.15 | 6.62  | 0.09 | -3.87 |
| 41 | 1184.28 | 1.09 | 97.56 | 1184.25 | 1.09 | 7.14  | 0.13 | -4.28 |
| 42 | 1213.41 | 1.19 | 94.53 | 1213.37 | 1.03 | 7.71  | 0.12 | -4.73 |
| 43 | 1242.35 | 1.29 | 95.78 | 1242.30 | 0.97 | 8.34  | 0.11 | -5.21 |
| 44 | 1271.14 | 1.42 | 97.11 | 1271.08 | 0.89 | 9.01  | 0.14 | -5.74 |
| 45 | 1300.39 | 1.55 | 99.42 | 1300.32 | 0.78 | 9.76  | 0.15 | -6.35 |
| 46 | 1329.50 | 1.71 | 99.35 | 1329.42 | 0.65 | 10.58 | 0.16 | -7.02 |

|    |         |      |        |         |       |       |      |        |
|----|---------|------|--------|---------|-------|-------|------|--------|
| 47 | 1358.36 | 1.82 | 100.74 | 1358.27 | 0.49  | 11.45 | 0.12 | -7.75  |
| 48 | 1387.20 | 1.88 | 98.03  | 1387.09 | 0.34  | 12.37 | 0.11 | -8.51  |
| 49 | 1416.21 | 1.98 | 99.32  | 1416.09 | 0.20  | 13.34 | 0.11 | -9.29  |
| 50 | 1445.16 | 2.06 | 99.81  | 1445.02 | 0.03  | 14.35 | 0.08 | -10.13 |
| 51 | 1473.97 | 2.20 | 100.57 | 1473.81 | -0.16 | 15.40 | 0.15 | -11.00 |
| 52 | 1502.84 | 2.28 | 99.44  | 1502.66 | -0.36 | 16.51 | 0.09 | -11.93 |
| 53 | 1531.64 | 2.41 | 103.17 | 1531.43 | -0.59 | 17.66 | 0.21 | -12.91 |
| 54 | 1560.34 | 2.46 | 102.08 | 1560.11 | -0.86 | 18.85 | 0.07 | -13.94 |
| 55 | 1589.25 | 2.55 | 104.39 | 1588.99 | -1.15 | 20.08 | 0.14 | -15.01 |
| 56 | 1618.02 | 2.68 | 104.24 | 1617.73 | -1.47 | 21.36 | 0.14 | -16.14 |
| 57 | 1646.92 | 2.84 | 104.86 | 1646.6  | -1.82 | 22.70 | 0.17 | -17.34 |
| 58 | 1675.62 | 2.87 | 103.6  | 1675.26 | -2.17 | 24.09 | 0.07 | -18.57 |
| 59 | 1704.47 | 2.95 | 105.61 | 1704.07 | -2.54 | 25.51 | 0.13 | -19.83 |
| 60 | 1733.30 | 3.12 | 106.59 | 1732.86 | -2.97 | 26.97 | 0.18 | -21.17 |
| 61 | 1762.16 | 3.11 | 107.65 | 1761.68 | -3.43 | 28.47 | 0.06 | -22.56 |
| 62 | 1791.03 | 3.1  | 105.63 | 1790.51 | -3.88 | 29.97 | 0.11 | -23.93 |
| 63 | 1819.88 | 2.94 | 106.39 | 1819.32 | -4.29 | 31.43 | 0.17 | -25.26 |
| 64 | 1848.66 | 2.96 | 105.97 | 1848.06 | -4.71 | 32.85 | 0.03 | -26.56 |
| 65 | 1877.50 | 2.97 | 107.23 | 1876.86 | -5.13 | 34.28 | 0.07 | -27.87 |
| 66 | 1906.25 | 2.96 | 107.87 | 1905.57 | -5.58 | 35.70 | 0.04 | -29.19 |
| 67 | 1935.05 | 2.95 | 106.8  | 1934.33 | -6.02 | 37.12 | 0.06 | -30.51 |
| 68 | 1963.99 | 3.03 | 106.22 | 1963.24 | -6.45 | 38.56 | 0.09 | -31.83 |
| 69 | 1992.84 | 3    | 105.49 | 1992.05 | -6.87 | 40.02 | 0.05 | -33.16 |
| 70 | 2021.64 | 2.93 | 106.51 | 2020.81 | -7.28 | 41.46 | 0.09 | -34.46 |
| 71 | 2050.53 | 3.03 | 107.88 | 2049.66 | -7.72 | 42.89 | 0.13 | -35.79 |
| 72 | 2079.35 | 3.07 | 106.83 | 2078.44 | -8.18 | 44.35 | 0.07 | -37.15 |
| 73 | 2108.11 | 3.00 | 108.22 | 2107.16 | -8.64 | 45.81 | 0.11 | -38.50 |

|    |         |      |        |         |        |       |      |        |
|----|---------|------|--------|---------|--------|-------|------|--------|
| 74 | 2136.91 | 2.97 | 106.88 | 2135.92 | -9.09  | 47.24 | 0.08 | -39.83 |
| 75 | 2165.81 | 2.82 | 106.83 | 2164.78 | -9.51  | 48.63 | 0.16 | -41.12 |
| 76 | 2194.63 | 2.69 | 106.68 | 2193.57 | -9.91  | 49.96 | 0.14 | -42.34 |
| 77 | 2223.49 | 2.55 | 105.62 | 2222.4  | -10.28 | 51.23 | 0.15 | -43.49 |
| 78 | 2252.27 | 2.37 | 106.68 | 2251.15 | -10.62 | 52.41 | 0.19 | -44.57 |
| 79 | 2281.01 | 2.34 | 107.43 | 2279.87 | -10.97 | 53.54 | 0.04 | -45.62 |
| 80 | 2309.87 | 2.11 | 105.31 | 2308.7  | -11.29 | 54.62 | 0.25 | -46.60 |
| 81 | 2338.44 | 1.96 | 104.72 | 2337.26 | -11.55 | 55.60 | 0.16 | -47.48 |
| 82 | 2367.46 | 1.67 | 105.45 | 2366.26 | -11.79 | 56.48 | 0.3  | -48.28 |
| 83 | 2396.33 | 1.42 | 104.1  | 2395.12 | -11.99 | 57.24 | 0.26 | -48.95 |
| 84 | 2424.40 | 1.29 | 104.84 | 2423.18 | -12.15 | 57.88 | 0.14 | -49.52 |
| 85 | 2517.87 | 1.41 | 109.98 | 2516.63 | -12.82 | 59.98 | 0.05 | -51.47 |
| 86 | 2623.70 | 1.25 | 107.59 | 2622.43 | -13.61 | 62.30 | 0.05 | -53.68 |
| 87 | 2729.53 | 1.11 | 107.34 | 2728.24 | -14.26 | 64.38 | 0.04 | -55.61 |
| 88 | 2825.61 | 1.05 | 105.14 | 2824.3  | -14.77 | 66.12 | 0.02 | -57.2  |
| 89 | 2921.74 | 0.95 | 117.54 | 2920.42 | -15.37 | 67.67 | 0.07 | -58.72 |
| 90 | 3037.36 | 0.91 | 105.62 | 3036.02 | -16.06 | 69.41 | 0.05 | -60.44 |
| 91 | 3081.68 | 0.91 | 109.52 | 3080.33 | -16.27 | 70.08 | 0.04 | -61.06 |
| 92 | 3100.40 | 0.6  | 51.71  | 3099.05 | -16.26 | 70.30 | 1.25 | -61.21 |
| 93 | 3112.90 | 2.11 | 342.95 | 3111.55 | -16.00 | 70.28 | 4.74 | -61.01 |
| 94 | 3122.44 | 4.2  | 333.36 | 3121.07 | -15.52 | 70.07 | 6.76 | -60.52 |
| 95 | 3132.65 | 6.14 | 329.34 | 3131.24 | -14.72 | 69.63 | 5.8  | -59.64 |
| 96 | 3141.99 | 7.6  | 328.64 | 3140.52 | -13.76 | 69.05 | 4.7  | -58.56 |

KOP

|     |         |       |        |         |        |       |      |        |
|-----|---------|-------|--------|---------|--------|-------|------|--------|
| 97  | 3152.10 | 8.87  | 327.01 | 3150.52 | -12.53 | 68.28 | 3.83 | -57.14 |
| 98  | 3161.20 | 9.81  | 323.7  | 3159.5  | -11.32 | 67.44 | 3.57 | -55.69 |
| 99  | 3171.00 | 10.64 | 319.31 | 3169.14 | -9.96  | 66.35 | 3.48 | -53.96 |
| 100 | 3181.00 | 11.49 | 318.41 | 3178.96 | -8.52  | 65.09 | 2.6  | -52.05 |
| 101 | 3190.18 | 12.19 | 316.12 | 3187.94 | -7.14  | 63.81 | 2.75 | -50.17 |
| 102 | 3199.76 | 12.76 | 313.39 | 3197.3  | -5.68  | 62.34 | 2.57 | -48.1  |
| 103 | 3209.79 | 13.5  | 312.11 | 3207.06 | -4.13  | 60.67 | 2.38 | -45.82 |
| 104 | 3218.95 | 14.37 | 313.06 | 3215.96 | -2.64  | 59.04 | 2.95 | -43.62 |
| 105 | 3228.80 | 15.61 | 314.68 | 3225.47 | -0.87  | 57.21 | 3.99 | -41.07 |
| 106 | 3238.80 | 16.86 | 314.79 | 3235.07 | 1.09   | 55.22 | 3.75 | -38.27 |
| 107 | 3248.80 | 18.3  | 315.51 | 3244.6  | 3.24   | 53.09 | 4.37 | -35.25 |
| 108 | 3257.50 | 19.36 | 315.46 | 3252.84 | 5.24   | 51.12 | 3.66 | -32.45 |
| 109 | 3268.07 | 20.82 | 315.08 | 3262.76 | 7.82   | 48.57 | 4.16 | -28.82 |
| 110 | 3277.71 | 22.03 | 314.67 | 3271.74 | 10.30  | 46.07 | 3.79 | -25.29 |

|     |         |       |        |         |        |         |       |        |  |
|-----|---------|-------|--------|---------|--------|---------|-------|--------|--|
| 111 | 3286.07 | 22.94 | 314.27 | 3279.46 | 12.54  | 43.79   | 3.31  | -22.1  |  |
| 112 | 3295.90 | 23.98 | 314.42 | 3288.48 | 15.28  | 40.99   | 3.18  | -18.18 |  |
| 113 | 3305.70 | 25.22 | 314.59 | 3297.39 | 18.14  | 38.08   | 3.8   | -14.11 |  |
| 114 | 3312.76 | 25.91 | 314.33 | 3303.76 | 20.27  | 35.91   | 2.97  | -11.06 |  |
| 115 | 3334.65 | 29.31 | 314.83 | 3323.15 | 27.39  | 28.69   | 4.67  | -0.92  |  |
| 116 | 3343.78 | 32.55 | 313.55 | 3330.98 | 30.66  | 25.32   | 10.86 | 3.78   |  |
| 117 | 3353.83 | 36.16 | 312.69 | 3339.28 | 34.53  | 21.18   | 10.87 | 9.44   |  |
| 118 | 3363.45 | 38.81 | 312.56 | 3346.91 | 38.50  | 16.87   | 8.27  | 15.29  |  |
| 119 | 3373.23 | 41.62 | 313.43 | 3354.38 | 42.80  | 12.26   | 8.79  | 21.6   |  |
| 120 | 3382.43 | 43.36 | 314.41 | 3361.16 | 47.12  | 7.78    | 6.07  | 27.81  |  |
| 121 | 3392.19 | 45.72 | 315.06 | 3368.12 | 51.93  | 2.92    | 7.39  | 34.66  |  |
| 122 | 3401.66 | 47.88 | 315.81 | 3374.6  | 56.85  | -1.93   | 7.06  | 41.56  |  |
| 123 | 3411.13 | 49.51 | 316    | 3380.85 | 61.96  | -6.88   | 5.18  | 48.68  |  |
| 124 | 3419.70 | 50.91 | 316.1  | 3386.34 | 66.70  | -11.45  | 4.91  | 55.26  |  |
| 125 | 3423.83 | 52.24 | 315.97 | 3388.9  | 69.03  | -13.69  | 9.69  | 58.49  |  |
| 126 | 3441.90 | 57.49 | 314    | 3400.58 | 79.47  | -24.14  | 9.12  | 73.27  |  |
| 127 | 3451.60 | 61.07 | 313.26 | 3405.91 | 85.22  | -30.18  | 11.22 | 81.6   |  |
| 128 | 3458.17 | 63.18 | 312.25 | 3407.33 | 89.16  | -34.44  | 10.5  | 87.4   |  |
| 129 | 3469    | 66.95 | 310.94 | 3411.89 | 95.68  | -41.79  | 10.95 | 97.2   |  |
| 130 | 3478.2  | 72    | 310.83 | 3415.12 | 101.32 | -48.3   | 16.47 | 105.79 |  |
| 131 | 3485.3  | 76.95 | 310.54 | 3417.02 | 105.77 | -53.49  | 20.95 | 112.61 |  |
| 132 | 3496.8  | 85.16 | 311.2  | 3418.8  | 113.2  | -62.07  | 21.48 | 123.93 |  |
| 133 | 3503.12 | 89.3  | 311.6  | 3419.11 | 117.37 | -66.8   | 19.74 | 130.23 |  |
| 134 | 3507.5  | 90.98 | 311.18 | 3419.1  | 120.27 | -70.09  | 11.86 | 134.6  |  |
| 135 | 3517.2  | 90.14 | 310.35 | 3419    | 126.6  | -77.43  | 3.65  | 144.28 |  |
| 136 | 3526.9  | 89.65 | 311.18 | 3419.02 | 132.94 | -84.78  | 2.98  | 153.95 |  |
| 137 | 3536.7  | 88.67 | 310.37 | 3419.17 | 139.34 | -92.2   | 3.89  | 163.72 |  |
| 138 | 3544.8  | 87.2  | 309.26 | 3419.46 | 144.52 | -98.42  | 6.82  | 171.78 |  |
| 139 | 3555.8  | 88.81 | 309.31 | 3419.84 | 151.48 | -106.92 | 4.39  | 182.72 |  |
| 140 | 3565.3  | 89.51 | 310.25 | 3419.98 | 157.55 | -114.22 | 3.7   | 192.18 |  |

|     |         |       |        |         |        |         |      |        |  |
|-----|---------|-------|--------|---------|--------|---------|------|--------|--|
| 141 | 3574.8  | 91.47 | 309.75 | 3419.9  | 163.66 | -121.5  | 6.39 | 201.64 |  |
| 142 | 3584.9  | 91.75 | 309.88 | 3419.61 | 170.12 | -129.25 | 0.92 | 211.7  |  |
| 143 | 3593.65 | 90.7  | 309.85 | 3419.43 | 175.73 | -135.97 | 3.6  | 220.41 |  |
| 144 | 3604.5  | 90.21 | 310.43 | 3419.34 | 182.72 | -144.26 | 2.1  | 231.22 |  |
| 145 | 3613.6  | 90.28 | 310.72 | 3419.3  | 188.64 | -151.17 | 0.98 | 240.3  |  |
| 146 | 3622.16 | 89.37 | 311.35 | 3419.33 | 194.26 | -157.63 | 3.88 | 248.83 |  |

|     |         |       |        |         |        |         |      |        |  |
|-----|---------|-------|--------|---------|--------|---------|------|--------|--|
| 147 | 3629.35 | 88.11 | 311.78 | 3419.49 | 199.03 | -163.01 | 5.55 | 256.01 |  |
| 148 | 3641.24 | 85.31 | 311.47 | 3420.17 | 206.92 | -171.88 | 7.11 | 267.86 |  |
| 149 | 3652    | 85.24 | 311.47 | 3421.06 | 214.06 | -179.97 | 0.2  | 278.56 |  |
| 150 | 3663.16 | 86.99 | 311.51 | 3422.11 | 221.39 | -188.25 | 4.74 | 289.66 |  |
| 151 | 3669.74 | 87.41 | 311.6  | 3422.43 | 225.75 | -193.17 | 1.96 | 296.22 |  |
| 152 | 3677.29 | 88.32 | 311.74 | 3422.72 | 230.77 | -198.81 | 3.66 | 303.76 |  |
| 153 | 3687    | 89.3  | 312.19 | 3422.92 | 237.26 | -206.03 | 3.33 | 313.45 |  |
| 154 | 3696.9  | 89.23 | 312.14 | 3423.04 | 243.91 | -213.36 | 0.26 | 323.34 |  |
| 155 | 3706.75 | 88.81 | 311.99 | 3423.21 | 250.5  | -220.68 | 1.36 | 333.17 |  |
| 156 | 3717.14 | 89.65 | 312.46 | 3423.35 | 257.49 | -228.37 | 2.78 | 343.55 |  |
| 157 | 3726.4  | 91.05 | 313.22 | 3423.3  | 263.78 | -235.16 | 5.16 | 352.8  |  |
| 158 | 3736.8  | 91.19 | 313.68 | 3423.09 | 270.93 | -242.71 | 1.39 | 363.2  |  |
| 159 | 3745.2  | 89.3  | 314.16 | 3423.06 | 276.76 | -248.76 | 6.96 | 371.6  |  |
| 160 | 3754.96 | 87.76 | 315.25 | 3423.31 | 283.62 | -255.69 | 5.8  | 381.35 |  |
| 161 | 3763.19 | 88.04 | 315.44 | 3423.61 | 289.47 | -261.47 | 1.23 | 389.58 |  |
| 162 | 3774.36 | 88.6  | 315.38 | 3423.94 | 297.42 | -269.31 | 1.51 | 400.74 |  |
| 163 | 3785.2  | 87.34 | 315.17 | 3424.32 | 305.12 | -276.93 | 3.54 | 411.57 |  |
| 164 | 3794.8  | 86.92 | 315    | 3424.8  | 311.91 | -283.7  | 1.42 | 421.16 |  |
| 165 | 3803.8  | 86.78 | 315.31 | 3425.3  | 318.28 | -290.04 | 1.13 | 430.15 |  |
| 166 | 3812.78 | 86.85 | 315.23 | 3425.79 | 324.65 | -296.35 | 0.35 | 439.11 |  |

|     |         |       |        |         |        |         |       |        |    |
|-----|---------|-------|--------|---------|--------|---------|-------|--------|----|
| 167 | 3821.22 | 86.92 | 315.48 | 3426.25 | 330.65 | -302.27 | 0.92  | 447.54 |    |
| 168 | 3831.7  | 87.41 | 315.1  | 3426.77 | 338.09 | -309.64 | 1.77  | 458.01 |    |
| 169 | 3841.8  | 87.41 | 315.02 | 3427.23 | 345.23 | -316.76 | 0.24  | 468.1  |    |
| 170 | 3852.6  | 86.99 | 314.76 | 3427.75 | 352.84 | -324.41 | 1.37  | 478.89 |    |
| 171 | 3862.38 | 87.13 | 314.6  | 3428.26 | 359.71 | -331.35 | 0.43  | 488.65 |    |
| 172 | 3871.12 | 87.55 | 314.33 | 3428.66 | 365.82 | -337.58 | 1.44  | 497.38 |    |
| 173 | 3882.3  | 88.18 | 314.28 | 3429.08 | 373.63 | -345.58 | 1.69  | 508.55 |    |
| 174 | 3891.6  | 88.53 | 314.17 | 3429.35 | 380.11 | -352.24 | 1.13  | 517.85 |    |
| 175 | 3901.5  | 88.46 | 314    | 3429.61 | 387    | -359.35 | -0.21 | 527.74 |    |
| 176 | 3910.8  | 87.97 | 314.2  | 3429.9  | 393.47 | -366.02 | -1.58 | 537.04 |    |
| 177 | 3920.91 | 87.83 | 314.19 | 3430.27 | 400.51 | -373.27 | -0.42 | 547.14 |    |
| 178 | 3929.56 | 86.85 | 314.1  | 3430.67 | 406.53 | -379.47 | -3.4  | 555.78 |    |
| 179 | 3939.6  | 85.8  | 313.8  | 3431.31 | 413.48 | -386.68 | -3.14 | 565.8  |    |
| 180 | 3949.4  | 85.94 | 313.58 | 3432.02 | 420.23 | -393.75 | 0.43  | 575.57 |    |
| 181 | 3970.55 | 86.15 | 313.6  | 3433.48 | 434.78 | -409.03 | 0.3   | 596.66 | TD |